



European Hyperloop Week 2022

Final Demonstration Documentation

by

HYPERLINK



Illustration by Katarzyna Hawliczek, Marketing Team at Hyperlink.

Table of Contents

1. General	8
1.1 Introduction	8
1.2 Team Members	9
1.3 Development Environment	11
1.4 Research Objectives	12
1.5 Budget & Funding	13
1.6 Manufacturing Method	13
1.7 Hyperlink Representative	14
1.8 Design Competition Award	14
2. System	14
2.1 Propulsion	17
2.1.1 Technical Description of the System	17
2.1.1.1 Theory and principle physics of desired functionality	17
2.1.1.1.1 Polyphase excitation	19
2.1.1.1.2 Faraday's Law of Induction	20
2.1.1.1.3 Eddy Currents	21
2.1.1.1.4 Lorentz Force	21
2.1.1.1.5 End-Effects:	22
2.1.1.2 Design Process	23
2.1.1.2.1 Average Force Required	23
2.1.1.2.2 Friction Forces	24
2.1.1.2.3 Proportionality	26
2.1.1.3 Free Body Diagrams to define load cases for simulations.	29
2.1.1.4 Simulations Validating the Theory & Results Analysis	29
2.1.1.4.1 Simulation Process	29
2.1.1.5 Dimensioning process	37
2.1.1.5.1 Data analysis	38
2.1.1.6 Manufacturing Processes	42
2.1.1.6.1 Manufacturing of the stator	42
2.1.1.6.2 Manufacturing of the coils	43
2.1.1.6.3 Combination of stator and coils	45
2.1.2 Size, Components, Appearance	46
2.1.2.1 Evidence of CAD models	46
2.1.2.2 Technical Drawings	48
2.1.3 Integration into a Subordinate Structure/System	49

2.1.4 Demonstration Plan	50
2.1.4.1 Parts List	50
2.2 Braking	50
2.2.1 Technical Description of the System	50
2.2.1.1 Theory and principle physics of desired functionality	50
2.2.1.1.1 Air Reservoir	53
2.2.1.1.2 Brake Cylinder	53
2.2.1.1.3 Brake Pads	54
2.2.1.1.4 Ball Valve	54
2.2.1.1.5 Fittings and Pipes	54
2.2.1.1.6 Solenoid Control Valve	54
2.2.1.1.7 Brake Spring	54
2.2.1.2 Design Process and Dimensioning Process	54
2.2.1.2.1 Braking Force Requirement	55
2.2.1.3 Free Body Diagrams to define load cases for simulations.	64
2.2.1.6 Description of the manufacturing processes.	65
2.2.2 Size, Components, Appearance	65
2.2.2.1 Evidence of CAD models	65
2.2.2.2 Technical drawings	74
2.2.3 Integration into a Subordinate Structure/System	80
2.2.4 Demonstration Plan	81
2.2.4.1 Parts List/BOM	82
2.2.4.2 Demonstration Setup	83
2.3 Suspension	85
2.3.1 Technical Description of the System	85
2.3.1.1 Theory and principle physics of desired functionality	85
2.3.1.2 Description of design process taken.	88
2.3.1.2.1 Shock Absorbers	89
2.3.1.2.2 Wheel and Shaft	90
2.3.1.2.3 Wheel housing and Fixtures	91
2.3.1.3 Free Body Diagrams	92
2.3.1.4 Evidence of simulations	94
2.3.1.5 Description of the manufacturing processes.	96
2.3.2 Size, Components, Appearance	97
2.3.2.1 Evidence of CAD models	97
2.3.3 Integration into a Subordinate Structure/System	98
2.3.4 Demonstration Plan	99

2.3.4.1 Parts List	99
2.4 Structures	100
2.4.1 Technical Description of the System	100
2.4.1.1 Theory and principle physics of desired functionality	100
2.4.1.1.1 Frame	100
2.4.1.1.2 Shell	101
2.4.1.2 Design process	103
2.4.1.2.1 Shell	103
2.4.1.2.2 Frame	104
2.4.1.3 Free Body Diagrams to define load cases for simulations.	106
2.4.1.4 Evidence of simulations validating the theory, and detailed analysis of results.	107
2.4.1.4.1 Static Operation	107
2.4.1.4.2 Dynamic Operation	108
2.4.1.4.3 Braking Operation	110
2.4.1.5 Dimensioning process	111
2.4.1.6 Manufacturing Processes	113
2.4.2 Size, Components, Appearance	114
2.4.2.1 Evidence of CAD models	114
2.4.2.2 Technical drawings	116
2.4.3 Integration into a Subordinate Structure/System	117
2.4.4 Demonstration Plan	117
2.4.4.1 Parts List	117
2.5 Electronics & Power	118
2.5.1 Technical Description of the System	118
2.5.1.1 Theory and principle physics of desired functionality	118
2.5.1.2 Description of design process taken.	118
2.5.1.4 Description of the manufacturing processes.	122
2.5.2 Size, Components, Appearance	122
2.5.2.1 Evidence of CAD models	122
2.5.2.2 Technical drawings	126
2.5.3 Integration into a Subordinate Structure/System	130
2.5.4 Demonstration Plan	130
2.5.4.1 Parts List	131
2.6 Software	133
2.6.1 Environments and packages	133
2.6.1.1 STM32CubeIDE	133
2.6.1.2 TouchGFX	133

2.6.1.3 HAL	133
2.6.2 System Software Flowcharts	134
2.6.2.1 System Flow Diagram	134
2.6.2.2 Further description of flow states	134
2.6.2.3 Protocol for decelerating pod (flowchart)	136
2.6.3 Graphical User Interface	137
2.6.3.1 Initial Menu Interface (concept)	137
2.6.3.2 Configuration and testing interface (concept)	138
2.6.3.3 View Pod Data Page (concept)	139
2.6.3.4 Configure Pod Page (concept)	140
2.6.3.5 Live running interface (implemented using TouchGFX)	141
2.6.4 UML Diagrams	142
2.6.4.1 Class Diagrams	142
2.6.4.2 Class Diagram: Key Methods and variables	142
2.6.5 Hardware and their application	144
2.6.5.1 Photoelectric reflective sensor	144
2.6.5.2 Encoders	144
2.6.5.3 Temperature Sensor:	144
2.6.5 Demonstration Plan	144
2.6.5.1 Demonstration Setup	144
2.6.6 Equipment & Infrastructure	145
3. Safety	145
3.1 Propulsion	146
3.4.1 FMEA & Risk Mitigation	146
3.4.2 Procedure in case of Failure	147
3.4.3 Energy Storage	147
3.4.4 Special Transport, Storage and Lifting Requirements	147
3.2 Braking	148
3.4.1 FMEA & Risk Mitigation	148
3.4.2 Procedure in case of Failure	150
3.4.3 Energy Storage	151
3.3 Suspension	152
3.4.1 FMEA & Risk Mitigation	152
3.4.4 Special Transport, Storage and Lifting Requirements	154
3.4 Structures	154
3.4.1 FMEA & Risk Mitigation	154
3.4.2 Procedure in case of Failure	155

3.4.3 Energy Storage	155
3.4.4 Special Transport, Storage and Lifting Requirements	155
3.5 Electronics & Power & Software	156
3.5.1 FMEA & Risk Mitigation	156
3.4.2 Procedure in case of Failure	157
3.4.3 Special Transport, Storage and Lifting Requirements	157
4. Logistics & Safety	158
 4.1 Transport, Lifting & Lift Plan	158
4.1.1 Specification of transportation procedures	162
4.1.1.1 Lifting the pod	162
4.1.1.2 Moving the crane around EHW premises	162
4.1.1.3 Descending the pod at the storage area, demonstration area, or display area	162
 4.2 Storage	162
4.2.1 Storage Procedure	163
4.2.2 Potential Energy Safe Storage	163
 4.3 Demonstration procedures	164
4.3.1 Pre-demonstration procedure	166
4.3.2 Demonstration procedure	167
4.3.3 Post-demonstration procedure	168
5. Testing	168
 5.1 Testing Facility	169
 5.1.1 Propulsion	169
5.1.1.1 Manufacturing & Testing Procedures	169
5.1.1.2 Testing Plan & Methodology	170
5.1.1.3 Expected Results	171
 5.1.2 Braking	171
5.1.2.1 Manufacturing & Testing Procedures	171
5.1.2.2 Testing Plan & Methodology	172
5.1.2.3 Expected Results	173
 5.1.3 Suspension	173
5.1.3.1 Manufacturing & Testing Procedures	173
5.1.3.1.1 Load Test	174
5.1.3.1.2 Speed Test	174
5.1.3.1.3 Complete Test	175
5.1.3.2 Testing Plan & Methodology.	175
5.1.3.2.1 Load test	175

5.1.3.2.2 Speed Test	175
5.1.3.2.3 Complete Test	175
5.1.3.3 Expected Results	176
5.1.3.3.1 Load Test	176
5.1.3.3.2 Speed Test	176
5.1.3.3.3 Complete Test	176
5.1.4 Structures	176
5.1.4.1 Manufacturing & Testing Procedures	176
5.1.4.2 Testing Plan & Methodology	176
5.1.4.2.1 Load test	176
5.1.4.2.2 Mounting test	176
5.1.4.2.3 Component test	176
5.1.4.2.4 Active test	177
5.1.4.3 Expected Results	177
5.1.5 Electronics & Power	177
5.1.5.1 Manufacturing & Testing Procedures	177
5.1.5.2 Testing Plan & Methodology	177
5.1.5.3 Expected Results	178
5.1.6 Software	178

1. General

1.1 Introduction

Hyperlink is a student Hyperloop team based in London. It was founded in September 2020 and is currently operating from Queen Mary University of London. The team consists of 65 members from 5 different universities - Queen Mary University of London, University College London, King's College London, University of the Arts London, Lancaster University.

Hyperlink was started as the response to meet unfulfilled demand for engineering teams at the Queen Mary University of London campus. The team was created to provide ambitious students interested in Hyperloop, technology, and business with dynamic and exciting opportunities to apply their skills in a large-scale project. We are driven by the vision of accelerating the implementation of Hyperloop and developing an innovative mode of transportation.

The team's long-term vision is to create a truly London-wide initiative by uniting the city's best universities and creating a strong Hyperloop development hub. We believe that London, being one of the world's top tech startup hubs, would be the perfect place to accelerate the development of the first economically and technologically viable Hyperloop network.

Hyperlink is composed of 3 main divisions: Engineering, Research and Operations.

Engineering department is responsible for designing, manufacturing and testing the pod. Within the department there are 6 teams which can be categorised into Mechanical and Electrical departments. The Mechanical department is responsible for developing the propulsion, brakes and structural parts of the pod. It is composed of 4 teams: Propulsion, Braking, Suspension, Structures. The Electrical department works on pod's control and emergency protocol and is divided into 2 teams: Electronics & Power, and Software.

Research department consists of Biomedical and Scalability divisions which focus on developing research papers on Hyperloop technology. The Biomedical team is studying the effects of prolonged exposure to magnetic fields and designing a magnetic shield to prevent the field from impacting passengers in any significant way. They also focus on designing ergonomic and safe passenger seating that would enable safe emergency braking and investigate the maximum safe braking force. The Scalability department performs studies on concepts of making Hyperloop

technology more inclusive and socially sustainable, through researching factors like sustainable Hyperloop station placement, changing inequality indices, and ESG financing.

The Operations department consists of the marketing, social media, and partnerships teams. They focus on public relations, upkeeping our social media presence, and obtaining sponsors for the team.

1.2 Team Members

Table 1.2.1 List of Committee Members

Committee	
President, Director of Research	Marcin Bielicki
Director of Engineering	Katarzyna Lichy
Director of Operations	Sahil Sharma
Treasurer	Rajmony Hasan

Table 1.2.2 List of Engineering Department Members

Engineering Department			
Mechanical		Electrical	
Mechanical Project Manager	Saad Ali	Electrical Project Manager	Michał Makówka
Propulsion			
Team Head	Matthew Clisby	Team Head	Michał Makówka
Team Members	Somaan Bhatti	Team Members	Gleb Smantcer
Electronics & Power			
Team Head	Michael Levitt	Team Head	Louie Ormstrom
	Dalir Kosimov	Team Members	Mikolaj Konko
Software			
	Shahaab Qureshi		Piotr Kurek
	Yathavan Sriskantharajah		Vedika Abhaykumar Barde
	Divyank Yarravarapu		

Braking	
Team Head	Andela Vasilijevic
Team Members	Abdulgani Abdilahi
	Theo Achilleos
	Manas Chaubey
Structures	
Team Head	Alex Pinel Neparidze
Team Members	Arman Kaplan
	Ezzedin Khaled Hassan Mohamed Nour
Suspension	
Team Head	Saad Ali
Team Members	Anisa Ahmad
	Melos Krasniqi
	Daniyaal Zahid

Table 1.2.3 List of Research Department Members

Research Department			
Scalability		Biomedical	
Team Head	Weronika Janusek	Team Head	Balvinder Dhillon
Members	Ilham Esse	Members	Sanka Wijayarathne
	Ahmed Galgal		Lucia Moreno
	Miklos Kralik		
	Hamza Mohammad		

	Govarthan Ramaneshan

Table 1.2.4 List of Operations Department Members

Operations Department			
Partnerships		Logistics	
Team Head	Taer Jan Jawasreh	Team Head	Rajmony Hasan
Members	Jonathan Bosquet	Members	Aleksandra Rebotenko
	Vasileios Vogiatzis		Alexandra Olid Stepanchuk
	Wiktoria Mroz	Social Media	
	Mojtaba Sidiqi	Members	Samuel Thomas Astaire
	Natalia Wasinska		Amir Dlimi
Members	Daim Choudhary		Carolina Tani

1.3 Development Environment

Our Hyperloop pod is being developed at Queen Mary University of London campus. For the manufacturing process, Hyperlink is utilising the lab facilities available at the School of Engineering and Materials Science and School of Electronic Engineering and Computer Science. Moreover, the Engineering Department is working closely with Hyperlink's industry partners to gain necessary experience and knowledge. Our industry parents provide the team with assistance on the manufacturing process, verification of the design and its integrity.

1.4 Research Objectives

As it is commonly known, Hyperloop is a very money and resource consuming project. Costs of technology and infrastructure constitute major limitations and delay towards making Hyperloop a reality. As a team, we want to push the Hyperloop industry forward, making it achievable, inclusive and more sustainable. Therefore, we decided for the theme of 2021/2022 academic year to be **Economic Feasibility**.

The main research objective is to develop a fully operational pod, while maintaining a high performance to cost ratio. This is achieved by implementing recycled materials, using a more efficient battery management system and designing a sustainable shell of the pod.

Throughout the development process, our second objective is to build a strong knowledge and experience base. It will serve as a strong foundation for the improved versions of our first pod to be developed in the upcoming years. With support from university, companies and previous research, our team aims to achieve high knowledge of Hyperloop technology and implement it in our design. Furthermore, we believe that involvement in this project will allow us to contribute to the growth of an innovative transportation system.

Our development process consists of 5 main milestones:

1. Final Design Specification - creation of a document that contains the final design choices for all subsystems, including the estimated costs and outputs the respective system will produce e.g. thrust force or braking force.

2. Final Design Package - creation of the final CAD assembly and the final Bill of Materials.

3. Start of Manufacturing - manufacturing begins in the Queen Mary University of London labs. Parts will be obtained from trusted manufacturers and some specific components, such as laminated cores, will be developed to our specifications by industry partners.

4. Testing and Optimisation - after manufacturing is complete, additional tests will be designed and carried out to ensure proper operation and a high level of safety for the demonstration at European Hyperloop Week. If needed, at this step any necessary improvements will be implemented and all tests will be repeated.

5. Delivery - the pod is ready for demonstration at the European Hyperloop Week.

1.5 Budget & Funding

As a university team, we received support from the School of Engineering and Materials Science at Queen Mary University of London. They are our main sponsor, as they provide us with 60% of the funding. Moreover, our second biggest sponsor is the metal manufacturing company Slovas, who provides us with approximately 30% of the whole financial funding, through in-kind manufacturing of all metal parts. Another source of funding were memberships for Hyperlink society, managed by Queen Mary Student's Union. Lastly, we have received funding from the university through the Society Development Fund. The above will allow us to fully manufacture, test and transport our pod at EHW 2022 safely and effectively.

Our partnerships team is still working on securing more funding, which will mostly be used for merchandising and improving our display booth at EHW.

The current sponsorship makeup is as follows:

Table 1.5.1 - Hyperlink's budget

Sponsor	Value (cash or in-kind)
School of Engineering, QMUL	£7000
QMUL, Society Development Fund	£800
Slovas	~£5000 (in-kind, manufacturing of all metal parts)
Team Membership Fees	£1200
Cash	£1000
Total	£16000

1.6 Manufacturing Method

Hyperlink's pod is designed for both, in-house and outsourced manufacturing techniques. The in-house manufacturing site is at the MakerSpace and Electrical laboratory at Queen Mary University of London. All components are assembled and tested in-house. Activities such as metal cutting, forming, 3D printing, welding were performed onsite in the laboratory. However, individual components such as air tanks, shock absorbers, springs were either outsourced or purchased.

The team works closely with industry partners such as Slovas who sponsor all our metal parts. The company uses laser cutting, metal bending and welding techniques to provide us with most ready-to-use metal parts such as the frame, mounting fixtures, wheels. The stator metal sheets were manufactured at Slovas and the LIM was assembled at the MakerSpace. Battery pack was outsourced, as well as electronics boards. For a detailed manufacturing process of individual subsystems, please refer to point 2. System.

1.7 Hyperlink Representative

The team's representative who will be in correspondence with EHW is Marcin Bielicki, current president of Hyperlink. He can be reached at bielicki.mar@gmail.com or at +44 7564523311. If necessary, the team email is: hyperlink@qmsu.org.

1.8 Design Competition Award

In the ITD, the categories of Design Competition Awards Hyperlink applied for are the following:

- Best Mechanical Subsystem Award.
- Best Electrical Subsystem Award.
- Complete Pod Award
- Full-Scale Award - Technical Aspects of Hyperloop System
- Full-Scale Award - Socioeconomic Aspects of Hyperloop Development

2. System

Hyperlink's pod is composed of the following subsystems: propulsion, braking, suspension, power, electronics, software and structures. The whole system is intended to weigh no more than 150kg and to fit into the dimensions of 2.101m x 0.456m x 0.577m (length x height x width).

The pod is propelled by a double-sided Linear Induction Motor (LIM). The design is providing the pod with necessary thrust to accelerate up to 50km/h. The main components of the system are the stator and the rotor. Hyperlink's propulsion design is described in more detail in section 2.1 *Propulsion*.

The braking system is one of the most important ones in the hyperloop. Braking is synchronously collaborating with two other sub teams, structures, and suspension in order to create a successful braking system which will effectively stop the pod

completely. The braking system is designed to provide sufficient braking force to the pod, both during the run and in emergency situations. The pod is equipped with pneumatic brakes designed to produce the deceleration force of 7.5kN. The braking system is constructed to be engaged by default to ensure additional safety of the design. It means that the power is required to disengage them and allow the pod to move. Braking is described further in section 2.2 *Braking*.

The suspension is a system composed of vertical and horizontal wheel sets which ensure horizontal and vertical stability. Due to the wheel alignment, the pod is able to move only in one direction, forward and back along the I-beam. Moreover, the system is designed to account for any possible deflection and to always bring the pod to its intended trajectory. Due to the shock-absorber and spring system on wheels, the system is designed to cease the effect of any unexpected bumps, allowing for the smooth run. The placement of two suspension sets is at the front and back of the pod. One set of suspension is composed of a pair of vertical wheels which are placed on top of the I-beam, and 2 pairs of vertical wheels distributed on both sides of the middle part of the track. Additionally, extra two horizontal wheels are added in the centre of mass, as a support for the primary suspension sets. Further details on suspension are in section 2.3 *Suspension*.

The pod's structure is composed of two main elements: a shell and a frame. The frame is a metal construction that accommodates all the subsystems, allowing for even mass distribution. The shell is designed to cover all the internal subsystems of the pod. It is composed of two main parts, a nose and a body. The nose is equipped with an air inlet at the front of the pod, allowing the air to travel through the pod cooling the subsystems. The shell is outsourced and manufactured from a glass-plastic reinforced composite. For detailed description of Structures please refer to section 2.4 *Structures*.

The suspension and structures' frame together constitute the chassis of the pod.

The power system will consist of an outsourced battery pack. The high-capacity power system consists of a number of Lithium Ion batteries, designed for high and low voltage application, Battery Management System (BMS), and a number of PCB modules responsible for Propulsion and Braking control. The internal power network for all the subsystems will distribute 24V DC current across the vehicle systems. This will be manufactured to our specification. Further details on Power are provided in section 2.6 *Electronics & Power*.

For the Electronics and Software subsystem, they are decentralised in that each of the above systems have their own unique electronic modules for the measurement, communication, and control of important variables for these subsystems, with integral software ensuring the state of these systems is monitored and the appropriate action is communicated to the systems or user so it can be implemented, especially in case of an emergency such as a sudden power loss. The pod is equipped with 3 position sensors, 2 encoders, a photoelectric reflective sensor, and a temperature sensor.

Passive components, wiring and circuit protection systems are placed between the subsystems and their respective electronics modules, which lead to the centralised battery pack where power is provided. For further details on Electronics & Power and Software, please refer to sections 2.5 and 2.6, respectively.

Figure below shows the Hyperlink's pod design with the transparent shell. In reality, the shell is not transparent, however, it is used here to allow for visualisation of the internal components.

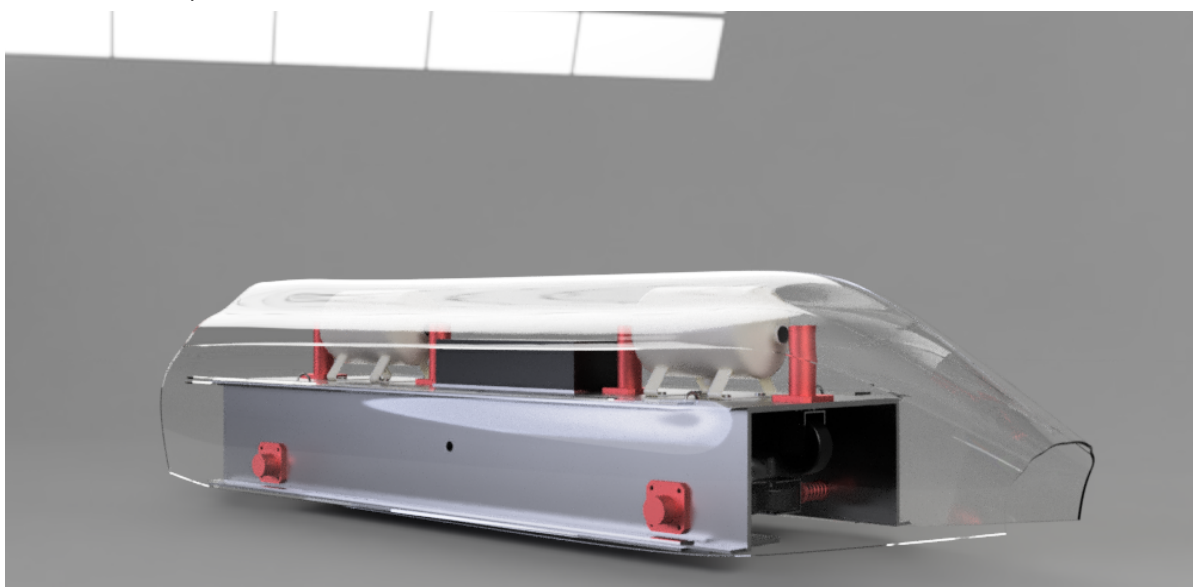


Figure 2.1. Hyperlink's pod render

The realistic render of the shell is presented on the figure below.



Figure 2.2 Hyperlink's Shell - Realistic View

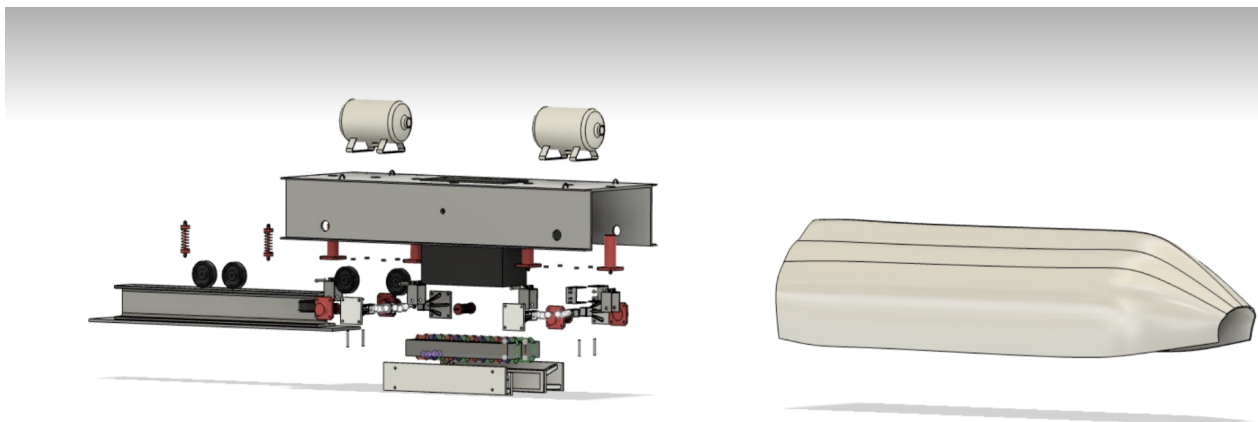


Figure 2.3 Exploded View Pod

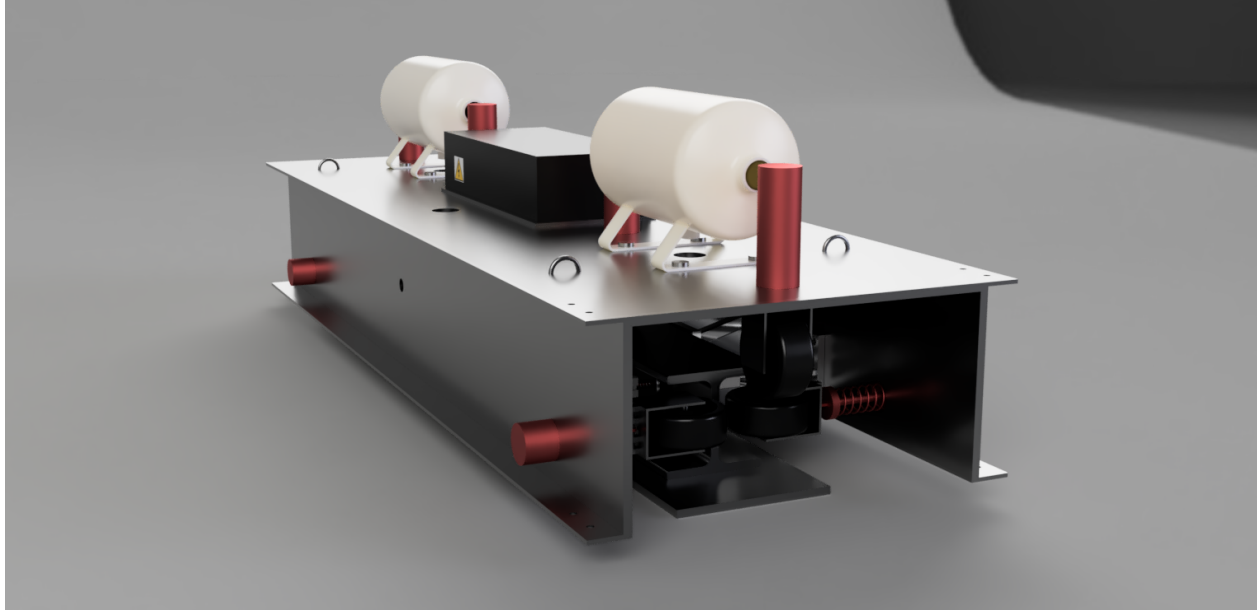


Figure 2.4 Internal view of the pod

2.1 Propulsion

The pod is propelled using a double-sided Linear Induction Motor (DSLIM). This motor is designed to accelerate the pod to speeds up to 50 km/h. The motor consists of two main components: a stator and a rotor. The rotor is the I-beam, made from aluminium 6061 T6 and the stator is made from Stainless Steel WN.1.4034 wound with 120 coils per phase of 2mm copper wiring. This design choice is made due to its capability of handling an adequate current whilst being thin enough to enable the maximum number of windings within the gap between the teeth.

2.1.1 Technical Description of the System

2.1.1.1 Theory and principle physics of desired functionality

The theory of Linear Induction Motors (LIM) can be described similarly to conventional rotary motors. However, the main difference between the two concepts lies in their respective geometries. The working principle of a conventional motor is changing of the primary current in the wires to produce a fluctuating magnetic field in the stator. These fluctuations cause eddy currents to flow in the stator which subsequently produce a magnetic force (or torque) on the rotor. A LIM is similar, except the geometry is linear so the eddy currents produce a linear magnetic force on the rotor. Hyperlink's design uses a double-sided LIM (DSLIM) on an I-beam, hence the primary is moving and the secondary remains stationary.

For any numerical analysis, the equations used are Maxwell's equations and are the following:

$$\nabla \times E = -\frac{\partial B}{\partial t}$$

$$\nabla \times H = J + \frac{\partial D}{\partial t}$$

$$\nabla \cdot D = \rho v$$

$$\nabla \cdot B = 0$$

Where E is the electric field strength, H is the magnetic field strength, B is the magnetic flux density, D is the electric flux density and J is the electric current density and ρ_v is the charge density.

As mentioned previously, the motion of a double-sided linear induction motor is similar to a conventional rotary motor. Although, in a rotary motor the motion is transferred rotationally, whereas in a linear induction motor the motion is produced and transferred linearly. This section focuses on the fundamentals of forward thrust, its production, and the crucial theory needed in the designing process of the LIM.

A rotary motor consists of two parts: the stator and the rotor. The stator is the stationary part of a rotary system which provides a magnetic field. It interacts with the rotor by inducing eddy currents. The crucial parts of the LIM are the windings wrapped around the teeth of the stator core, which serve as the motor's input. The actual stator core comprises the teeth and the yoke. The rotor is the moving component of the motor, and in a rotary motor, the rotor is rotating inside of the stator. A combination of those two parts with an air gap between the two components generates a force. The induced eddy currents produce an equal and opposite magnetic field that is attracted to the source magnetic field produced by the stator. However, as discussed, in a rotary motor, a torque is generated and causes the rotor to rotate.

To generate linear motion, a few changes are required to be implemented to the rotary motor. To create a linear motor, the motor was 'flattened' and 'rolled out' to ensure that the stator and rotor are placed parallel to one another. There are two main considerations concerning the magnetic fields between a rotary motor and a linear motor. The linear motor has continuing air gaps at each end which leads to end-effects. The origins and implication of end-effects are discussed in the section *2.1.1.5 End Effects*. A further difference to consider is that the end rings of a rotor are

no longer present in a linear motor. The rotor is simplified into a solid conductive plate. Therefore, the travelling stator field is distributed continuously. The linear driving force of a linear induction motor is thus the result of the induction of a travelling stator field from polyphase excitation.

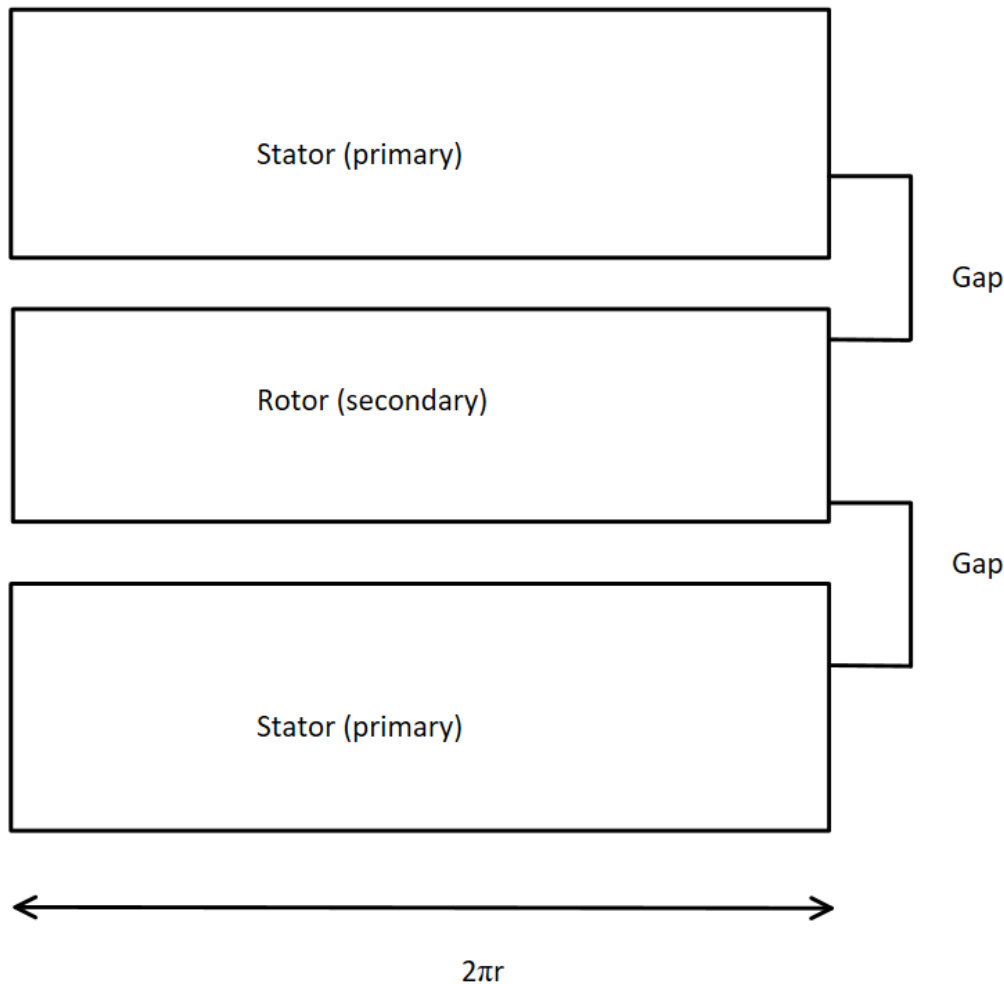


Figure 2.1.1.1.1 flattened induction motor with parallel stator and rotor system

2.1.1.1 Polyphase excitation

Polyphase excitation is an excitation where the input is split among multiple signals of equal amplitude, with varying phase delays. To start an AC input source is approximated using a DC-AC inverter (see section *Electronics*) to produce the desired

sine wave. The sine wave oscillates between its maxima and minima between each cycle. This AC current excites the linear motor producing magnetic fields. The signals from the field interact with the rotor, and as a result of Lenz's law, pulls the rotor resulting in a linear thrust. The thrust is the strongest at the maximum amplitude. In between the maximums the signal is lost, leading to zero thrust. To counteract this phenomenon, the AC input wave is split into 3 with a phase delay of 120° . This change not only prevents the signal loss but, if evenly distributed, also allows the field's maximum to constantly alternate between each input. If the phase delays between the input signals are evenly distributed, a nearly constant travelling field is produced.

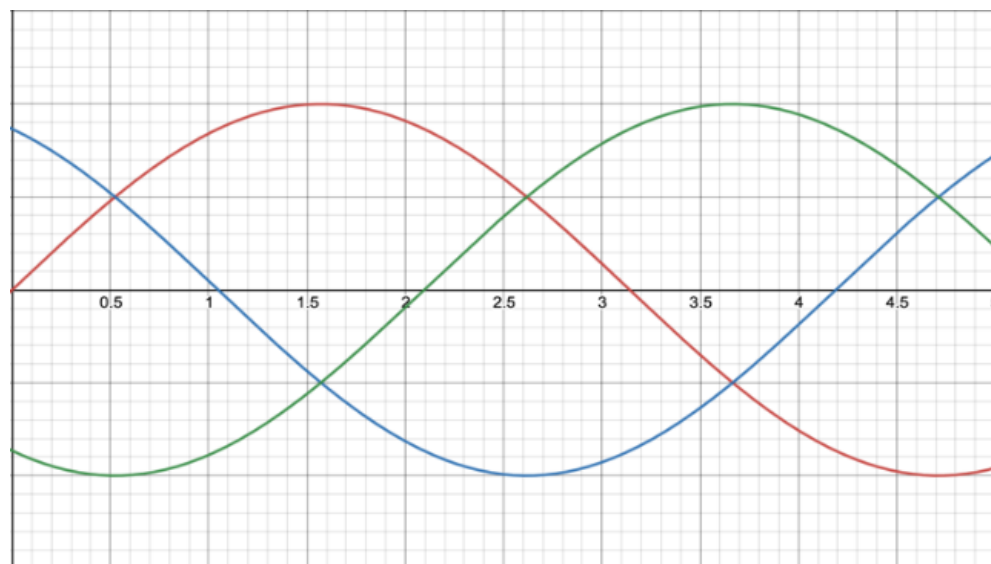


Figure 2.1.1.1.1 Polyphase excitation 3 phase AC

2.1.1.2 Faraday's Law of Induction

Current flows across the coil windings as a result of the varying electric potential. A magnetic field around the coil exists around the coil. A change in the magnetic flux over time produces a current that flows around a coil of windings, which in turn generates an electromagnetic force across the windings. This is Faraday's law of induction which states that the magnitude of the emf induced in a circuit is proportional to the rate of change of the magnetic flux that cuts across the circuit.

$$\varepsilon = - N \Delta \Phi / \Delta t$$

The equation above states that the electromotive force is directly proportional to the number of turns, and the rate of change of the magnetic flux. It is of great importance to notice that the direction of the EMF is negative due to Lenz's law.

According to Faraday's Law, the EMF across the windings causes a corresponding current to flow, which produces the stator magnetic field. Since the excitation originates from a simultaneous 3-phase source, the magnetic field in the stator fluctuates in position and sweeps across the length of the stator.

The flux interacts with the rotor as the travelling stator magnetic field sweeps along the stator. This interaction induces eddy currents according to the Maxwell-Faraday law:

$$\nabla \times E = -\frac{\partial B}{\partial t}$$

The induced eddy currents in the rotor are proportional to the stator's time varying magnetic field. These eddy currents that ultimately generate thrust in the double-sided linear induction motor.

2.1.1.3 Eddy Currents

The eddy currents are induced from the EMF across the stator (as discussed earlier in the section). These eddy currents are crucial to propulsion's design, as they provide the key force for the LIM. The eddy currents induce the magnetic field which allows the pod to accelerate. The magnetic field induced by the eddy current is equal and opposite to the initial magnetic field which induced the eddy current itself. The eddy currents are 3-phase alternating just like the initial current that was applied.

2.1.1.4 Lorentz Force

The Lorentz force relates the magnetic field produced by the eddy current to the mechanical force on the pod. The field produced by the eddy current is marginally slower than the initial field produced by the initial current. The difference is given by the slip. This slip delay is linear and always moving along the stator with the progression of the travelling field. The constant difference between the stator field and induced field of the rotor creates the opportunity for a magnetic force. The Lorentz force of moving particles in a magnetic field is given by:

$$F = Q(E + v \times B)$$

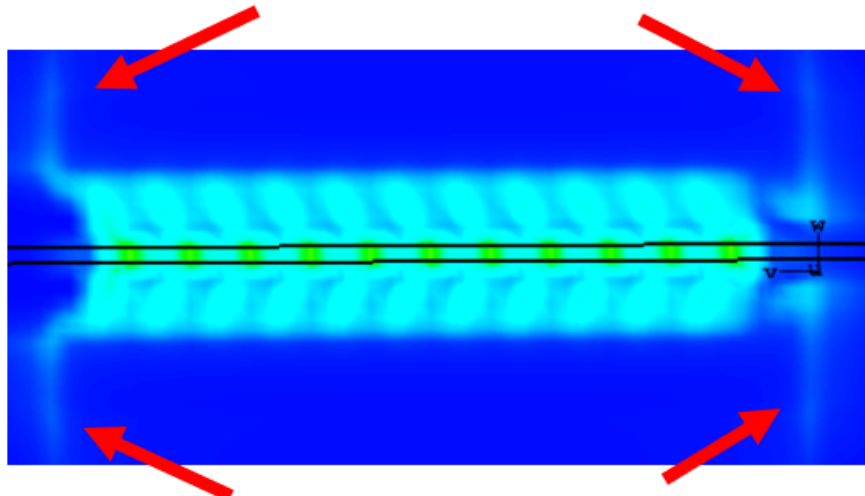
Where F is the force, E is the electric field strength, v is the velocity of the particle, Q is the charge of the particle and B is the magnetic flux.

2.1.1.5 End-Effects:

In a standard rotary induction motor, the rotor (secondary) and stator are circular so the magnetic fields can stay connected, unlike in a linear induction motor where the rotor and stator are unrolled, and the beginning and end of the magnetic fields are unconnected. The relative movement of the stator causes a distortion in the magnetic fields, resulting in longitudinal end effects in the direction of motion reducing the force output of the motor. End effects in other directions are insignificant because the stator will be stabilised in those directions. In the longitudinal direction, there are entry and exit end effects of which only the entry end effects are significant. There are a number of ways to reduce the end effects such as:

- Increasing the frequency of the input current
- Increasing the number of poles in the stator
- Operating in a low slip region
- Decreasing the air gap thickness
- Increasing the stator length
- Increasing the teeth size at the ends of the stator.

However, at low speeds the end effects will not reduce the force output of the stator by a significant amount, so it was deemed that no special changes need to be made to the design.



2.1.1.5.1 Visual representation of end effects from the simulation process

2.1.1.2 Design Process

2.1.1.2.1 Average Force Required

The minimum average force required to accelerate to 50 km/h on a 150m track is determined with an assumption of no air resistance. The force required to overcome air resistance is calculated separately.

The distance over which the pod is accelerated is to be 40% of the track length to allow for the braking distance while still maintaining a safe distance to the end of the track, which is 60m. As the pod starts from rest and accelerating to a target of 50 km/h, the minimum average acceleration can be calculated as follows:

$$v^2 = u^2 + 2as$$

$$a = \frac{v^2}{2s}$$

$$a = \frac{50 \cdot \frac{1000}{3600}}{2 \cdot 60} = \frac{13.8}{120}$$

$$a \approx 1.61 \text{ m/s}$$

This means the minimum average force without air resistance is

$$F = ma$$

$$F = 150 \cdot 1.61 = 241.5 \text{ N (150kg pod)}$$

Therefore, the time t taken to reach 50 km/h is:

$$s = \frac{1}{2}(v + u)t$$

$$t = \frac{2s}{v}$$

$$t = \frac{2 \cdot 60}{13.8}$$

$$t = 8.64 \text{ s}$$

The drag force due to air resistance can be approximated by:

$$F_D = \frac{1}{2} \rho v^2 C_D A$$

For a streamlined half-body, C_D can be approximated as 0.09, where $A = \frac{1}{8}\pi D^2$ and the diameter D of the pod is estimated as 0.7m. This would mean the estimated drag force F_D due to air resistance would be:

$$F_D = \frac{1}{16} \rho v^2 C_D \pi D^2$$

$$F_D = \frac{1}{16} \cdot 1.225 \cdot 13.8 \cdot 0.09 \cdot \pi \cdot 0.7^2$$

$$F_D \approx 2.05 \text{ N}$$

Therefore, the overall minimum average required force to accelerate the pod to 50 km/h over 60m of track is:

$$\text{for } m_{\text{pod}} = 100 \text{ kg: } F = 163.05 \text{ N}$$

$$\text{for } m_{\text{pod}} = 150 \text{ kg: } F = 243.55 \text{ N}$$

$$\text{for } m_{\text{pod}} = 200 \text{ kg: } F = 325.05 \text{ N}$$

2.1.1.2.2 Friction Forces

Relating the thrust force and the eddy current density represented using the following equation:

$$F_{\text{thrust}} = D \cdot dr \int_0^L \text{Re}\{J_z(y, t) \cdot B_x^*(y, t)\} dy$$

Where B_x^* is the flux density conjugate along the motor, J_z is the eddy current density, L is the length of the stator, D is the stator depth and dr is the rotor thickness.

This equation is written as a MATLAB script:

```

function F = ForceProduction(I, N)
%FORCEPRODUCTION Returns initial force production for a given parameters
%   Input parameters are:
%   - I = current (A)
%   - N = number of coil windings per phase per pole

%Initialise parameters
D = 0.05;           %stator width
dr = 0.0105;         %secondary thickness
sigma = 3.99e6;       %rotor conductivity
f = 60;              %current frequency
L = 0.5;             %stator length
tp = L/4;            %pole pitch
vs = 2*tp*f;          %synchronous speed
vr = 0;               %stator speed
w = 2*pi*f;           %angular frequency of wave
g = 2*0.005+dr;        %longitudinal air gap
mu = 1.256665e-6;      %magnetic permeability of secondary
t = 1;                %time

%Calculate initial force production
syms y
B1 = (3.*sqrt(2).*N.*I)./sqrt((pi.*g./mu).^2+(vs-vr) ...
.^2*(sigma.*dr.*tp).^2);
phi = atan(pi.*g./(mu.*sigma.*dr.*tp.*(vs-vr)));

F = D*dr*int(sigma.*B1.^2.*((vs-vr)).*(cos((pi.*y./tp)-w.*t+phi) ...
.*cos(-(pi.*y./tp)+w.*t-phi)-sin((pi.*y./tp)-w.*t+phi) ...
.*sin(-(pi.*y./tp)+w.*t-phi)),y,[0,L]);
end

```

The function is then run in the command window using the following code:

```

>> I = 0:0.5:100;
>> x=[];
>> for i=0:0.5:100
x(end+1)=ForceProduction(i, 25);
end
>> plot(I,x)

```

The following graph is produced relating the inputted current and the thrust force F_D :

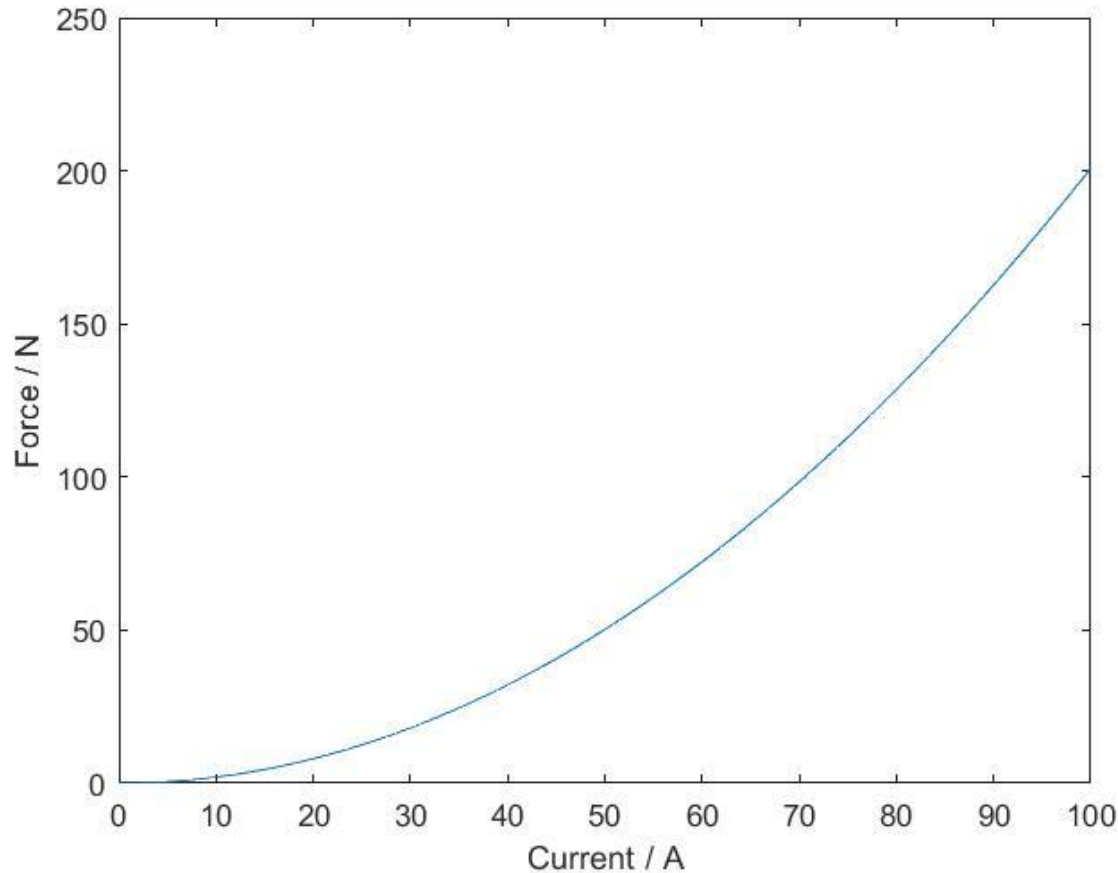


Figure 2.1.1.2.2.1. Thrust force vs Current Input

The outcome of the performed simulation is that the thrust force is maximised when the input current is maximised.

2.1.1.2.1 Proportionality

The following data has been conducted by ETH Zurich (Timperio, C.L., 2018. *Linear Induction Motor (LIM) for Hyperloop Pod Prototypes*. ETH Zurich: Institute of Electromagnetic Fields (IEF)), and was used to set down the foundational parameters of a design of a linear induction motor. These parameters are used in the simulation process to yield the values that are later used to design and manufacture the double-sided linear induction motor for Hyperlink's pod.

Table 2.1.1.2.1.1 LIM Parameters, Effect and Thrust Force

Parameters	Effect on thrust
Air gap	Reducing the air gap between the stator and the I-beam maximises the thrust force.
Active surface area	Increasing the active surface area increases the magnetic flux that passes through the stator and increases the stack width, which increases the thrust produced.
Saturation	Increasing the active surface area reduces the saturation of the iron core. This is useful, as oversaturation leads to an increase in heat, which reduces thrust by the stator.
Turn number	More turns, or coils, produce a larger MMF which increases thrust. However, increasing turn number also increases the voltage induced, which, if not supported by the power source, will reduce the maximum thrust produced.
Slot size	More slots allow for more turns per tooth and approximate the stator close to that of a sine wave, which increases the thrust.
Yoke height	Short yokes make the core oversaturated and may lead to over heating, tall yokes will be heavier and have unused space. The ideal yoke height is equal to the tooth height.
Input current	Passing high current through the windings increases MMF but also heats up the coils, which increases the resistance and drops the thrust. This needs to be taken into consideration in the design process.

From this data, several conclusions were drawn to define some pre-simulation parameters:

- The maximum thrust of the double-sided LIM is determined when the turn number per phase is maximised.
- As the maximum height of the stator is 100mm, the tooth height and the yoke height is 50mm each.
- The tooth width to slot ratio is approximately 1:1, meaning the slot size is 20mm, which will need to accommodate a rectangular winding bundle of the same width. Conservatively, the maximum wire diameter was found to be 3.37mm.

- A copper wire with diameter of 3.37mm has an AWG of 7-8, which has a maximum current load of around 70A at 90°C, which is the approximate temperature of operation, within the predicted operational and safety limits.
- For a 13-tooth design, the stator length is 500mm with 12 slots to accommodate the windings. The maximum width of the stator is limited by the dimensions of the I-beam, allowing for around 50mm of leeway. A bigger width decreases the stator saturation, which maximises thrust, so the width of the stator is maximised to 50mm.
- As a single bulk of iron produces overheating, thin laminations are fixed together instead, to make the stator body.
- A double LIM generates more thrust than a single LIM.
- For the 3 phase AC to generate a moving magnetic field, the different phases must overlap, such that when one bundle has forward moving current, the adjacent bundle has backwards moving current. This results in a simple winding design, which can be reiterated to accommodate the length of the motor:

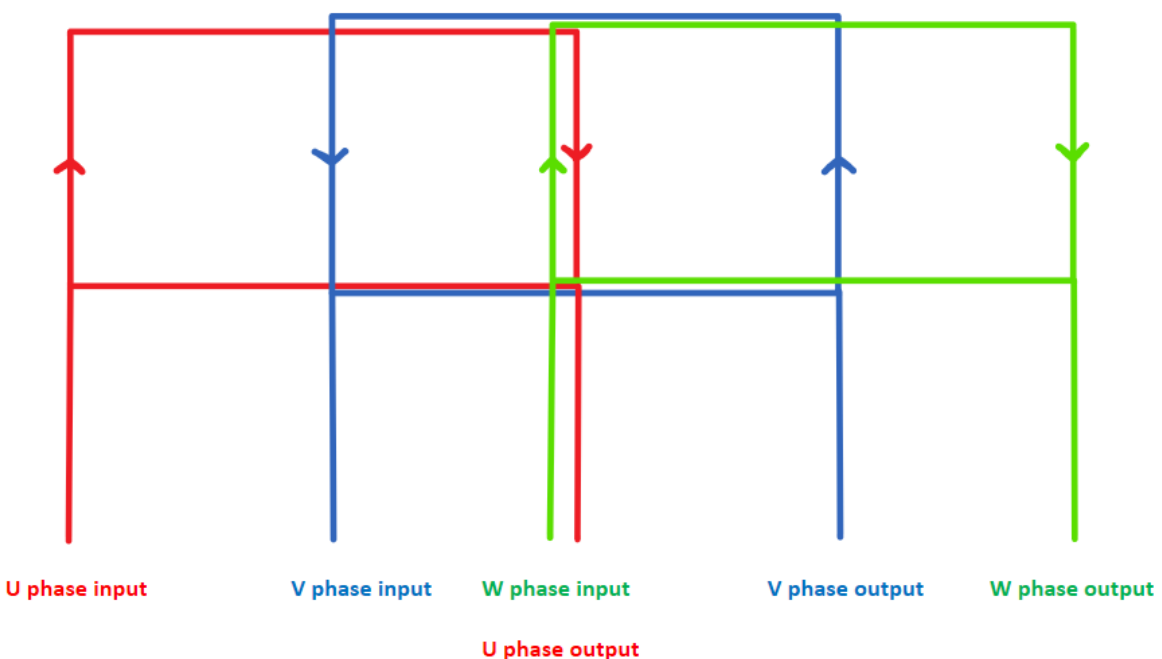


Figure 2.1.1.2.1.13 3 phase wire configuration

These parameters acted as the independent variables in the simulation process, where each variable was constrained optimally to maximise the thrust force.

2.1.1.3 Free Body Diagrams to define load cases for simulations.

The loads on the propulsion system are presented below. The main forces acting on LIM during the pod's acceleration phase are levitation, guidance and thrust. From the parameters discussed in 2.1.1.2.1 *Proportionality*, it's found that a double LIM is the most optimal design. The free body diagrams were constructed accordingly:

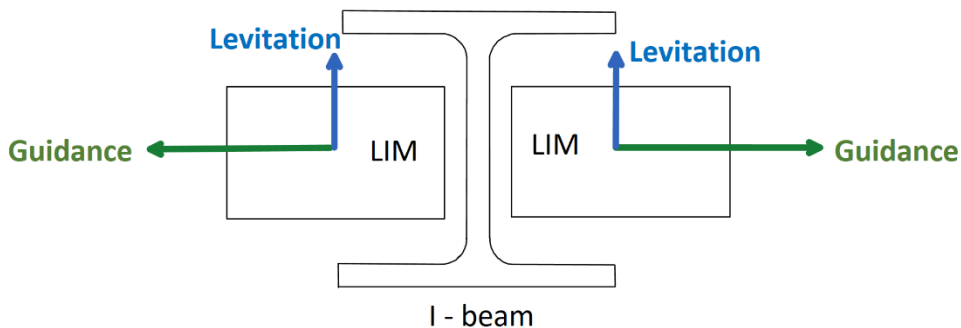


Figure 2.1.1.3.1 Front view of free body diagram of a dual LIM

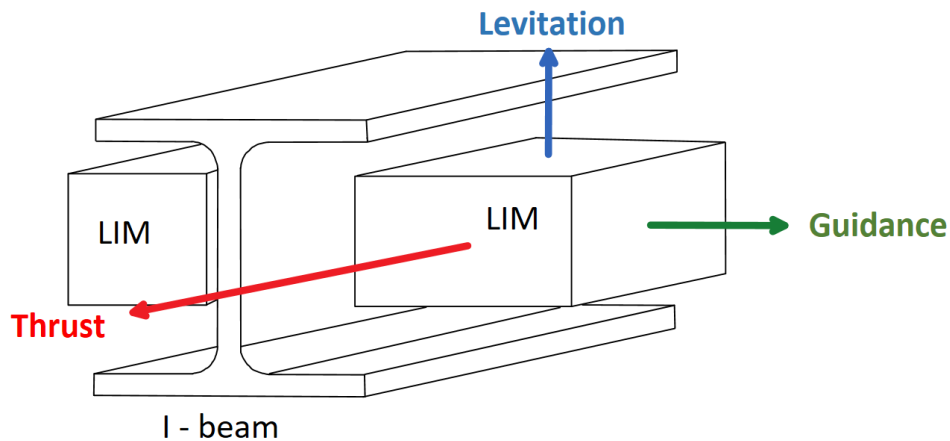


Figure 2.1.1.3.2 Perspective view of the free body diagram of the dual LIM

2.1.1.4 Simulations Validating the Theory & Results Analysis

2.1.1.4.1 Simulation Process

To determine the optimal parameters of the stator and windings, a control simulation is performed and a number of parameters are varied in a range to determine their impact on the thrust force. The parameters chosen to be varied were

the air gap, number of windings, input voltage and the ratio between the teeth width and the gaps between them.

The simulation process is run in CST Studio using the Statics/Low Frequency application area and the Electromechanical Devices workflow. The workflow automatically sets the background and boundary conditions and M-Static solver to reasonable values for a linear induction motor.

To model the stator, a cross-section is drawn and then extruded. The coils are modelled by extruding a cross-section along a path curve and then copying the coils to their positions on the stator. The coils are modelled at an angle to the horizontal to reduce the guidance force the linear induction motor produces. The secondary is modelled as an extruded cross-section similar to the stator.

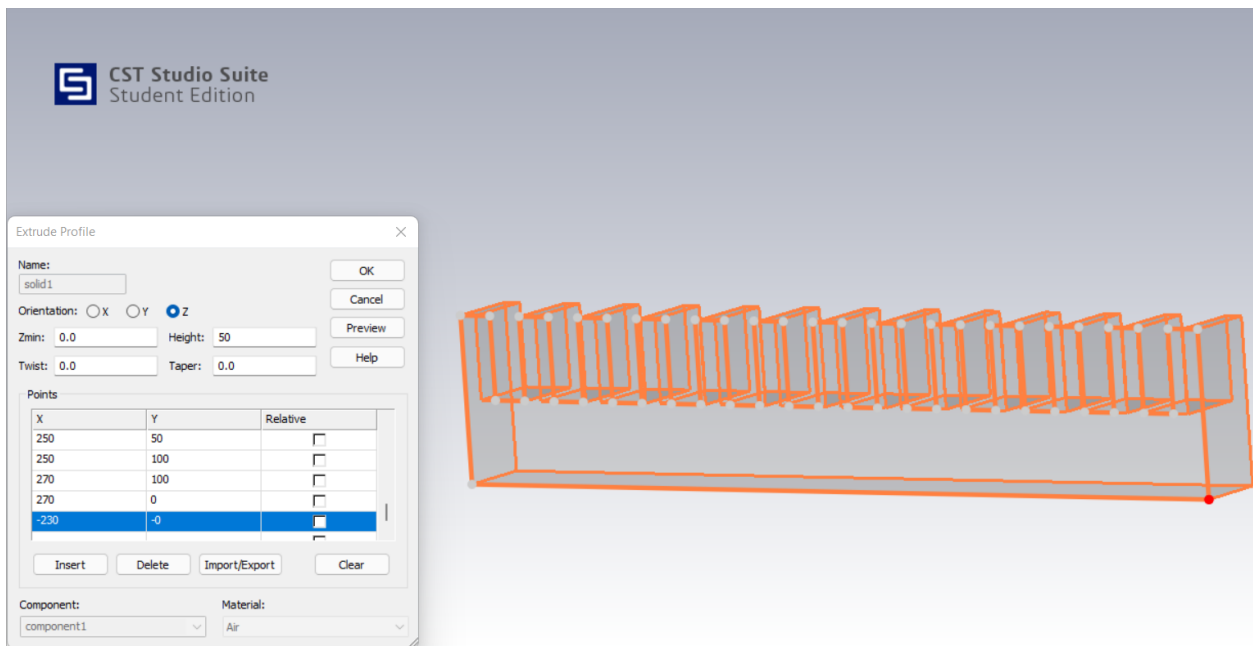


Figure 2.1.1.4.1.1. Modelling Stator



Figure 2.1.1.4.1.2. Modelling Coil

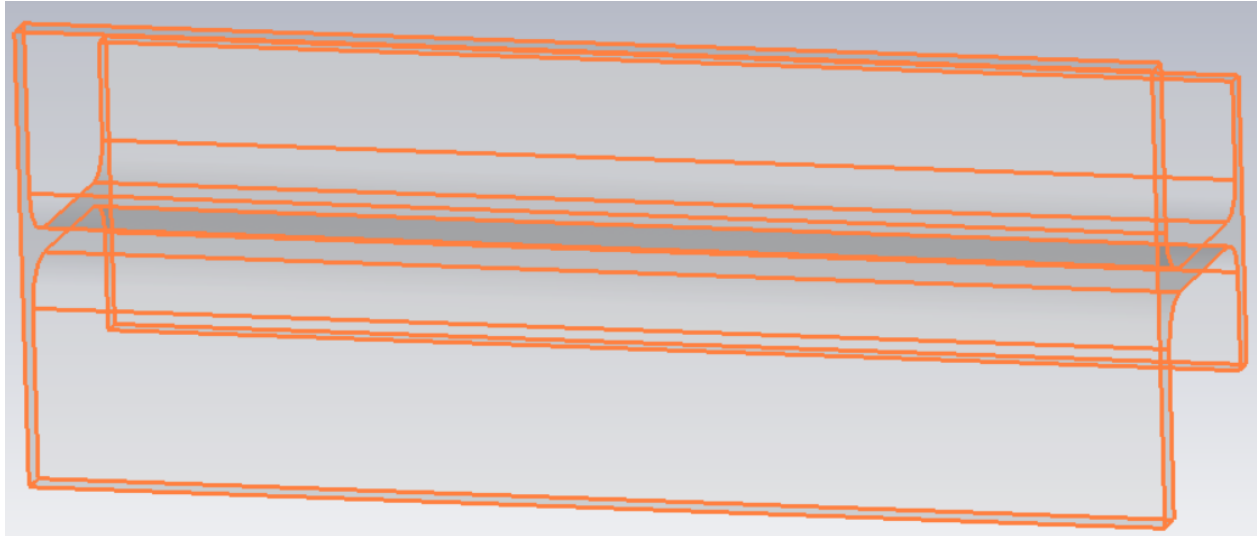


Figure 2.1.1.4.1.3 Modelling Secondary

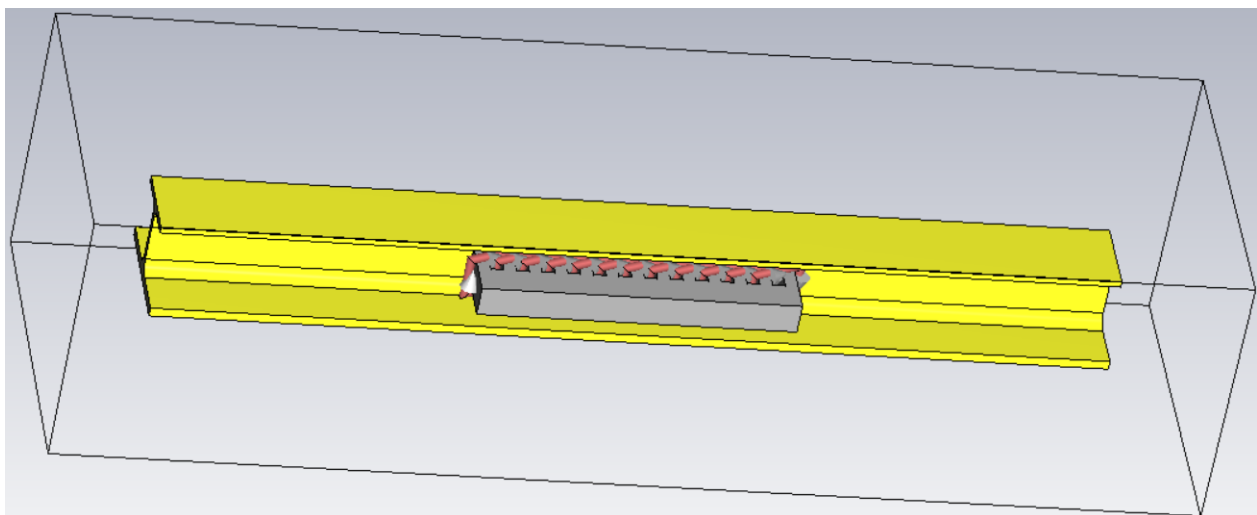


Figure 2.1.1.4.1.4 Modelling Full Simulation

The materials chosen for the parts of the model are Steel-1008 for the stator, Aluminium 6061 T6 for the secondary and annealed Copper for the coils.

Table 2.1.1.4.2 The Electrical and Magnetic Properties of the Materials Used

	Steel-1008	Aluminium	Annealed Copper
Electrical Conductivity (S/m)	7.7×10^6	10^7	5.8×10^7
Young's Modulus (GPa)	200	69	120
Density (kg/m ³)	7870	2700	8930

Once the model is completed, the solver is run which computes the magnetic field strength and magnetic flux density in and around the model. The forces produced on the parts of the model are then calculated in the Post-Processing section of the software. For each variation of the model, the solver and forces have to be recalculated.

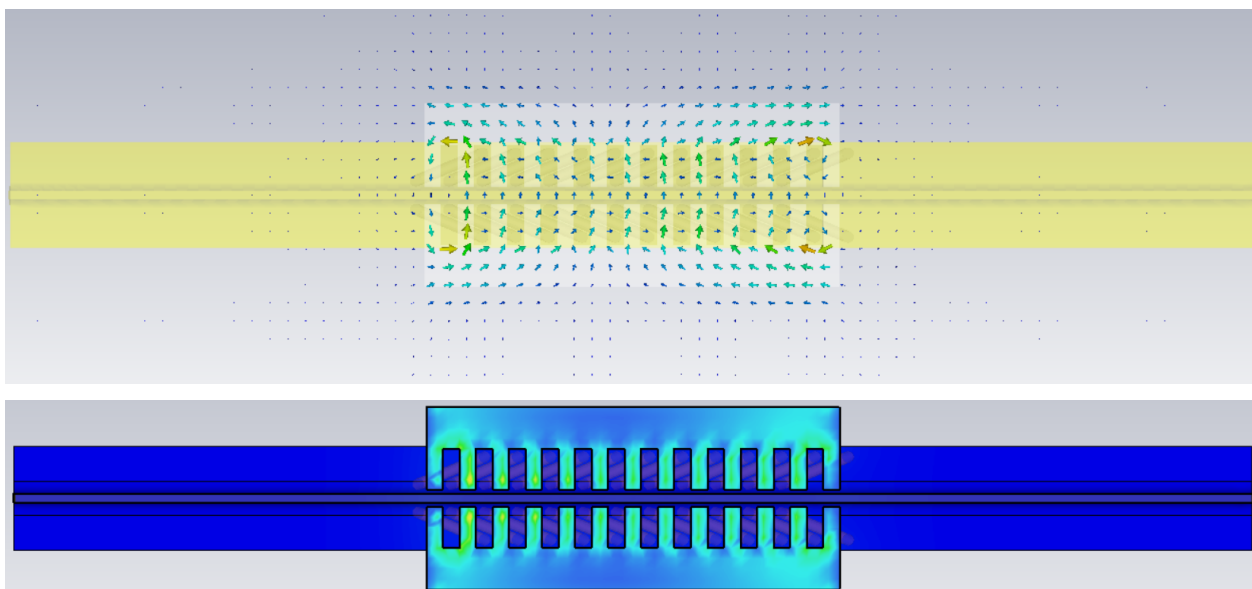
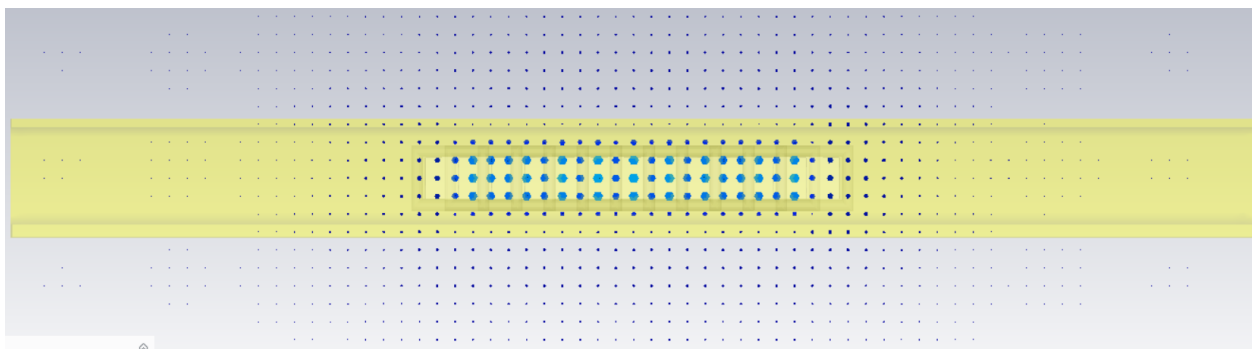


Figure 2.1.1.4.1.5 B-Field Vectors and Contours Z-Cut



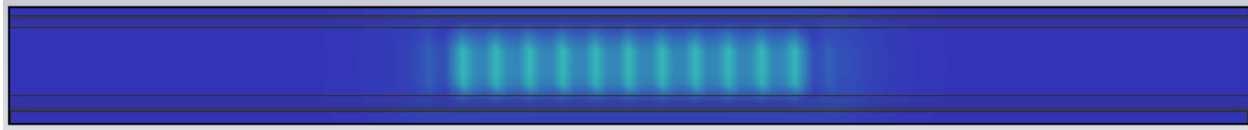


Figure 2.1.1.4.1.6 B-Field Vectors and Contours Y-Cut Secondary

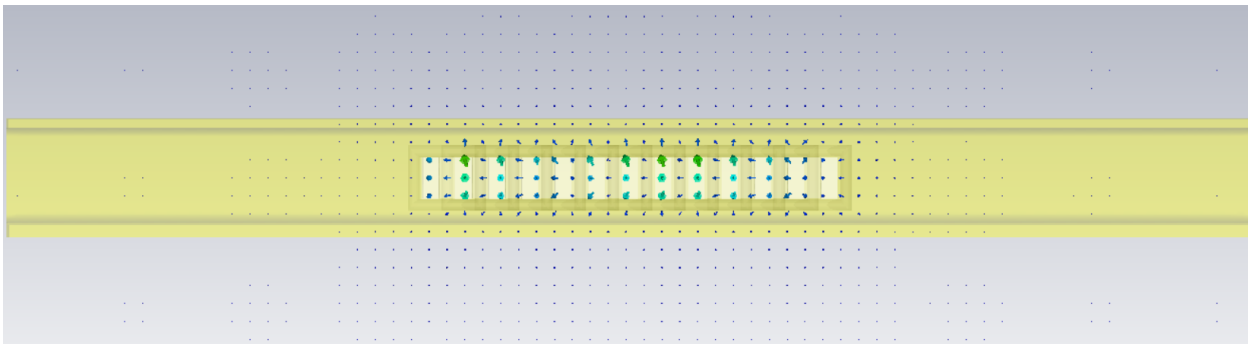


Figure 2.1.1.4.1.7 B-Field Vectors and Contours Y-Cut Teeth

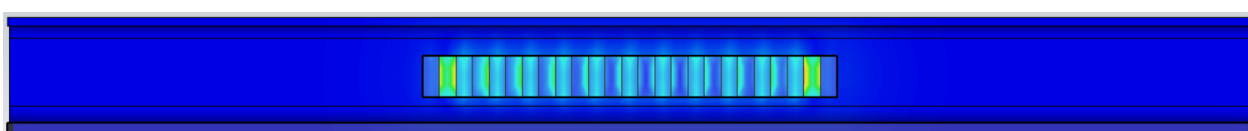
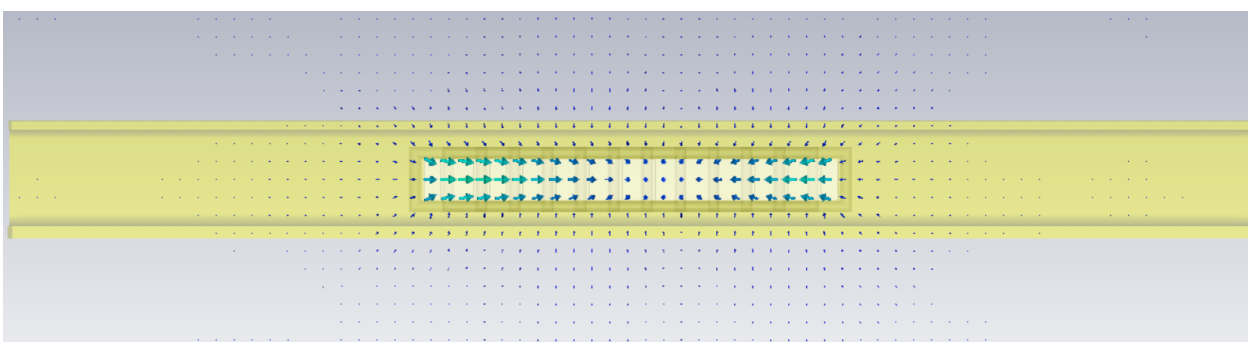


Figure 2.1.1.4.1.8. B-Field Vectors and Contours Y-Cut Yoke

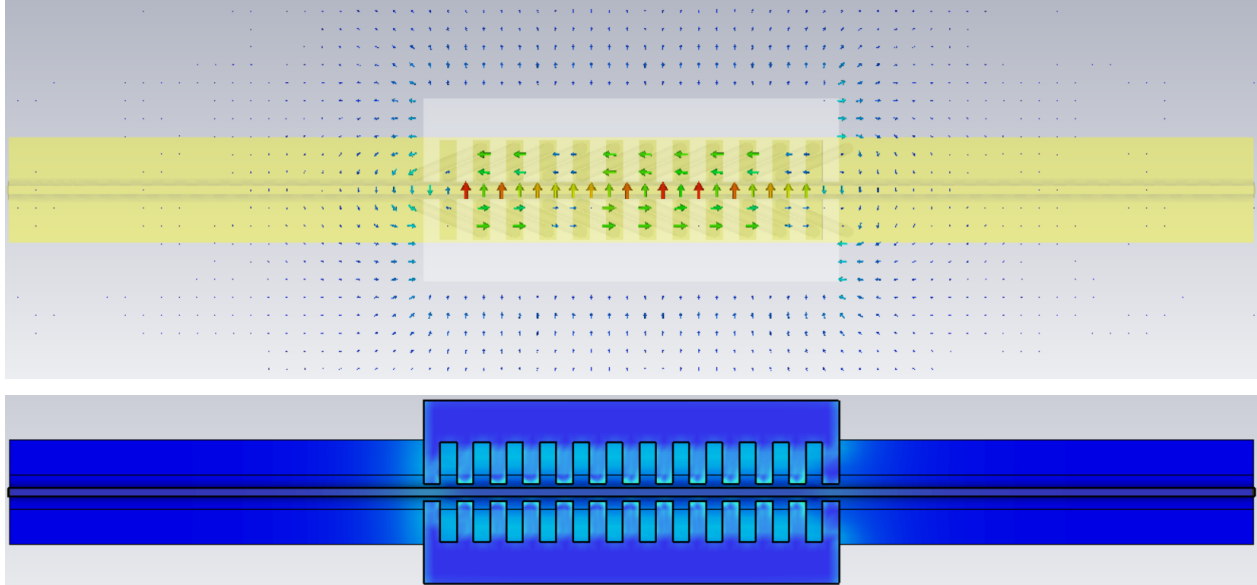


Figure 2.1.1.4.1.9. H-Field Vectors and Contours Z-Cut

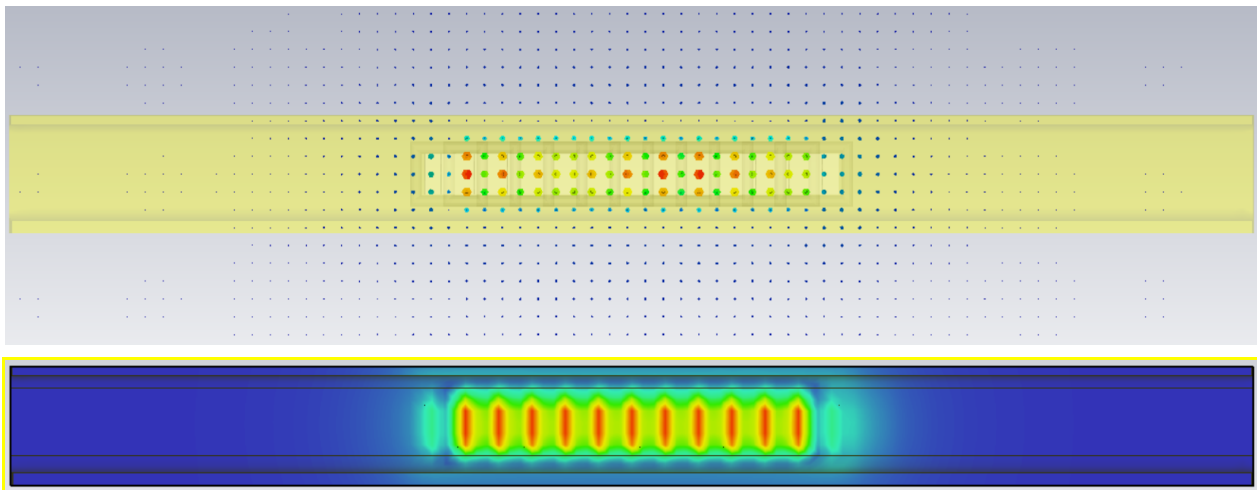
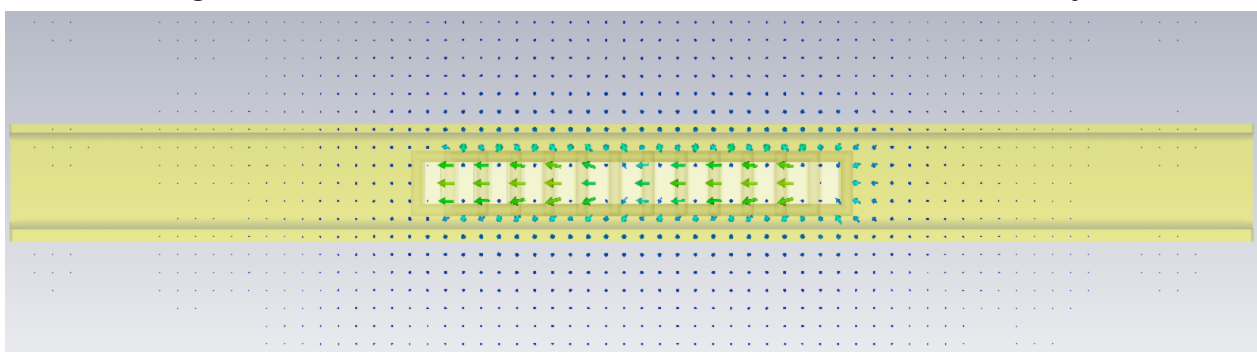


Figure 2.1.1.4.1.10 H-Field Vectors and Contours Y-Cut Secondary



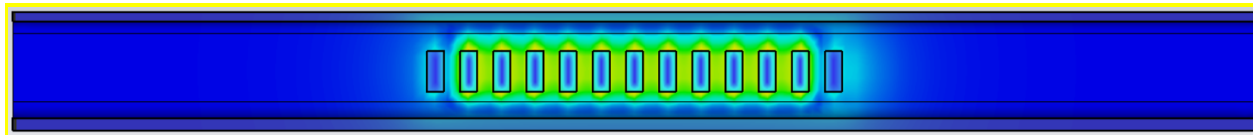


Figure 2.1.1.4.1.11. H-Field Vectors and Contours Y-Cut Teeth

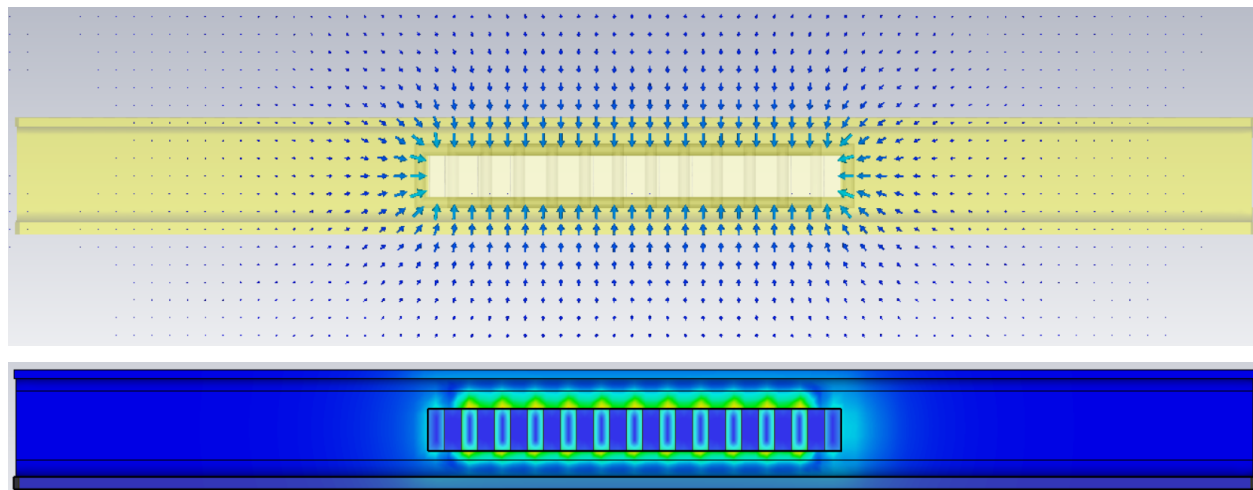


Figure 2.1.1.4.1.12. H-Field Vectors and Contours Y-Cut Yoke

The following data is obtained from the simulation process. Each parameter is set as an independent variable, with the H field, B field and thrust force being the dependent variables. The control variables are established as follows.

Table 2.1.1.4.3. Control Variables

Control Variable	Value
Gap width (mm)	10
Width of stator (mm)	50
Length of stator (mm)	500
Voltage input (V)	48
Current input (A)	10
Turn number	25
Tooth to Slot size ratio	1
Arrangement	Double
Rotor	I-beam

The first test measures how altering the number of windings changes the dependent variables:

Table 2.1.1.4.4. Simulation Data for Number of Windings

Number of windings	H field [A/m]	B field [Vs/m^2]	Thrust [N]
10	45441	0.317	-21.692
25	90857	0.622	-86.93
50	227000	1.29	-544.2
75	341000	1.81	-1223.2
100	459000	2.15	-2108.3

The same was done for voltage input:

Table 2.1.1.4.5. Simulation Data for Voltage Input

Voltage [V]	H field [A/m]	B field [Vs/m^2]	Thrust [N]
10	23673	0.163	-5.8722
20	47334	0.33	-23.54
50	118000	0.789	-147.47
80	189000	1.12	-337.84
100	236000	1.33	-590.51

For the air gap between the stator and the I beam:

Table 2.1.1.4.6. Simulation Data for the Ai Gap [in mm]

Air Gap [mm]	H field [A/m]	B field [Vs/m^2]	Thrust [N]
10	73408	2.04	-81.493
15	114000	0.761	-135.9

20	91489	0.735	-105.53
40	84446	0.641	-43.306
60	82200	0.612	-25.5624

And for the tooth to slot size ratio:

Table 2.1.1.4.7. Simulation Data for Tooth-to-slot-size Ratio

Tooth to Slot size ratio	Thrust [N]	H field [A/m]	B field [Vs/m²]
1/3	-94.103	109000	0.64
1/2	-107.46	109000	0.856
1	-112.66	103000	0.663
2	-125.27	182000	2.58
3	-134.25	244000	2.47

2.1.1.5 Dimensioning process

The thrust force is calculated for three different potential masses of the pod, and the time taken to reach the desired speed of 50km/h is calculated using basic SUVAT equations. Air resistance is then taken into account, and three final overall thrust forces are generated. These acted as the guideline for propulsion simulations, as the thrust generated by the motor must be larger than these theoretical values.

Using the MATLAB script to compute the eddy current density equation, it is found that the thrust force and input current have an almost exponential relationship, meaning the current should be set as high as possible while falling within the safety constraints.

From the proportionality section, a few key thrust altering parameters are identified i.e. the number of turns, voltage input, gap width and tooth to slot size ratio. These parameters act as independent variables in the simulation process, and raw data is collected to identify the optimal values of these parameters which maximises the

thrust force. Other parameters, such as stator width, are dimensionally constrained to the EHW regulations, and are not to be varied to test their effect on the thrust force.

The following section is an analysis of the data obtained from the simulation process.

2.1.1.5.1 Data analysis

Number of windings

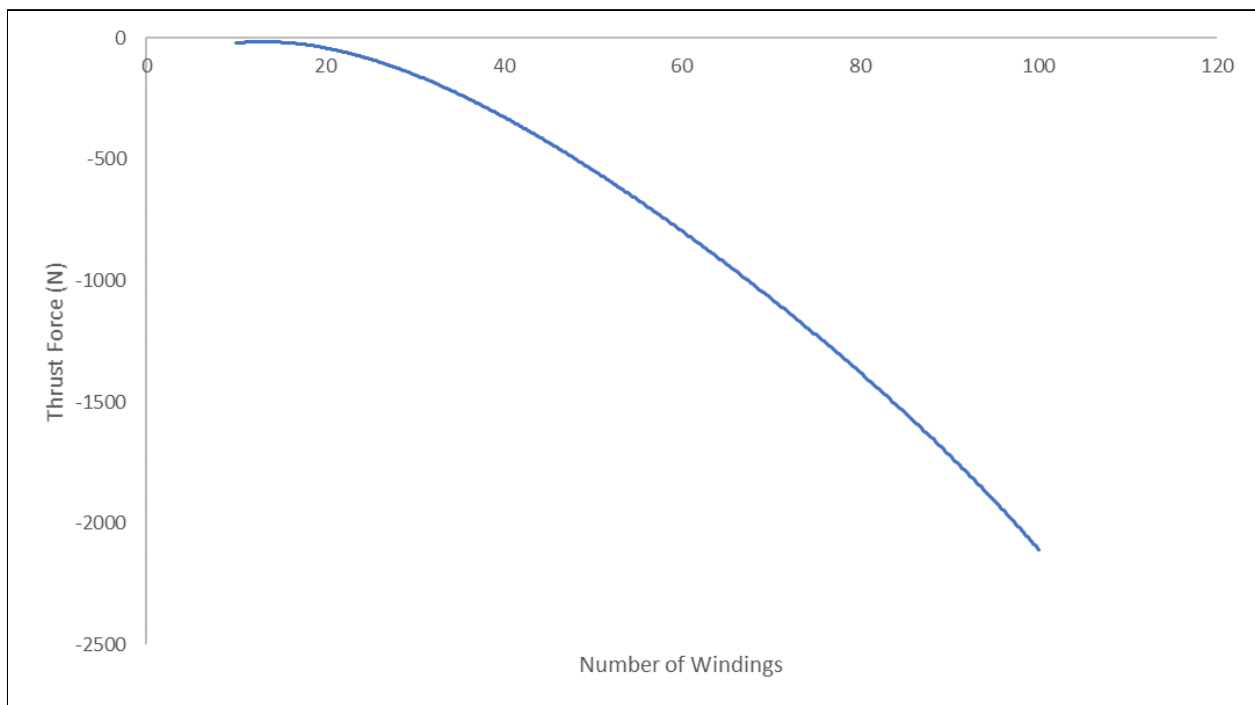


Figure 2.1.1.5.1.1. Thrust Force vs Number of Windings

The number of windings is the number of coil turns over two teeth and one slot. The winding number is varied by varying the coil number in every bundle against control variables. The results show an almost exponential relationship between turn number and thrust force, with the data being trendlined by a polynomial function of order 2. That being said, there does exist a physical constraint due to the slot size being 20mm; the maximum number of windings is only limited by the dimensions of the stator. Consequently, the ideal number of windings is optimally constrained to the size of the stator, which, after experimenting with the prototype, was found to be 35 windings.

Voltage input

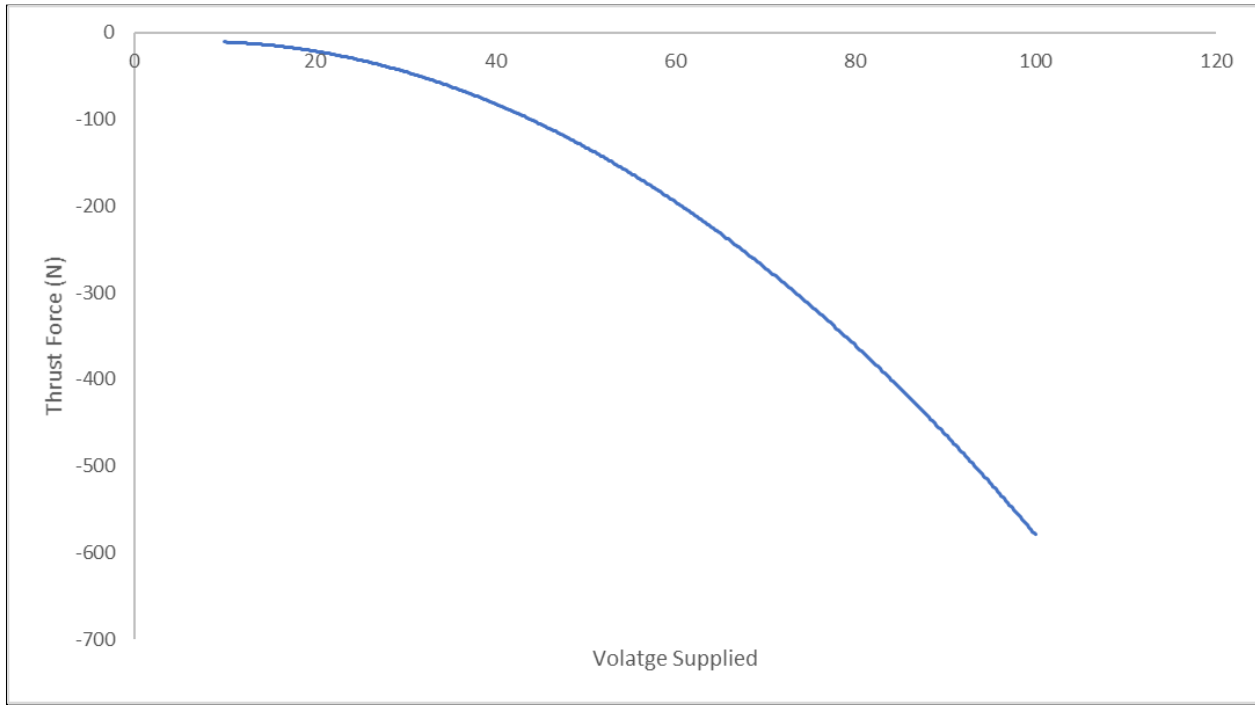


Figure 2.1.1.5.1.2 Thrust Force vs Voltage Supplied

The voltage is varied against control variables. The trend demonstrates that the thrust force is maximised as the voltage is maximised. However, the voltage is constrained by safety regulations, as a very high voltage input, while generating a high thrust force, will not only be energy demanding but also hazardous. The voltage must be optimally constrained to the maximum voltage that is within the safety regulations, which was found to be around 48 V.

Air Gap

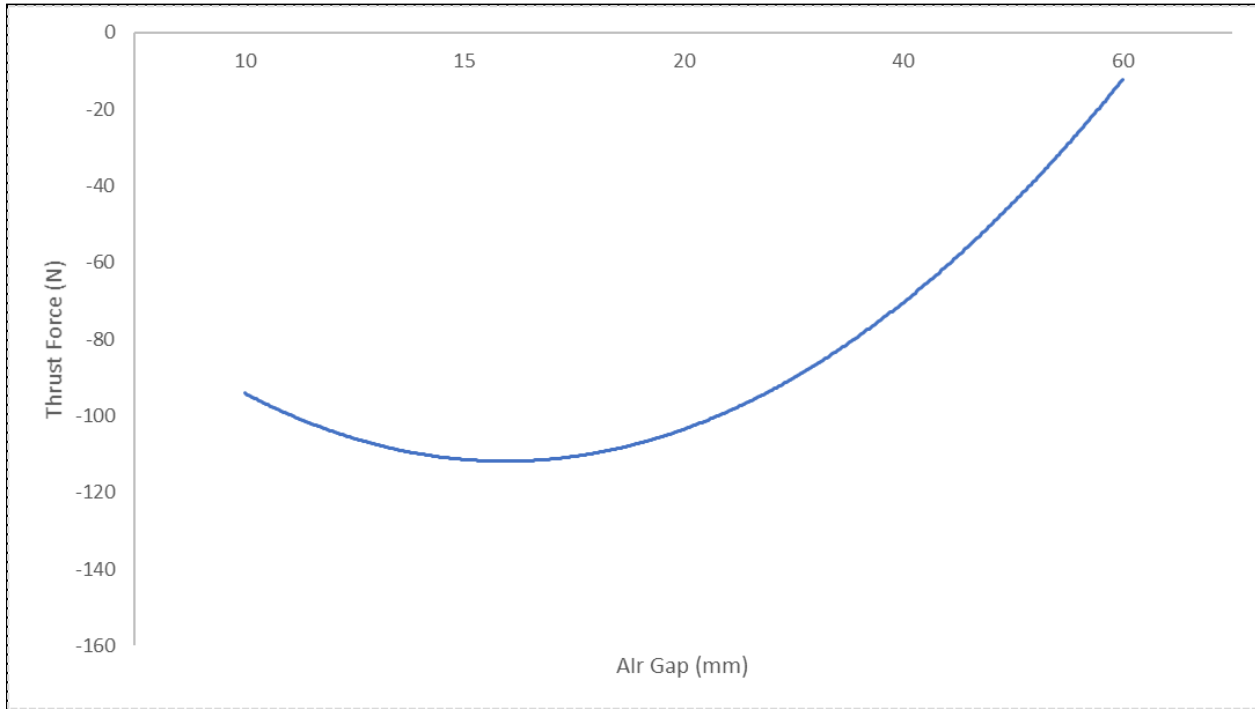


Figure 2.1.1.5.1.3. Thrust Force vs Air Gap Width

Air gap is the gap between the stator and the I beam. The data, being trendlined by a polynomial function of order 2, demonstrates a global maximum at around 15mm.

Tooth to slot ratio

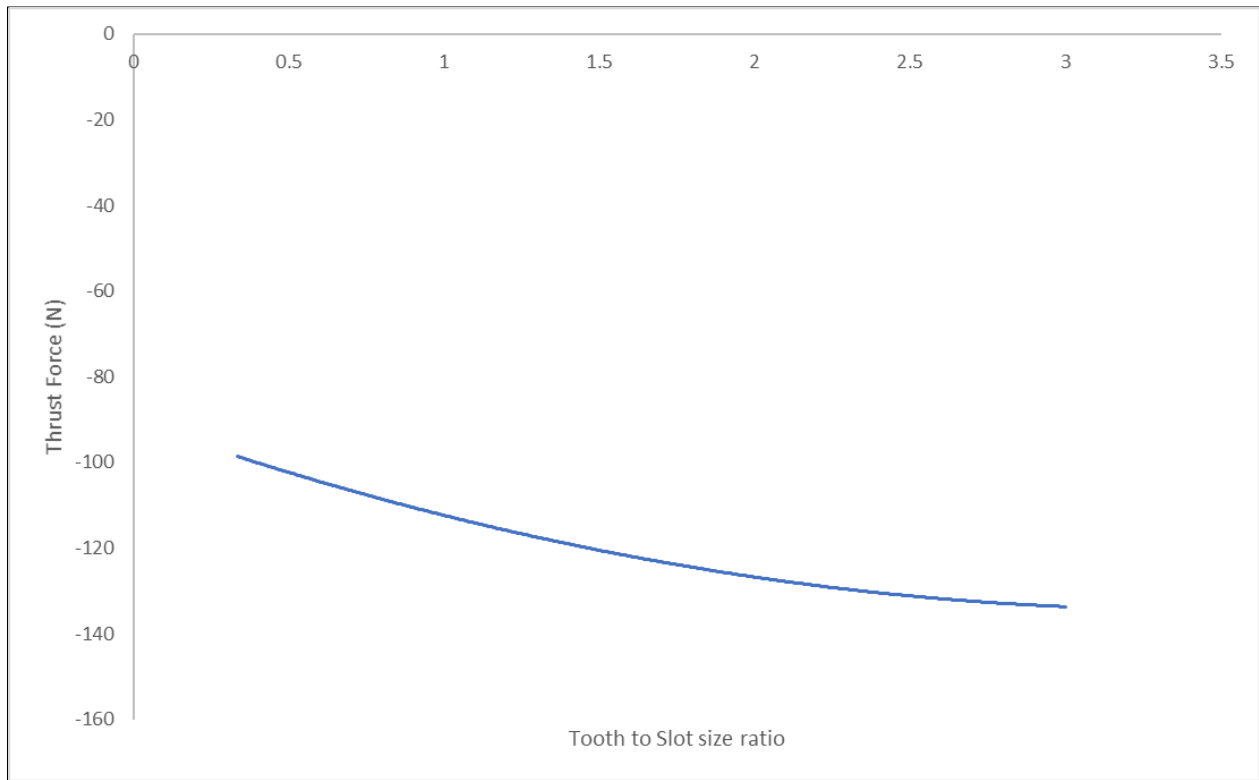


Figure 2.1.1.5.1.4. Thrust Force vs Tooth-to-slot ratio

This graph suggests that, with an increase in tooth to gap ratio, the thrust force is increased. However, increasing the tooth width will by default decrease the gap size, as the length of the stator is constrained to 500mm. This is problematic, as decreasing the gap size will reduce the maximum number of coil turns. Since the gradient of the polynomial function of the turn number is significantly greater than that of the tooth to slot ratio function, trading off a larger slot gap to accommodate more coil turns will result in the maximum thrust force produced.

Consequently, the tooth to gap ratio will be established as 1.

From these results, the final dimensions of the stator are concluded in the following table.

Table 2.1.1.4.8 Final Dimensions of Stator

Variables	Values
Stator tooth number	13
Stator slot number	12
Tooth height	50mm
Tooth width	20mm
Slot width	20mm
Slot to Tooth ratio	1
Stator material	Stainless Steel
Winding material	Copper
Winding diameter	2mm
Winding total length	50m
Winding per tooth	35
Winding per phase	420
Gap width	15mm
Input voltage	48v

Having obtained these results, the manufacturing process is initiated.

2.1.1.6 Manufacturing Processes

2.1.1.6.1 Manufacturing of the stator

Manufacturing the stator was performed in-house in the MakerSpace laboratory at Queen Mary University of London. The premise was to combine multiple thin sheets of the stator together with an epoxy. The epoxy is selected to be not conductive, so its function is to withstand high temperatures. The metal sheets for the stator are designed as specified in the section *2.1.1.5 Dimensioning Process* and outsourced to our sponsor, Slovas company. The company used cutting with a pulse plasma machine to obtain 35 2mm stainless steel sheets. The sheets were roughened to key

the surface to increase the adhesion of the epoxy. The stator sheets came ready-to-use, so they did not require any additional in-house machining.



Figure 2.1.1.6.1.1 Stainless Steel Stator Sheets received from manufacturer

For the manufacturing process of the LIM, the stator steel sheets are placed and fixed on a tray to ensure that the stator maintains its shape with the addition of each new layer. This tray consists of a wooden plank with metal rods that are positioned to keep the stator firmly in place while the epoxy is applied. Thus, an even spread of epoxy is achieved between each layer.

To aid the evening out of the epoxy, thin slices of polycarbonate were placed along the stator in a fixed pattern. The epoxy was then applied in a grooving pattern to maximise surface binding. The sheets were pressed together with a vice to ensure an even, constant load was exerted unto them. This procedure is repeated 25 times, until completion of the stator build.

2.1.1.6.2 Manufacturing of the coils

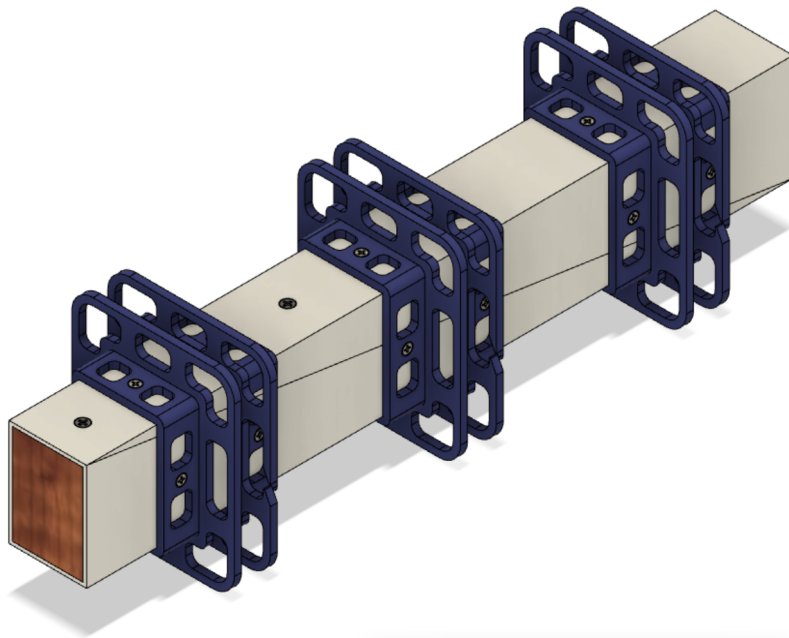


Figure 2.1.1.6.1.2. CAD model of winding loader with stoppers and acrylic coating

The main principle when formulating the desired coil configuration is to firstly, determine the accurate coil thickness, cross-section of winding, construct coil windings, and then apply them onto the stator. In the first step, a long block of wood is dimensioned and finely cut to match the dimensions of three stator teeth (two teeth and one slot), which are 50mm x 60mm. Then, the wire is wrapped around the block, as it is dimensionally equivalent to the stator.

Then, the block is cut diagonally, to allow for the coils to be easily removed from the wood. This is vital, as the pressure exerted on the wood by the coils is high, making the process of sliding the coils off the wood difficult. To accommodate this, PMMA is bonded using Tensol 12 Plastic Acrylic onto each side of the wood, to decrease the coefficient of friction of the block. The added thickness of the plastic made the dimensions of the coils 2mm bigger than the dimensions of the actual winding configuration. However, this is an advantageous, as the clearance is increased with a minimal effect on the induction.



Figure 2.1.1.6.1.3. Prototype winding loader

The stoppers presented on the figure above were 3D printed to keep the coil thickness down to a maximum of 20mm, which are placed at an even distance away from each other. The stoppers are drilled into position to restrict coil movement. Then, the bundle of coils is wrapped between each pair of stoppers 35 times. In the next step, the wire is wrapped around the space between the adjacent stoppers 3 times, to act as mediator between each bundle. This procedure is repeated 4 more times for one phase, and a total of 12 times for 3 phases. The coils are held together using adhesive tape to avoid their shape from deforming.

2.1.1.6.3 Combination of stator and coils

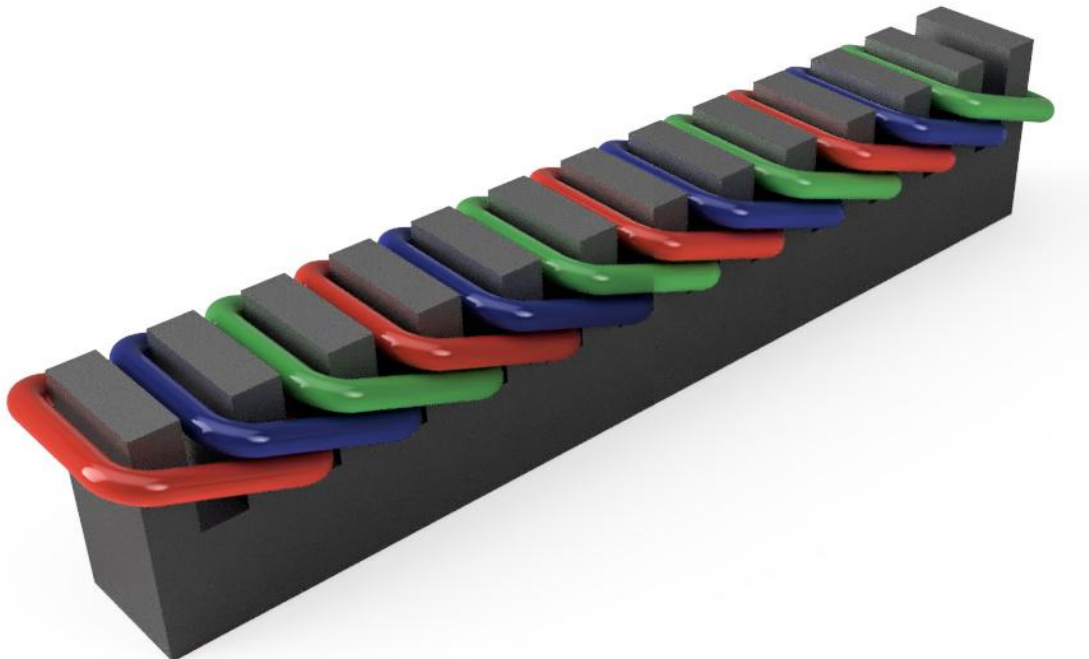
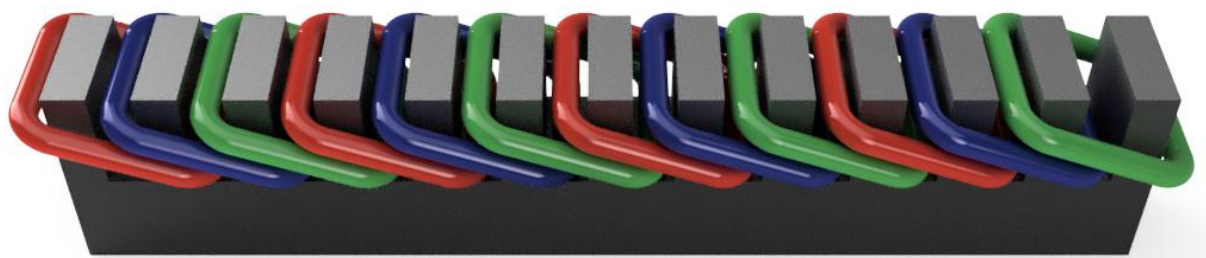
As described in the previous section, having the stator ready, and the coils bent to the correct dimensions, the windings are slid into the correct positions. First phase is slid on, then the second, then the third, up to the last winding. The input wires are set to be on one side of the motor, and the output wires are grounded on the opposite side.

All the steps presented in section 2.1.1.6 Manufacturing Process are repeated for the construction of the second linear induction motor, as the pod is designed to operate

with a Double-sided LIM. Therefore, the two motors act as mirror opposites of one another.

2.1.2 Size, Components, Appearance

2.1.2.1 Evidence of CAD models



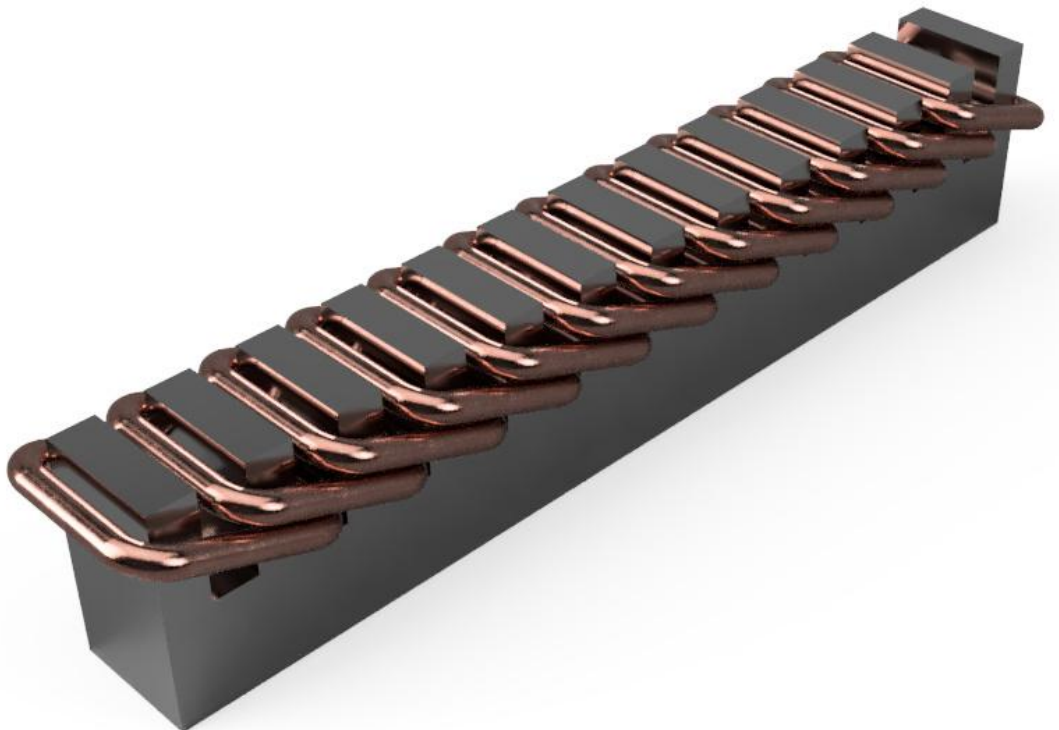


Figure 2.1.2.1.1. 3x Propulsion CAD Models

2.1.2.2 Technical Drawings

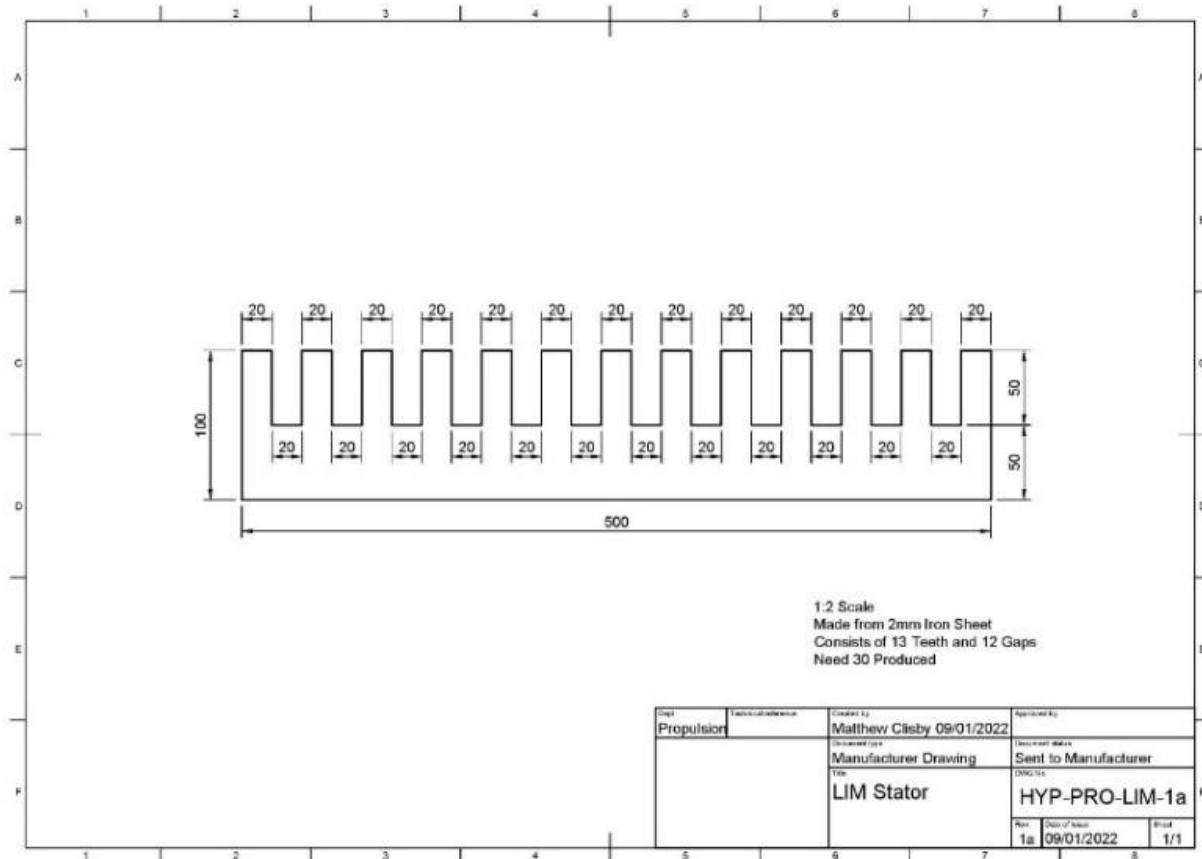


Figure 2.1.2.2.1. Engineering Drawing of a LIM's Stator Sheet

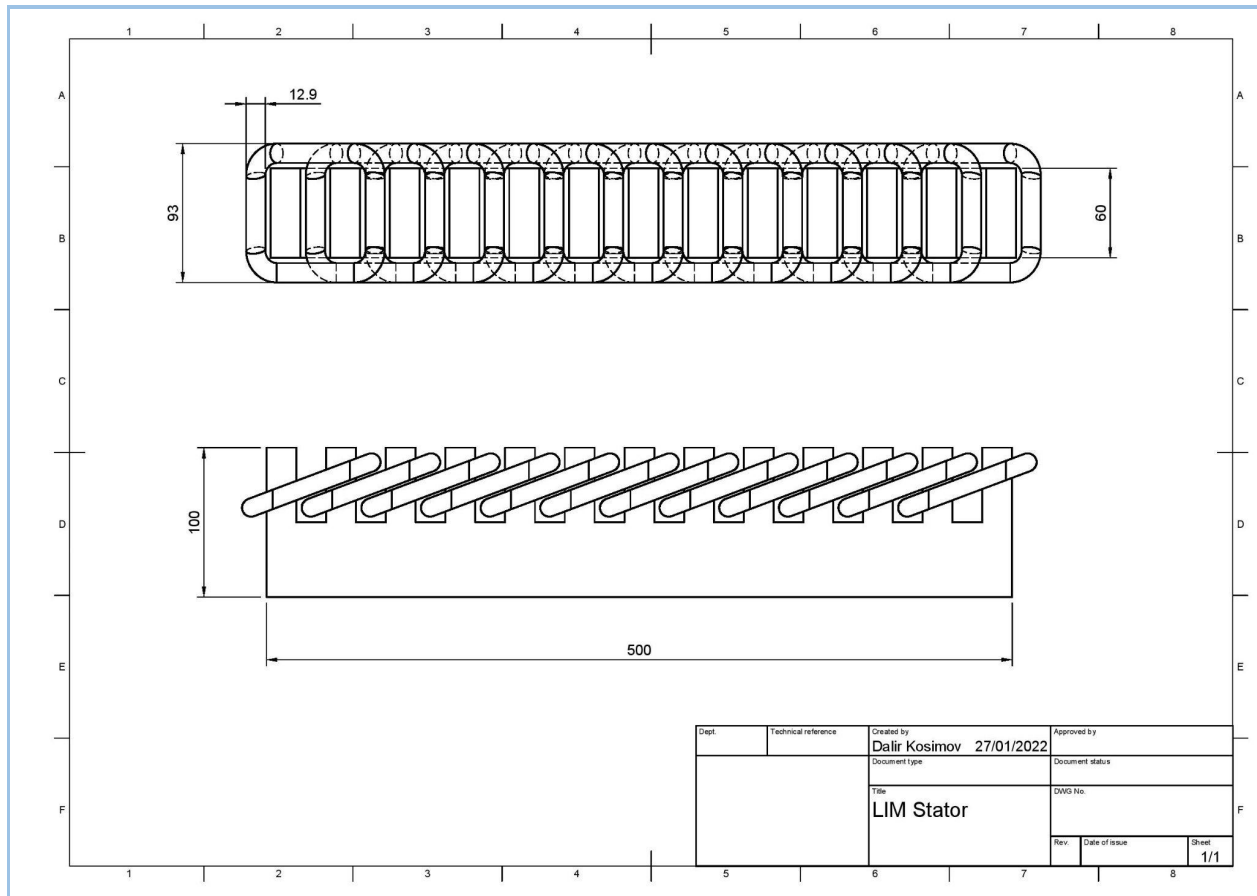


Figure 2.1.2.2.2. Engineering Drawing of a LIM's Stator with Coils

2.1.3 Integration into a Subordinate Structure/System

A special mounting fixture is designed on which the two linear induction motors can be safely attached and then bolted into the frame of the pod. These fixtures are made of Aluminium and have been subjected to simulations to ensure the motors stay in their expected positions at all times while also being light and easy to manufacture. Simulations for the propulsion mounting fixture are represented and analysed in the 2.4 Structures section.

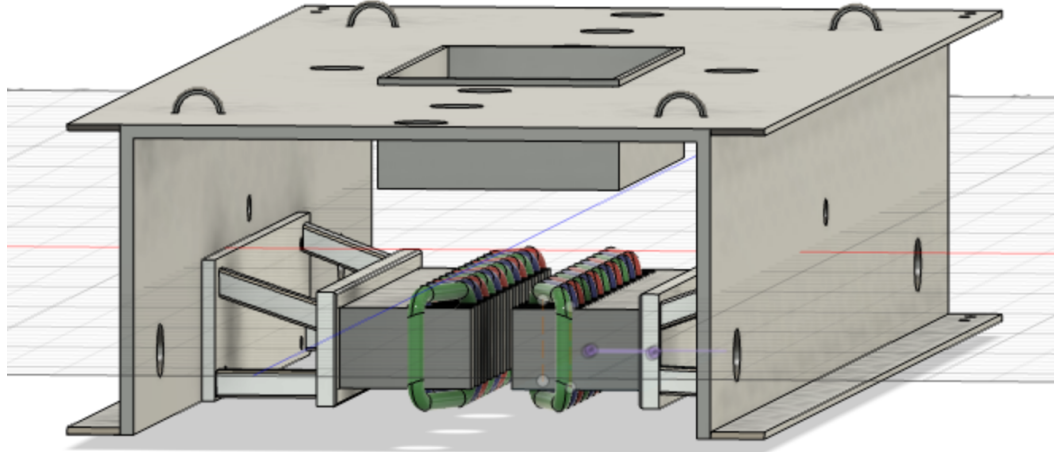


Figure 2.1.3.1. LIM's mounted on the frame

2.1.4 Demonstration Plan

2.1.4.1 Parts List

Table 2.1.4.1 Parts List of Double-sided LIM

Component	Quantity	Dimensions	Mass	Created
Stator	1	500x100x50mm	18kg	In-House
Coil Windings	3	37m x 2mm	1kg	In-House

2.2 Braking

2.2.1 Technical Description of the System

2.2.1.1 Theory and principle physics of desired functionality

Braking is a crucial part of the hyperloop system. It is intended to safely stop the pod both, in normal and emergency situations. The system was designed as a pneumatic braking system which generated a maximum braking force of 7.5kN. The main components of the brake system are, air reservoirs, pneumatic cylinder, brake spring,

brake pads, ball valves. All components are described in the further section of 2.2 *Braking*.

The pod is equipped with two braking systems: a primary and a secondary. The primary braking system is the main braking system of the pod used in the braking scenario I. The secondary braking system acts as an emergency braking system and is engaged in braking scenarios II and III.

Table 2.2.1.1.1. Braking Scenarios

Braking Scenario	Braking Systems Engaged	Description of the scenario
I	Primary	Normal demonstration, no emergency
II	Primary and Secondary	Emergency braking, provided primary braking is fully functioning
III	Secondary	Emergency braking in case of primary brake failure/malfunction

The pneumatic brake system is a type of braking system that utilises compressed air to produce braking force. The braking system consists of a series of valves and chambers that respond to a logic of pneumatic and mechanical interactions. Control valve is a component that controls the air flow throughout the pneumatic network. The chambers, on the other hand, are identified as the air reservoir and the pneumatic brake cylinder. These are connected to each other through small ducts in the control valve. The air reservoir is responsible for storing the air that is used to feed the brake cylinder in the brake application.

The brake cylinder is a pneumatic actuator that transforms the air pressure into brake force (potential energy into mechanical energy). Air has a natural tendency to move from a region of high pressure to a region of low pressure. This characteristic has been exploited within the braking system design to remove the need for a compressor. Pressurised air inside the air reservoir moves to the low pressure chamber of the brake cylinder where it pushes onto the piston.

The main components of the pneumatic braking system are:

- Air reservoir
- Brake cylinder

- Brake spring
- Brake pads
- Ball valves
- Fittings and Pipes
- Solenoid Control valve
- Brake Spring

The brake is engaged by default as a result of the preloaded spring fixed to the brake cylinder and control valve's default configuration. A puller brake cylinder was selected to work against the spring to disengage the brake when the cylinder is pressurised. An active input from the battery and electronics is required to disengage the braking system. The spring pushes the brake pad onto the I-beam to provide the normal reaction force necessary to generate a decelerating frictional force.

The air reservoir is charged by an external compressor of up to 10 bars. The maximum operational limit of the reservoir is 16 bars so the operation is within the safety region. When pressurising the air reservoir, readings from the pressure sensor are taken in order to control the rate of the pressurisation. A safety factor of 2 is implemented to ensure the pump does not exceed maximum tensile or pressure.

To disengage the brakes, the following steps are needed to be taken

- The external access ball valve is closed and the pump is detached
- The internal access ball valve is opened
- The solenoid control valve's pneumatic port, which is open to the atmosphere, is closed
- The solenoid control valve's pneumatic ports connecting the air reservoir and the brake cylinder are opened
- The pressure difference moves the air through the pipes and into the brake cylinder
- Pressure in the brake cylinder increases to the operational requirement
- All pneumatic ports of the solenoid valve are closed once brakes are disengaged

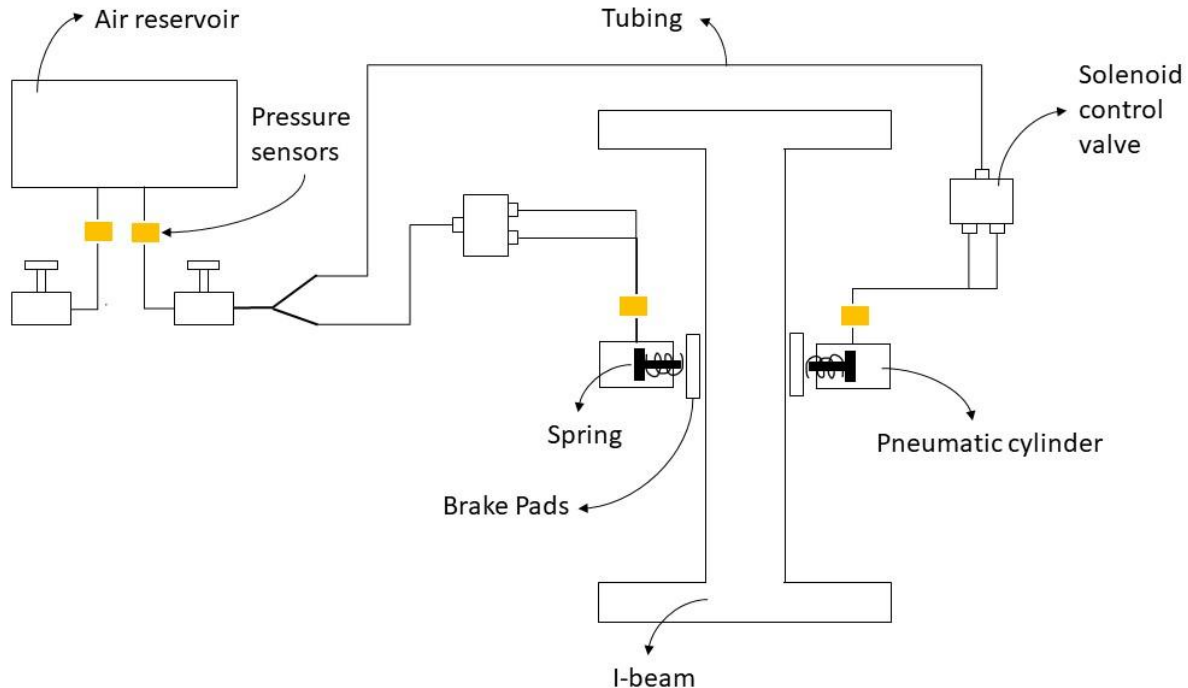


Figure 2.2.1.1.1. Block diagram representing the braking system

During the normal run, the engagement of braking is subjected to either propulsion achieving 50km/h speed or when the pod exceeds half the length of the track.

2.2.1.1.1 Air Reservoir

The purpose of an air reservoir in a pneumatic braking system is to store air from the external pump. Air is received, stored and then used to actuate the brake cylinder within the braking system. The use of an air reservoir requires additional equipment to achieve the desired compression value.

2.2.1.1.2 Brake Cylinder

The brake cylinder is responsible for providing the necessary force to compress the brake spring further and remove the brake pads from the I-beam. The brake cylinder must be a puller high operational limit to work against stiff springs

2.2.1.1.3 Brake Pads

The main application of the brake pads is to produce a frictional force when in contact with the I-beam. The frictional force produced is directly proportional to the normal reaction force (the force with which it is pushed onto the I-beam).

2.2.1.1.4 Ball Valve

Manual ball valves in order to restrict access of air to the pipe network or the atmosphere. The internal ball valve is connected to the braking system and restricts access while charging the air reservoir. The external ball valve is used as an access port for the external pump that fills the air reservoir with air.

2.2.1.1.5 Fittings and Pipes

Fitting and Pipes are components that allow the air to move between the braking components, assuring no leakage to the surroundings.

2.2.1.1.6 Solenoid Control Valve

The solenoid control valve is the main control device of the system. It is responsible for controlling the direction the air moves in within the pneumatic network. It can allow air to move from the air reservoir to the brake cylinder or evacuate the brake cylinder into the atmosphere. By default, it has one port always closed while one port is always open which prevents air from entering the brake cylinder. An electrical input is required to open or close the pneumatic ports.

2.2.1.1.7 Brake Spring

Brake Spring is responsible for generating the braking force to the pod. Its crucial design feature is spring constant which is directly proportional to the braking force. The spring exerts force on the pad which then exerts the force on the I-beam and successfully stops the pod.

2.2.1.2 Design Process and Dimensioning Process

The focus of the design process is to design a braking system that stops the pod quickly and safely. A robust system must be designed due to the fact that a lot of emergency routines rely on the braking system bringing the entire system to a halt.

2.2.1.2.1 Braking Force Requirement

The emergency braking distance (braking scenario II) was assumed to be 2m. Normal and emergency braking (braking scenario I and III) was designed to decelerate in less than 4 metres.

In order to calculate the maximum (emergency) braking force required to stop the pod in a distance of 1m, simple calculations from the dynamics of non-uniform linear motion with variable velocity and non-zero acceleration were used.

The maximum speed the pod is set to travel is 50km/h along a straight line of 168 metres. The braking is assumed to be applied when the goal speed of 50km/h is achieved or if not, 40m from the end (not taking into account emergency situations). Using linear equations and Newton's 2nd law of motion, the braking force was determined.

Table 2.2.1.2.1.1. Estimated values of braking distance, top speed, and mass of the pod

Braking distance	1m
Top speed	50km/h (13.883m/s)
Assumed Mass of the pod	150kg

The following equation of motion was used to calculate the deceleration of the pod in 1m.

$$v^2 = u^2 + 2as$$

$$a = \frac{-u^2}{2s} = \frac{-(13.883)^2}{2*4} = -24.10 \text{ m/s}^2$$

Braking force required of the pod with mass 150Kg

$$F = ma$$

$$F = 150 * 24.10 = 3615 N$$

Since we have two brake cylinders,

$$F_{braking} \approx 3.6 * 0.5 = 1.8kN$$

Assuming an average sliding friction coefficient of 0.5 between the brake pad and I-beam, we can determine the force that needs to be exerted by brake spring by using the formula

$$F_{braking} = \mu_k N$$

Where μ_k is the sliding friction coefficient and N is the force the brake pad is pressed onto the I-beam (the force that needs to be exerted by a spring). By substitute the necessary values, we get N equal to 3.6kN.

Braking spring selection:

The brake spring is an important component inside the pneumatic cylinder, it is there to provide final extension and retrieval of the piston. The type of spring we will be using in our system is compression spring.

Compression Springs are open-coil helical springs wound or constructed to oppose compression along the axis of wind. Helical Compression is the most common metal spring configuration. These coil springs can work independently, though often assembled over a guide rod or fitted inside a hole. When the load is placed on a compression coil spring, making it shorter, it pushes back against the load and tries to get back to its original length. Compression springs offer resistance to linear compressing forces (push) and one of the most efficient energy storage devices available.

The following parameters were used to choose the spring suitable for our system:

Rate: Spring rate is the change in load per unit deflection in Newtons per millimetre (N/mm).

Stress: The dimensions, along with the load and deflection requirements, determine the stresses in the spring. When a compression spring is loaded, the coiled wire is stressed in torsion. The stress is greatest at the surface of the wire; as the spring is deflected, the load varies, causing a range of operating stress. Stress and stress range govern the life of the spring. The wider the operating stress range, the lower the maximum stress must be to obtain comparable life. Relatively high stresses may be

used when the operating stress range is narrow or if the spring is subjected to static loads only.

Outside Diameter: The diameter of the cylindrical envelope formed by the outside surface of the coils of a spring.

Hole Diameter: This is a measurement of the space where you would insert a compression spring. It is the diameter of a mating part to a compression spring and often commonly mistaken for a dimension of the spring itself. The hole diameter should be designed larger than your compression spring's outside diameter factoring tolerance and spring expansion under load.

Rod Diameter: This is a measurement of the rod that goes through the inside of a compression spring. Essentially a mating part, this rod can work as a guide shaft to minimise spring buckling under load. The rod diameter should be designed smaller than your compression spring's inside diameter factoring tolerance; however, not too small or else it loses ability to minimise spring buckling.

Free Length: The length of a spring when it is not loaded. NOTE: In the case of extension springs, this may include the anchor ends.

Wire Diameter: This is a size measurement of the raw material used to form a spring. Usually, springs are made with round wires that are specified to a diameter.

Solid Height: This is a length dimension of a compression spring at its maximum loaded condition. Effectively, this is the compression spring's height when all the coils are pressed together.

Spring Set: This is an occurrence when a spring is loaded beyond its material elastic strength. It is a kind of permanent deformation that is noticeable when a spring does not return to its original length after releasing a deflection load. Depending on the application, spring sets can be either desirable or undesirable. In our case the desirable effect is the occurrence of the spring set because of safety factors. Meaning that if we need to efficiently and quickly stop the pod, the unplanned load would then occur on the spring, so it needs to be strong enough to withhold the load beyond its elastic limit.

Load at Solid Height: This is a measurement of the force required to completely deflect a compression spring to where the coils are fully pressed together. For product designers that want to avoid the occurrence of bottoming out a compression spring, Load at Solid Height is a quick reference property to find springs capable of handling an assembly's maximum operating load.

The length of the coiled spring L is the sum of the distance between the brake cylinder and the I-beam and the preload of the spring.

Using the Hooke's law equation, we can find the spring constant that we need in order to provide the desirable braking force.

The extension of an elastic object, such as a spring, is described by Hooke's law:

$$F = ke$$

Where F is the force, k is the spring constant, e is the extension of the spring.

This is when:

- force (F) is measured in newtons (N)
- spring constant (k) is measured in newtons per metre (N/m)
- extension (e), or increase in length, is measured in metres (m)

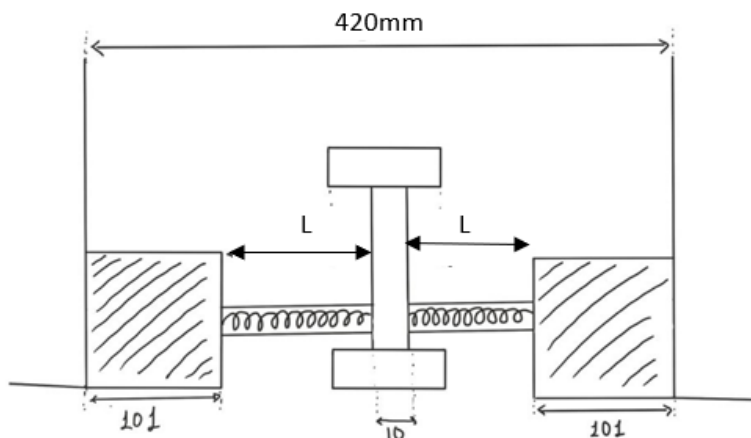


Figure 2.2.1.2.4 The block diagram representation of the lengths of the spring, I-beam, and structures

Assuming that spring needs to be compressed by 10mm (pre-loaded),

$$k = \frac{F}{e}$$

$$k = \frac{3615}{10} = 361.5 [N/mm]$$

This gives us a spring length of

$$L = \frac{420}{2} - 101 - 5 + 10 = 104\text{mm}$$

A spring of this length and spring rate will be customised by the manufacturer to suit our performance requirements.

Assuming a gap of 9mm between the brake pad and I-beam (when disengaged), the pulling force generated by the brake cylinder is equal to the sum of the return force of the spring due to preload and the additional compressive force required.

$$F = 360 * (10 + 8) = 6480N$$

Cylinder pressure requirements:

The assumption behind this is that initial pressure inside the brake cylinder is atmospheric pressure of 1 bar.

Piston diameter	100mm=0.1m
Max output force (approximately)	6480

Table 3. Given values for calculation of maximal cylinder pressure

The cross-section area of piston can be determined using simple equation for area of circle when its diameter is given:

$$A = \frac{\pi d^2}{4}$$

Where A is the cross-sectional area and d is the diameter of the piston whose value is given in Table 3.

$$A = \frac{\pi * 0.1^2}{4} = 0.00785 \text{ m}^2$$

The pressure difference can be then calculated using simple pressure difference formula:

$$\Delta p = \frac{F}{A} = \frac{6480}{0.00785} = 825059.225 \text{ Pa} = 8.25 \text{ bar}$$

From this pressure difference we can find the operating pressure on one side of the cylinder (it is assumed the other side has a pressure of 1bar)

$$\Delta p = p_2 - p_1$$

Where delta p is pressure difference, p_1 is pressure on the side of the brake cylinder piston open to air and p_2 is the pressure on the side of the piston connected to the pneumatic network. This gives a pressure of 9.25 bar. The air reservoir needs to have a pressure sufficiently higher than this to create pressure driven flow through the pipes.

Air reservoir selection and pressurisation:

The air reservoir was selected based on the following requirements presented below.

Table 2.2.1.2.1.2. Braking Air reservoir requirements

Maximal Pressurisation of cylinder, up to	9.25 bar
Initial volume of brake cylinder	84 224.5 mm ³
Atmospheric conditions (pressure)	1 bar
Atmospheric conditions (temperature)	288.16K
Molar mass of air	28.9647 * 10 ⁻³ kg/mol
Universal gas constant	8.314 J/(K*mol)

Table 2. Estimated values for air reservoir calculation

An air reservoir with a fixed volume of 5L is taken considering the space limitations of the pod. Once the air moves from the air reservoir to the brake cylinder, all the air occupies a total volume of 5.03L. The reduction in pressure must result in a pressure higher than the cylinder pressure requirement. Assuming an initial pressure of 13 bar in reservoir,

$$p_1 V_1 = p_2 V_2$$

$$p_2 = 13 \frac{5}{5.03} = 12.922\text{bar}$$

Hence, a pressurisation of 13 bar is sufficient to allow for multiple engagements..

Brake pad:

Brake pads are the parts of our braking system that take the brunt of the frictional force necessary to stop the pod. In a brake system, the brake rods activate a pneumatic line which squeezes the pistons and the spring towards the I-beam. Pads are positioned on the I-beam itself to absorb the energy and heat, then provide enough grip to stop the pod.

The material of which they are made is extremely important. For this we will make use of kinetic friction coefficient, hardness number (Brinell) and hardness number (Vickers) and specific heat capacity.

One of the best materials we have found so far is the Aluminium 6061 T6, whose properties will be listed below in Table 5.

One of the best materials we have found so far is the Aluminium 6061 T6, whose properties will be listed below in Table 5.

<u>Aluminium 6061 T6 properties</u>	<u>Values</u>
Brinell Hardness	95

Vickers Hardness	107
Rockwell Hardness	40(scale A), 60(scale B)
Specific heat capacity	900 J/Kg-K

Table 5. the Aluminium 6061 T6 specifications

The friction force is referred usually as “the resisting force tangential to the interface between two bodies when, under the action of an external force, one body moves or tends to move relative to the other” while the coefficient of friction (COF) is defined as “the ratio of the force resisting tangential motion between two bodies to the normal force pressing those bodies together”. Following the fundamentals of tribology, two types of COFs can be distinguished: the static friction coefficient (μ_s) and the kinetic friction coefficient (μ_k).

In the case of solid-on-solid friction (in dry or lubricated conditions), both coefficients are usually respectively defined in equations below.

$$\mathcal{M}s = F_s * P$$

$$\mathcal{M}k = F_k * P$$

Where forces F are respectively static and kinematic forces and P is the normal force

The kinetic friction coefficient between the I beam material (aluminium 6061 T6) and the brake block material can be found using a tribometer. A tribometer measures the friction coefficient between two materials under highly controlled conditions. Using a material database, we will be able to find a material that meets such requirements and be able to test the brake block material.

The material of the brake pad must meet certain requirements in order to be suitable for its purpose. It must have a high specific heat capacity. When the brake pad material is in contact with the I beam, made of aluminium 6061 T6, the friction coefficient should be around 1. The brake pad cannot damage the I beam so the brake pad material should have a lower hardness number than that of the I beam. Brake pad materials that could be used and meet the requirements are reinforced carbon-carbon, ceramic, or a type of leather material. In order to finalise the selection process an experiment to find the friction coefficient between the brake pad material and the I beam material must be completed. A tribometer can be used to find the friction coefficient between the I beam material and the tested brake block material. Whilst conducting the research contacting a materials researcher will strengthen the choices made and will improve the quality of the experiment and selection process.

In the below the application of brake block is shown on the I-beam.

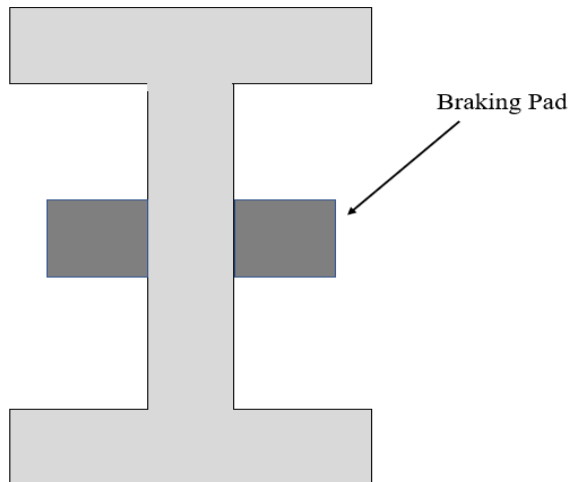


Figure 2.2.1.2.3. Application of break block to I-beam

2.2.1.3 Free Body Diagrams to define load cases for simulations.

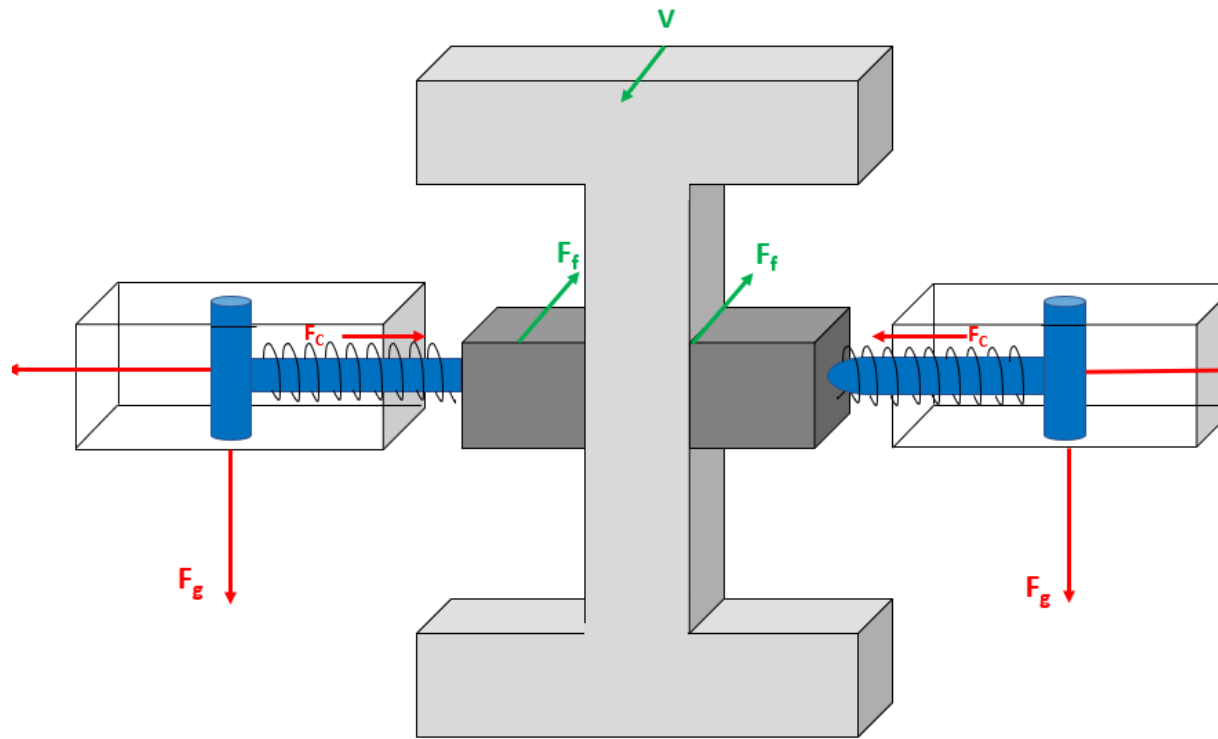


Figure 2.2.1.3.1 Free Body Diagram of braking system

The Free Body Diagram (FBD) presented above illustrates a single braking system (primary or secondary) when it is engaged. The force F_g represents the gravitational force or the weight of the system, F_p represents the pressure force exerted on the piston of cylinder, F_c is the compression force on spring due to piston pushing spring, F_f is the frictional force between the braking pads and I-beam which always has opposite direction from velocity V.

2.2.1.6 Description of the manufacturing processes.

All the components of both primary and secondary braking systems are purchased off-the-shelf from the suppliers listed in Section 2.2.4.1. *Parts List*. Therefore, the manufacturing of any components is not performed in-house. All components

purchased off-the-shelf are operating within its operational limits specified by the manufacturers. All technical data is uploaded to the ‘FDD Hyperlink 2022’ folder shared to EHW organisers. The whole braking system is assembled onsite at MakerSpace at Queen Mary University of London.

All the fittings will be connected to the appropriate components and sealant applied. All pipes will be connected as per the given schematic. No additional assembly is required.

2.2.2 Size, Components, Appearance

2.2.2.1 Evidence of CAD models

The following figures represent the CAD models of our purchased components.

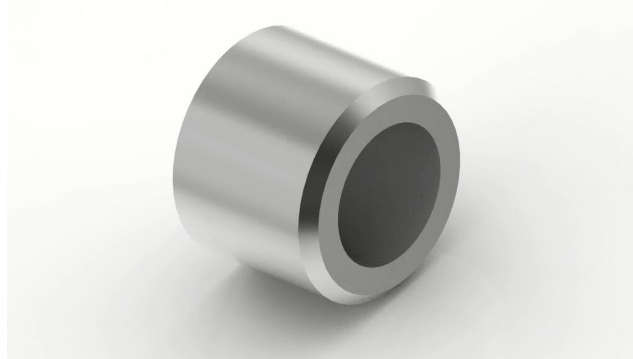


Figure 2.2.2.1.1. Fitting for cylinder

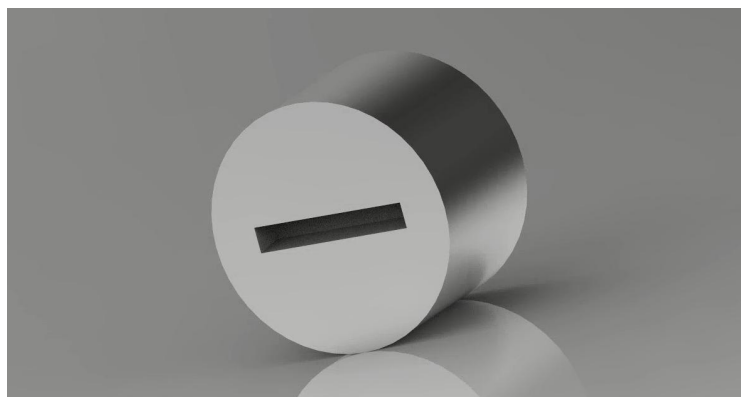


Figure 2.2.2.1.2. Fitting for cylinder

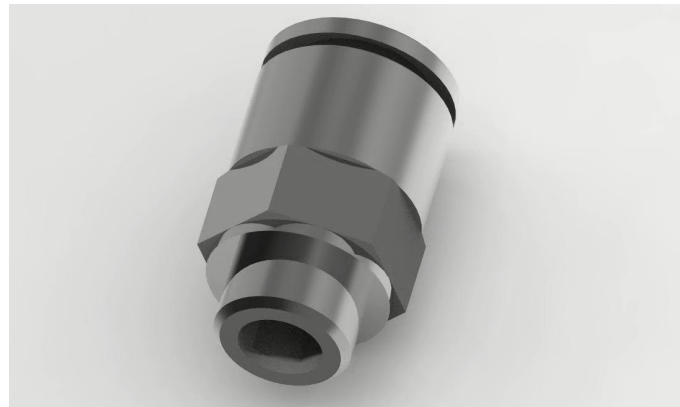


Figure 2.2.2.1.3 Fittings for valves



Figure 2.2.2.1.4 Fittings for valves

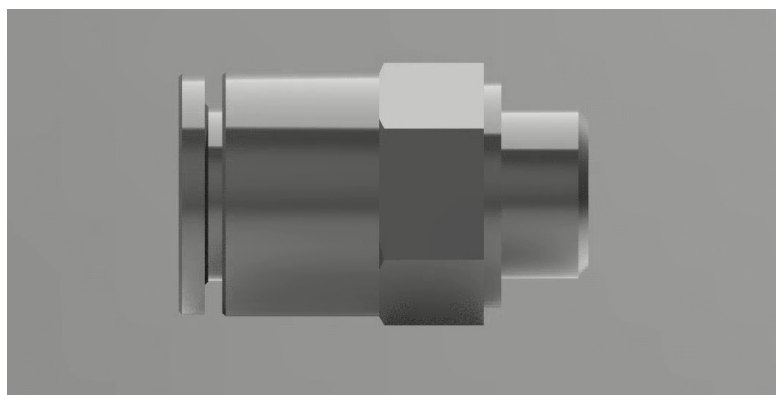


Figure 2.2.2.1.5 Fittings for valves

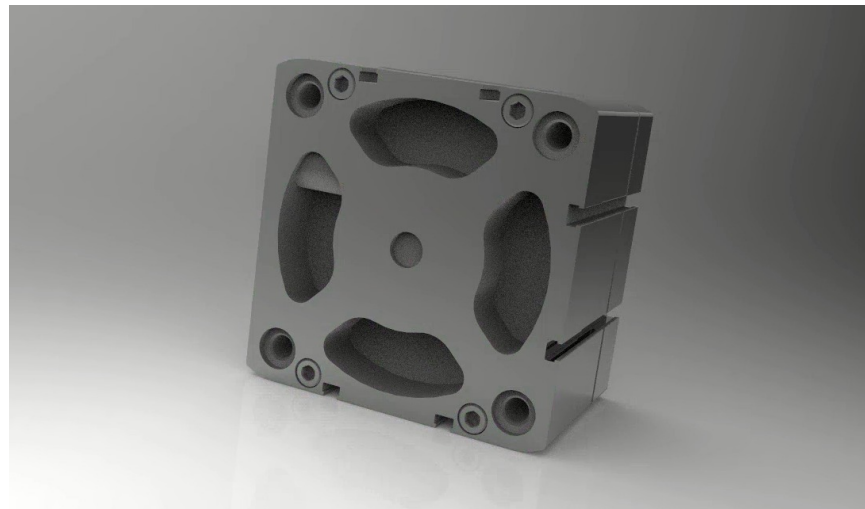


Figure 2.2.2.1.6 Pneumatic cylinder

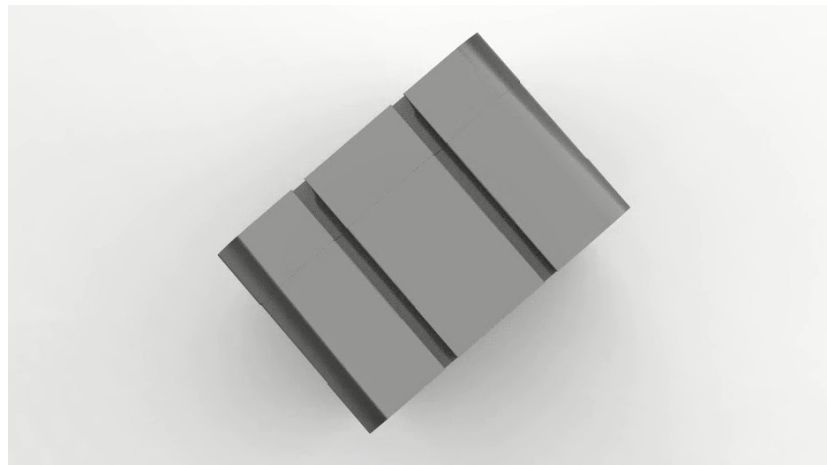


Figure 2.2.2.1.7 Pneumatic cylinder



Figure 2.2.2.1.8 Pneumatic cylinder



Figure 2.2.2.1.9 Piston for pneumatic cylinder

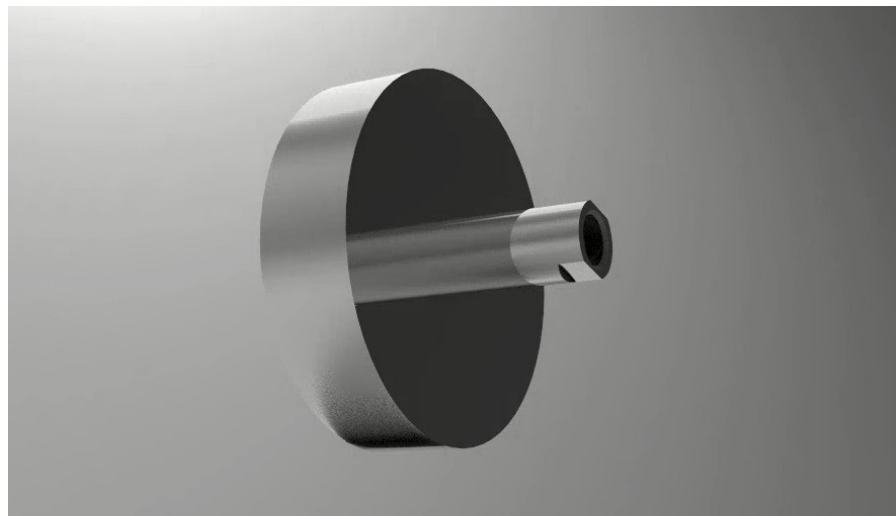


Figure 2.2.2.1.10 Piston for pneumatic cylinder

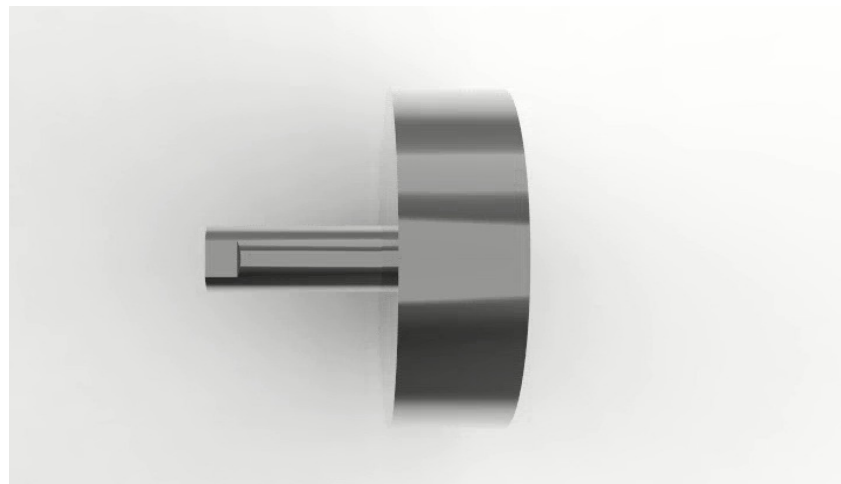


Figure 2.2.2.1.11 Piston for pneumatic cylinder

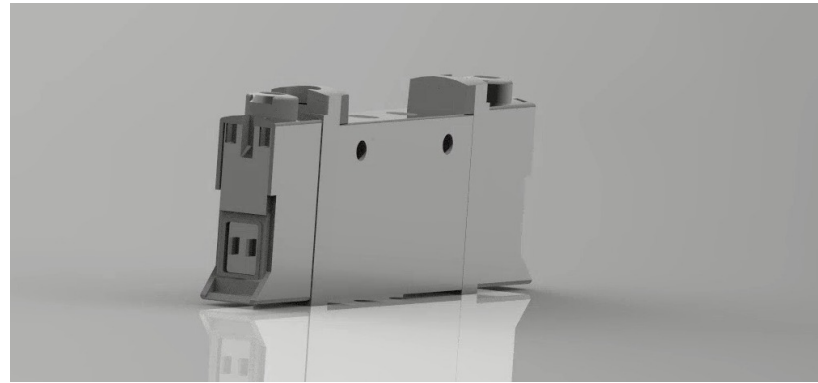


Figure 2.2.2.1.12 Solenoid Valve

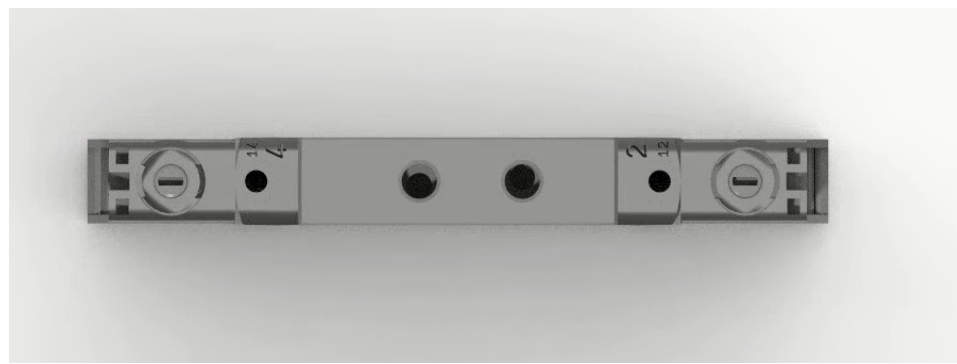


Figure 2.2.2.1.13 Solenoid Valve



Figure 2.2.2.1.14 Solenoid Valve



Figure 2.2.2.1.15 Tubing

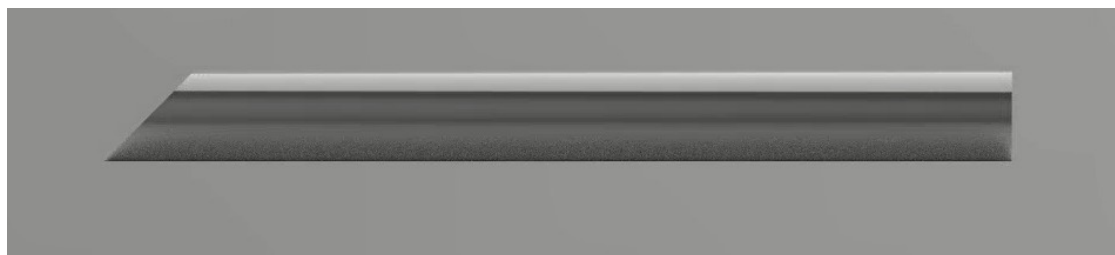


Figure 2.2.2.1.16 Tubing

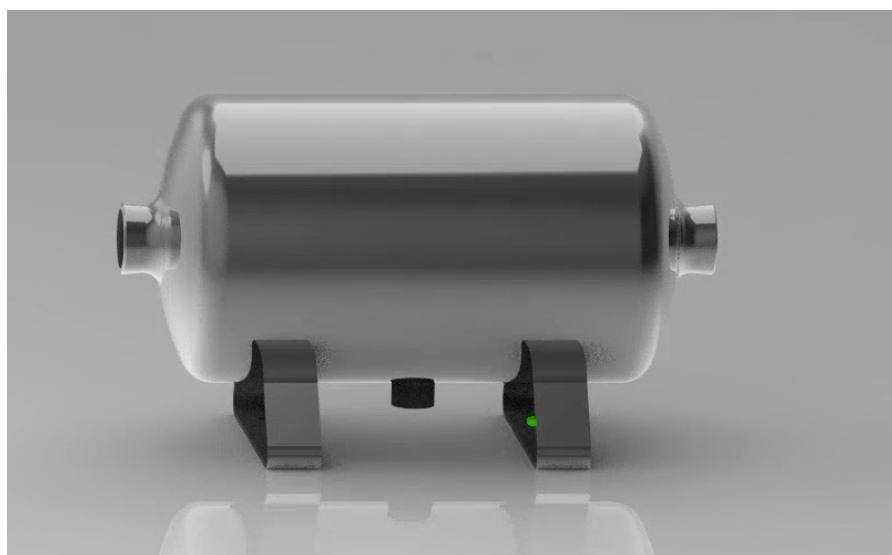


Figure 2.2.2.1.17 Air reservoir

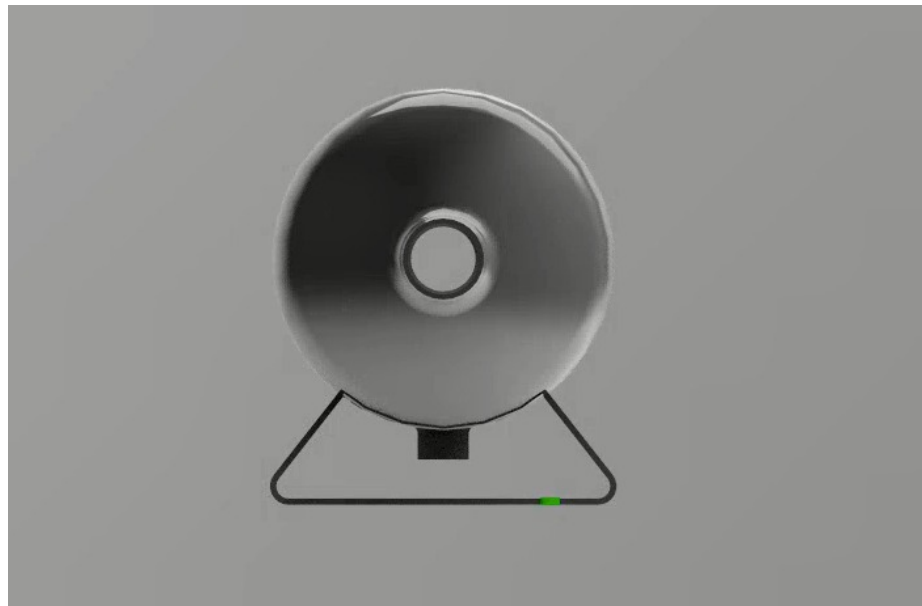


Figure 2.2.2.1.18 Air reservoir



Figure 2.2.2.1.19 Air reservoir



Figure 2.2.2.1.20 Air reservoir

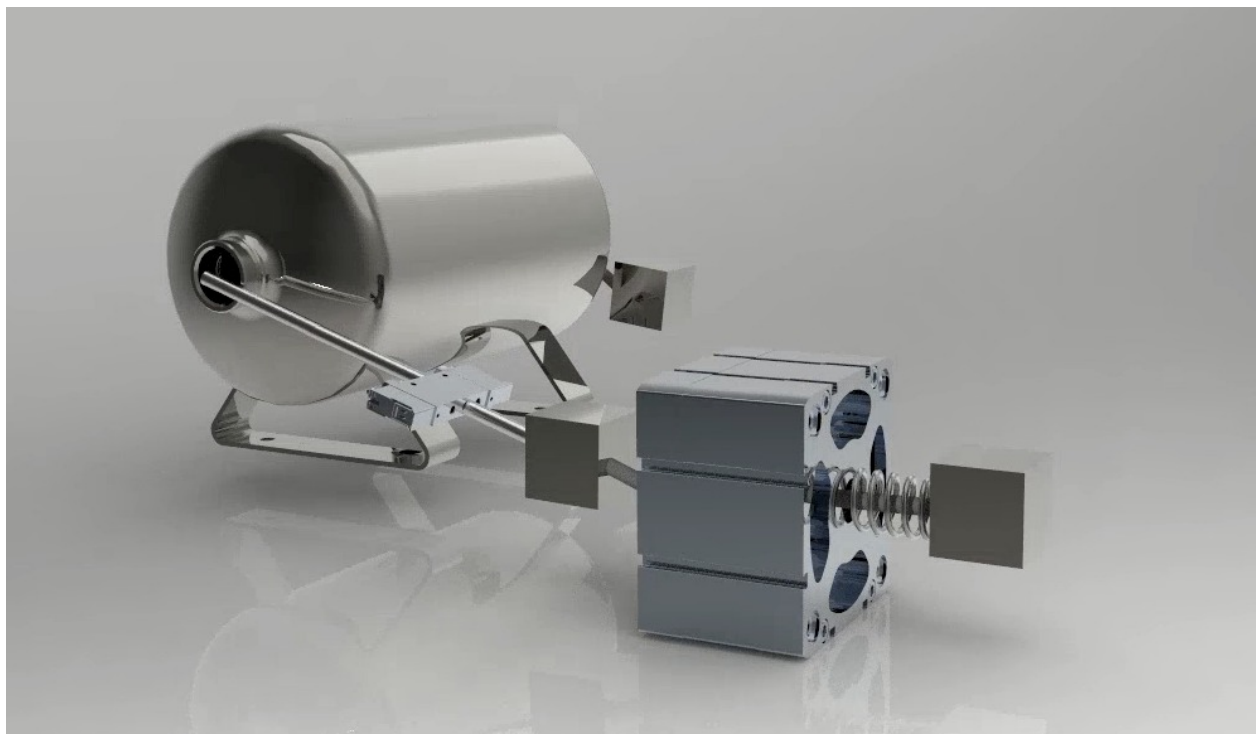


Figure 2.2.2.1.21 Assembly of braking system

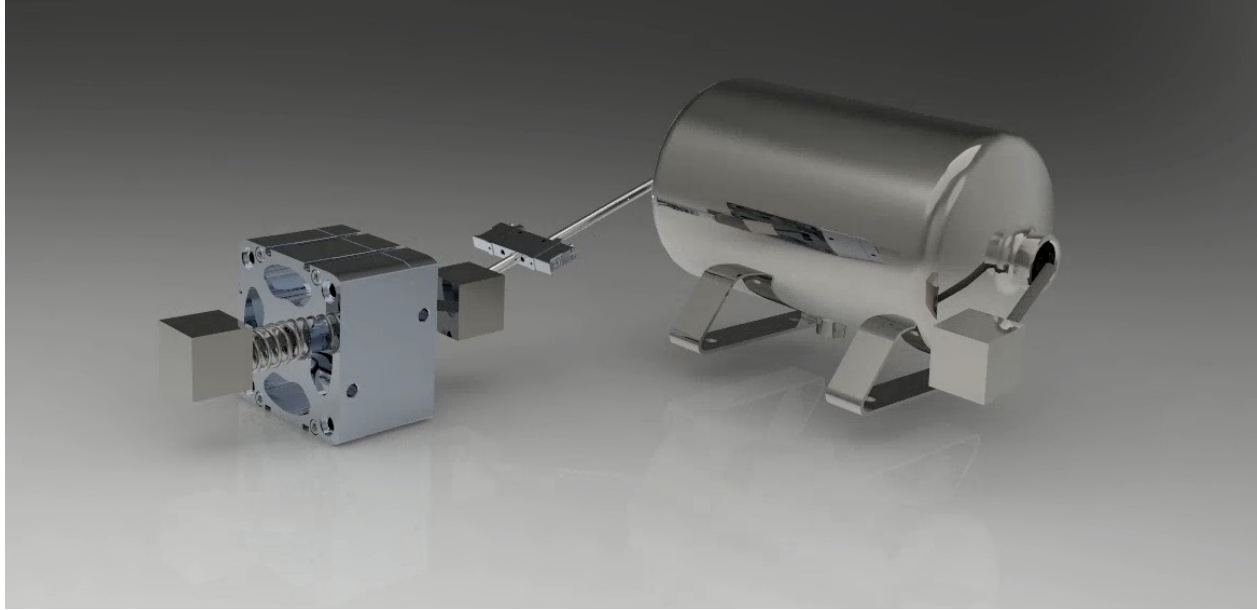


Figure 2.2.2.1.22 Assembly of braking system

2.2.2.2 Technical drawings

In the following figures, the engineering drawings for various purchased components will be visually presented.

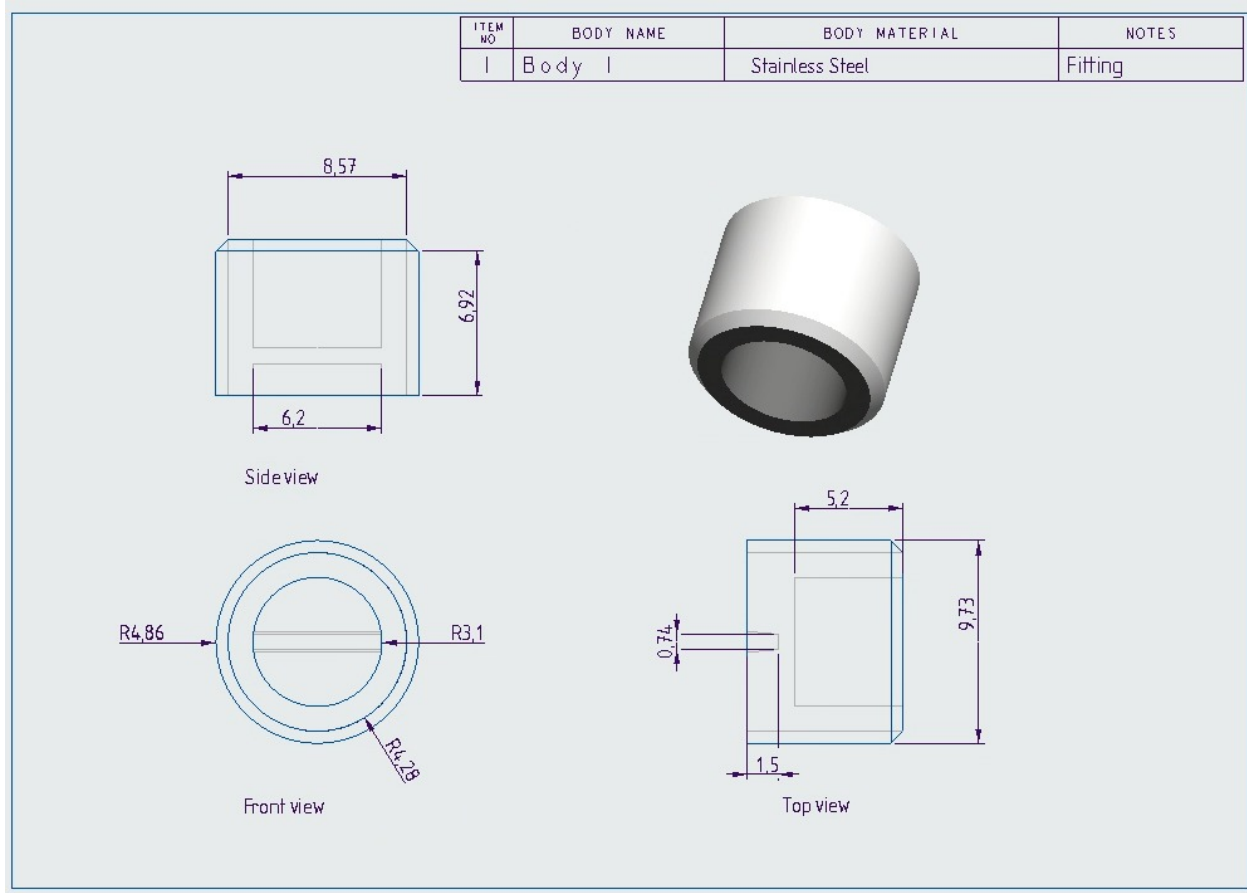


Figure 2.2.2.2.1 Engineering drawing of fitting for the cylinder

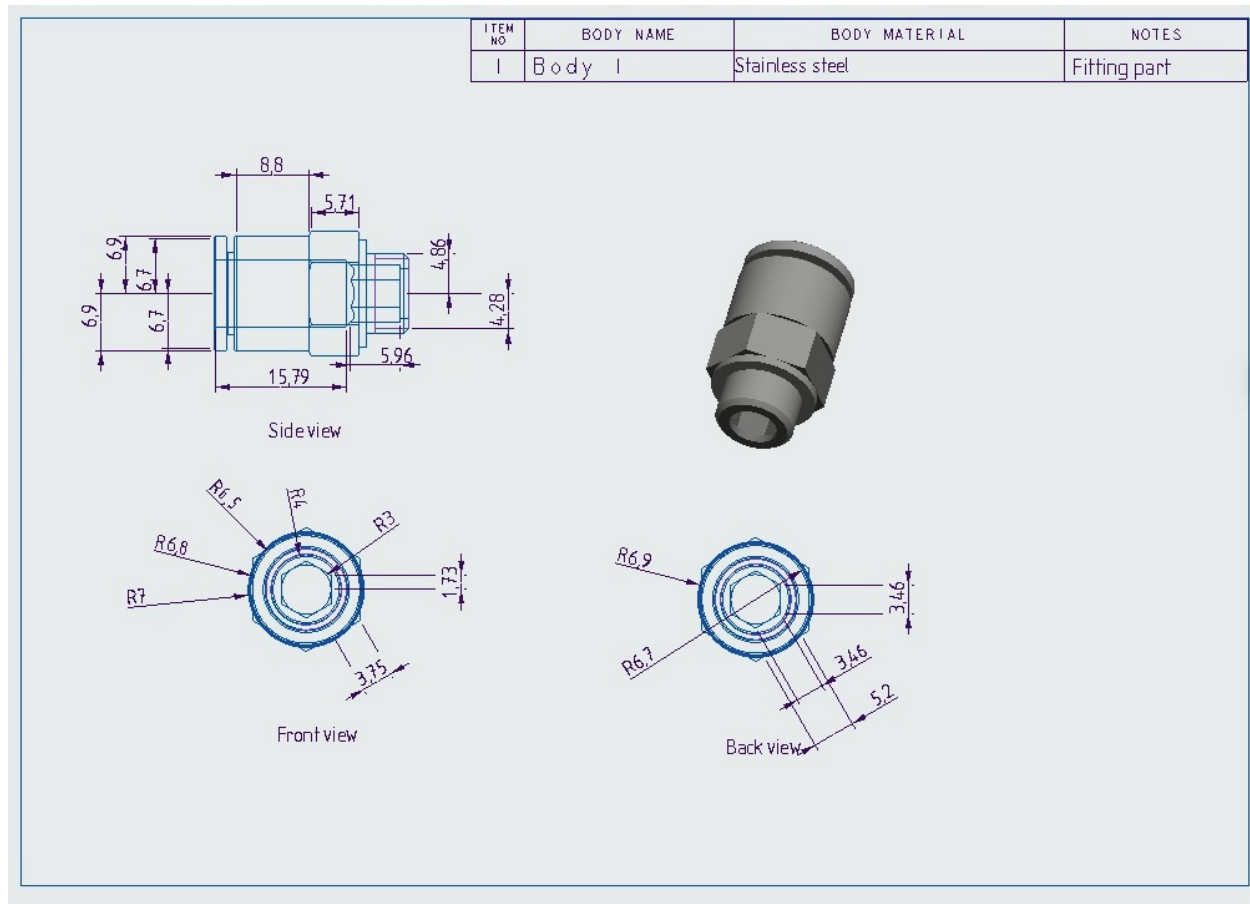


Figure 2.2.2.2.2 Engineering drawing of fitting for the valves

ITEM NO	PART NUMBER	QTY	DESCRIPTION	NOTES
			Pneumatic cylinder part	Stainless steel

Side view

Front view

Back view

Figure 2.2.2.2.3 Engineering drawing of pneumatic cylinder

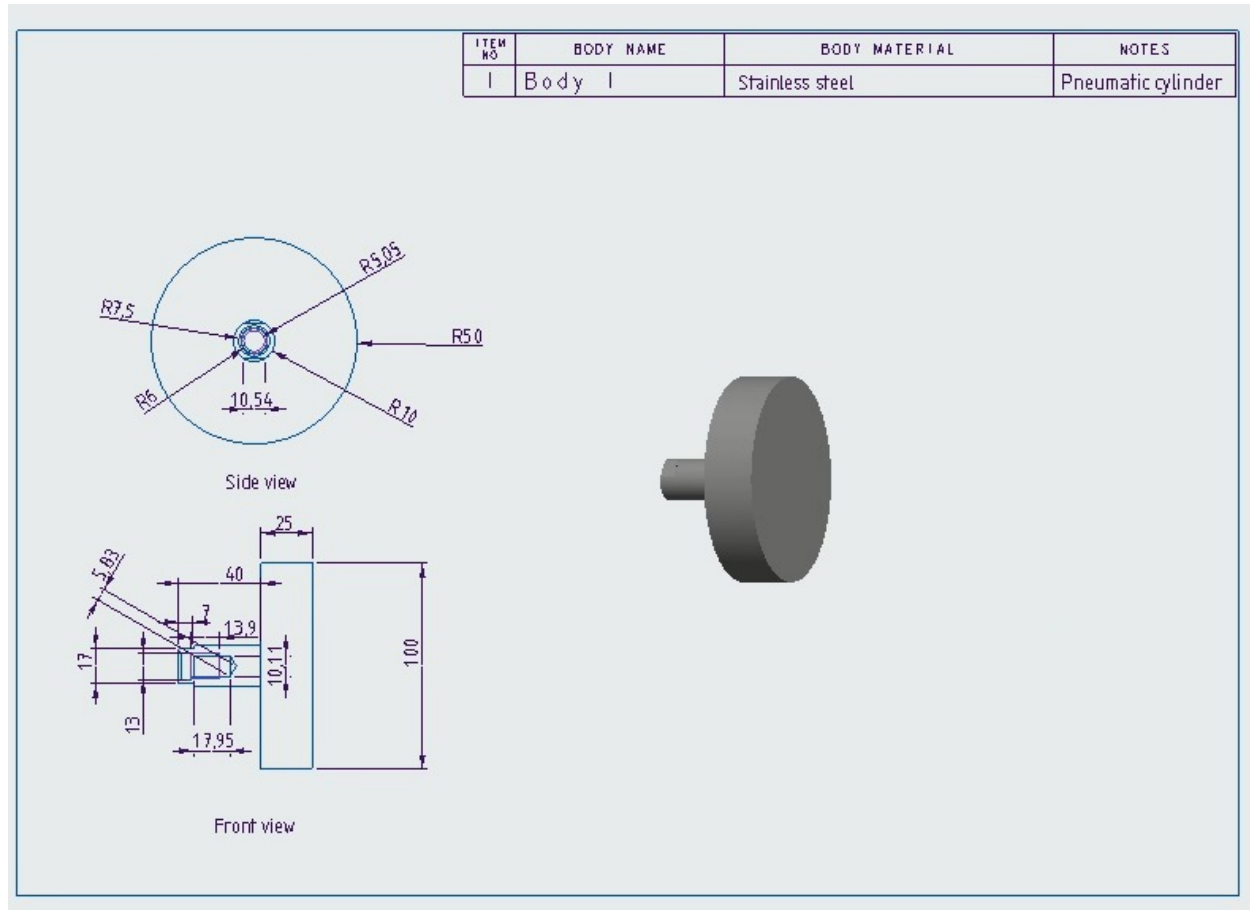


Figure 2.2.2.2.4 Engineering drawing of piston for pneumatic cylinder

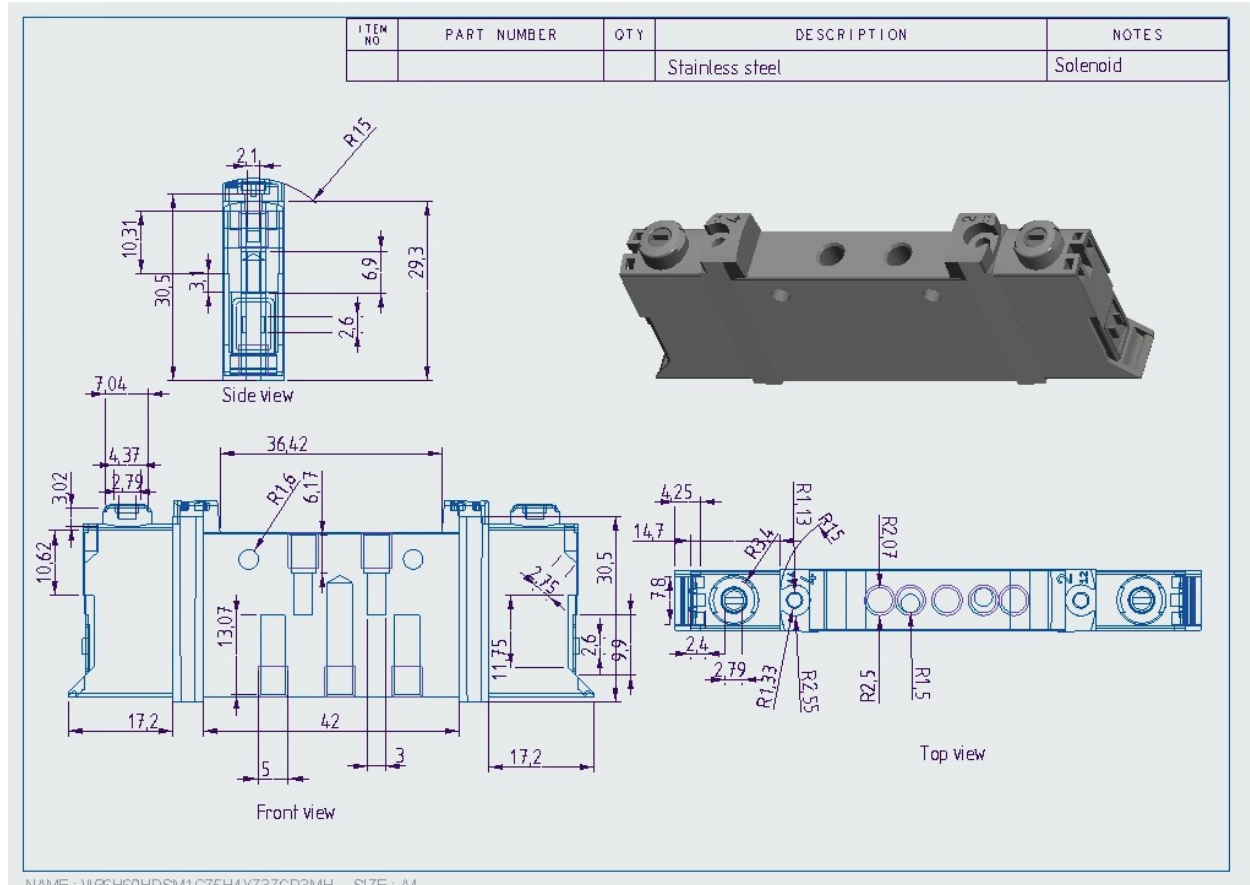


Figure 2.2.2.5 Engineering drawing of Solenoid valve

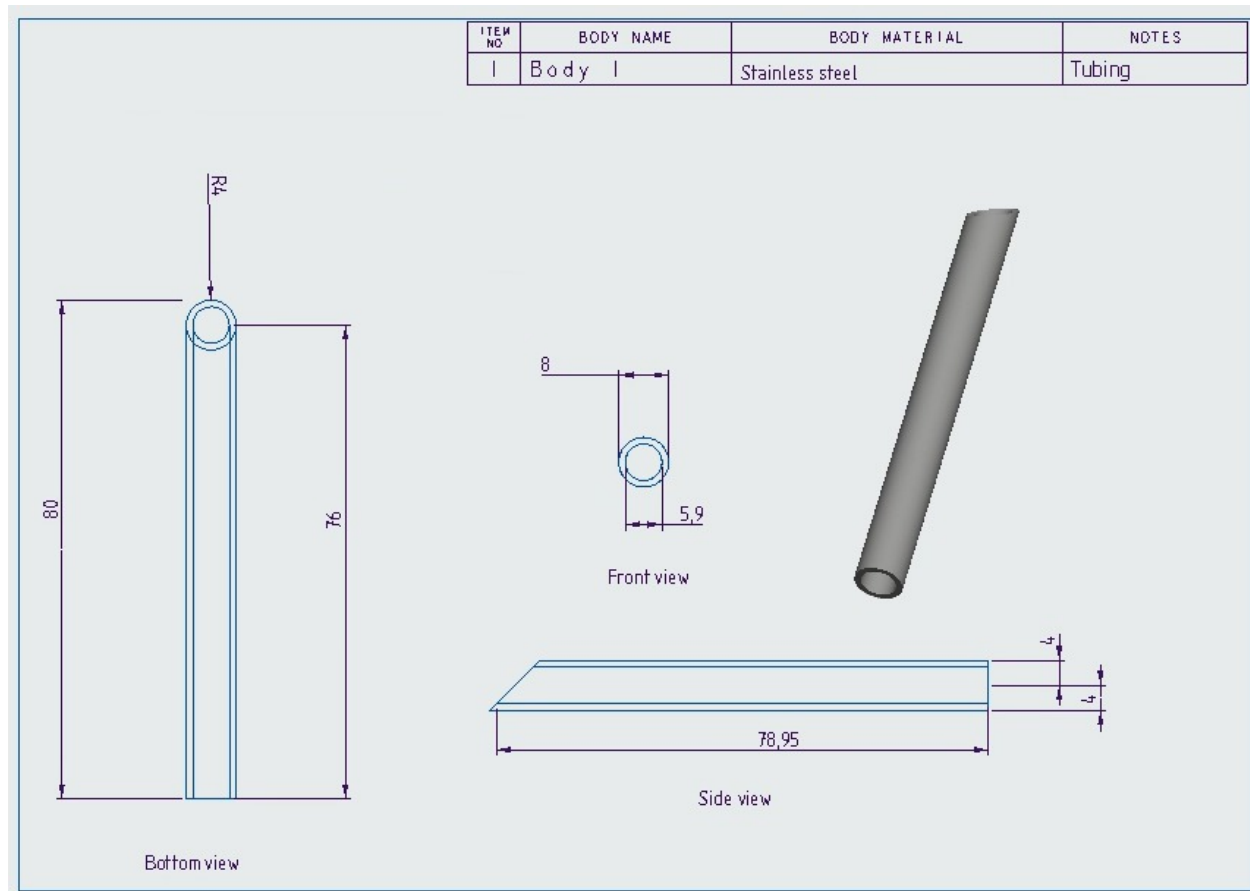


Figure 2.2.2.2.6 Engineering drawing of the tubing of system

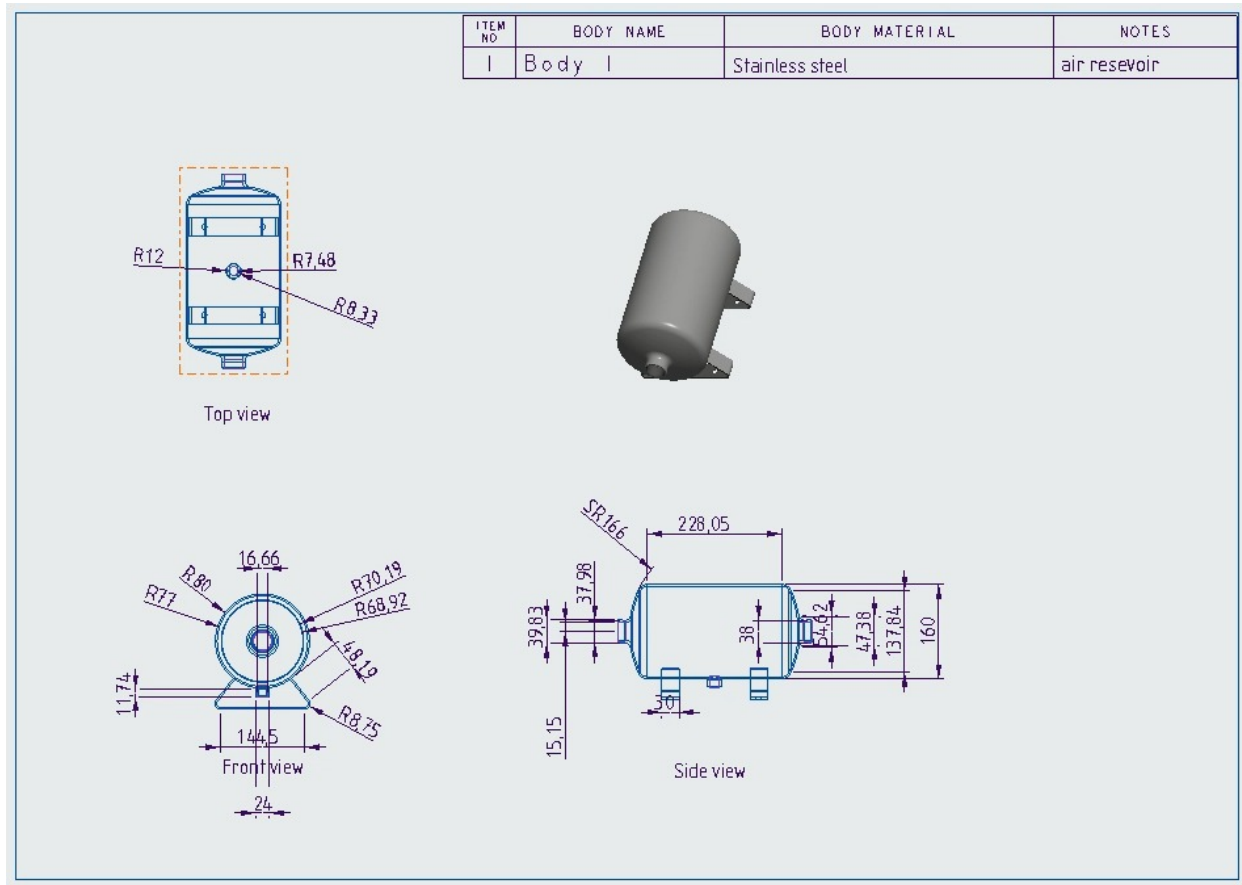


Figure 2.2.2.2.7 Engineering drawing of the air reservoir

2.2.3 Integration into a Subordinate Structure/System

The braking system will be integrated into the pod in a way that both air cylinders will be mounted to the frame while tubing and valves will be fixed between the air reservoir and cylinder. The pneumatic cylinder will be placed on plates on frame and it will be connected to the brake pads that once engaged will be in contact with I-beam.

2.2.4 Demonstration Plan

Setting up before run

From the point when pod is placed on the I-beam, for demonstration, the braking system will automatically have pressure inside the pneumatic cylinder equal to atmospheric and the brake pads will be in contact with I-beam applying the braking force on it. This way system will be engaged immediately once positioned to the beam.



Start of the run

In order to start the run we have to disengage the braking system. We will manage this by pumping the air to the air cylinder that will once valves are fully open pressurise the cylinder, pulling the piston backwards and extending the spring. This way brake pads will move away from I-beam and the pod will be ready to go once the valves get closed again



During the run

The valves that provide pressure from reservoir to the cylinder will be engaged all the time ensuring the piston is pulled and brake pads are away from the I-beam. Once the pod has reached maximum speed the valves for pressurization will close enabling the valves that have one side open to atmosphere open and produce enough mass flow rate of lower pressure in order to push the piston. When piston is pushed it compresses the spring and applies brakes to the I-beam. Regarding the braking scenario mentioned in Section 2.2.1.2. Description of design process being taken, either one or both braking systems will be engage



After the run

Once the pod has stop successfully, the valve with a connection to atmosphere will close and the valve that connects cylinder and reservoir will open pressurizing the pneumatic cylinder. Once enough pressure difference has been reached in pneumatic cylinder the piston will be pulled, extending the spring. This will enable brake pads to move from the I-beam so we can remove the pod after demonstration.

All of these steps mentioned above in the Algorithm, that shows a demonstration plan by explaining how the system is engaged by default, are crucial for the pod to stop successfully within desired braking distance.

2.2.4.1 Parts List/BOM

Table 2.2.4.1.1 Braking Parts List

PARTS LIST						
Part / part mass (kg)	Device quantity usage	Unit of measure	Unit cost	Device usage cost	Created	Supplier
Air Reservoir CRVZS-5 / 3.581kg	2	Each	/	/	Outsourced	Festo
G1/8 Male thread 8mm OD Y push fitting for pneumatic cylinder //	4	Each	£3.79	£15.16	Outsourced	Tamsen
G3/8 Male thread 8mm OD Y push fitting for air reservoir and ball valves //	4	Each	£4.16	£16.64	Outsourced	Tamsen
G1/8 Male thread 8mm OD push fitting for solenoid valve / 0.012kg	12	Each	/	/	Outsourced	Festo
Sealant //	1	Sold with cylinder	/	/	Outsourced	Festo
Pneumatic cylinder AEN-100 / 2.847 kg	4	Each	/	/	Outsourced	Festo
Compression Spring (custom made) //	4	Each	£16.06	£4.02	Outsourced	Lee Springs
Tubing PFAN-8X1 / 0.049kg/m	1	Each	/	/	Outsourced	Festo
Solenoid 3/2 way control valve VUVG-L14-T32H-MZT-G1 8-1P3 / 0.08 kg	4	Each	/	/	Outsourced	Festo

PARTS LIST						
External compressor 30MPa 1800W / 16.5kg	1	Each	£129.99	£129.99	Outsourced	Crenex
Ball Valves QH-3/8 //	4	Each	/	/	Outsourced	Festo
G3/8 Male thread 8mm OD push fitting for ball valve / 0.022kg	2	Each	/	/	Outsourced	Festo
Braking Plug B-1 / 0.123kg	4	Each	/	/	Outsourced	Festo
Brake pads for Aluminium rims //	4	Each	£22.96	£91.86	Outsourced	Tweeks

The prices of the components marked as "/" are not final yet, as the discussion with the provider Festo is still open. However, all the technical data and product's technical reports of each component are uploaded to the 'FDD Hyperlink 2022' folder in google docs. The folder is shared to EHW and the link to it is pasted in the Appendix.

2.2.4.2 Demonstration Setup

The demonstration setup will include all the components inside the pod that are mentioned in Section 2.2.4.1. Parts List and the additional external compressor that will pump the air inside the air cylinder when the time comes for the braking system to disengage.

The external compressor that we will use during demonstration is presented in Figure 2.2.4.2.1 This compressor measures the amount of pressure pumped inside the reservoir using the barometer which presents data analogically. The barometer can be seen in Fig. 2.2.4.2.2, since this measuring device is not precise we decided to implement pressure sensors at the entrance of the air reservoir that will measure exact pressure being applied.

The pressure sensor will be used continuously, meaning that when air gets pumped to a certain measure, we will wait until the system settles down to measure the magnitude of pressure until the desired level is reached, which is 13 bar. The pressure sensor will also be implemented before the pneumatic cylinder to sense the amount of pressure arriving to the cylinder at all times. The sensor will also send feedback to

control valves that will be opened and closed according to control that comes from software.

The equipment used in the mounting and pumping air in the reservoir using a cylinder consist of pipes, screws and plugs.



Figure 2.2.4.2.1 The External Compressor



Figure 2.2.4.2.2 Barometer



Figure 2.2.4.2.3 Equipment used to start the external compressor

At all times pressure in cylinders is measured as previously stated by a sensor and displayed in software which shows the health of the system and sends the imminent control to emergency valves in case of emergency i.e. overpressurization of the whole system.

2.3 Suspension

2.3.1 Technical Description of the System

2.3.1.1 Theory and principle physics of desired functionality

The primary purpose of the suspension system is to generate resistive forces against any disturbances acting on the pod during operation while also supporting the pod. It is composed of vertical and horizontal wheel sets which ensure horizontal and vertical stability. Due to the wheel alignment, the pod is able to move only in one direction, forward and back along the I-beam. The main components of the suspension system are the wheels and shock absorbers. The shock absorber is a combination of spring and damper.

Both the spring and damper generate forces that allow the system to return to equilibrium after a disturbance. The spring resists all compressive loads from the wheel or pod by converting the kinetic energy to elastic potential energy while also producing a returning force that brings the pod to its original alignment. The return force of the spring can be given by Hooke's law

$$F = kx$$

where k is the spring rate and x is the deflection.

The damper dissipates the extra energy present within the pod due to the work done by the disturbing forces. It consists of a piston head moving within a highly viscous fluid such as oil to generate friction. Friction converts kinetic energy present due to a disturbance to thermal energy. Without the damper, the pod will experience oscillations which would grow with any new disturbances. While the spring determines the maximum deflection of the pod for a given disturbing load, the damping coefficient of the damper determines the time taken to diminish the oscillations.

The possible disturbances include the following:

- Unevenness in track geometry
- Minor misalignments of the Propulsion system during mounting
- Asymmetry in the Braking Forces due to slight variations in brake pad roughness or small delay in engaging the brake pads to the I-beam.
- Possible micro-asymmetry in general loading such as aerodynamic forces, small variations of weight distribution.
-

However, as the track can be assumed to be reasonably smooth, the horizontal and vertical imperfections are not a source of big concern. Hyperlink's suspension system is designed to withstand any small imperfection that may occur along the pod's run, such as environmental disruptions and connections between parts of the I-beam.

Each shock absorber with the wheel is modelled as a simple mass spring damper system.(can you elaborate on this sentence, it's a bit out of the blue)

As the wheels are manufactured from (what metal, type and grade), the assumption made is that they are rigid and non-elastic. Therefore, any deflections are directly translated onto the suspension system, with negligible interference. All other unexpected disturbances are assumed to be sudden impulses acting on the pod.

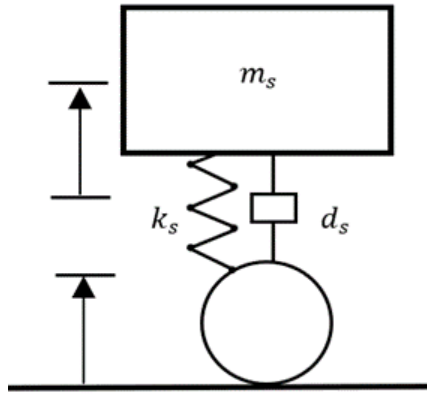


Figure 2.3.1.1.1 Mass-spring damper model

Thus, a force caused by a deflection is only opposed by the damping and spring forces, where the spring is constrained to move axially. Using balance of forces, the following is obtained

$$-F_s - F_D = ma$$

$$F = kx$$

$$F_D = cv$$

where F_s is the spring force, F_D is the resistive force from the damper, c is the damping coefficient, and v is the speed the wheel is being pushed upwards.

The above equations are all functions of time and displacement and thus can be rewritten based on displacement:

$$m \frac{d^2y}{dt^2} = -c \frac{dy}{dt} - ky$$

The suspension can be modelled as an inhomogeneous second order differential equation. An analytical solution to the differential equation is available and has been studied extensively.

The system consists of vertical and horizontal wheels and shock absorbers that provide horizontal and vertical stability. There are three vertical wheels that are the primary support of the pod and are located at the front, centre, and rear of the pod. Two pairs of horizontal wheels are located at the front and back of the pod.

As for the desired functionality of the suspension system, it must be able to dampen out any disturbances with minimum deflection to prevent collision of components such as the propulsion system. The position of the propulsion system is crucial as the air gap between the stator and the I-beam needs to be fixed at all times, as it influences the porpulsion's efficiency. The following section describes main components of suspension and their desired functionality.

a) Wheels

- Must be able to operate at speeds of 50km/h
- Must be able to bear loads larger than 60kg each
- Must be made of a material softer than Aluminium 6061 T6 not to damage the I-beam
- Must be wide enough to ensure pod's stability

b) Shock absorber

- Must keep horizontal deflections below 6mm to prevent the propulsion system from changing its position with respect to the I-beam
- Must keep vertical deflections below 10mm to prevent any component from interfering with the keep out zones during operation
- Must have damping coefficient high enough to allow near critical damping
- Must be able to prevent any rotation that could result in collision of critical components of the pod with the I beam
- Must be able to bear loads larger than 60kg

c) Structural Components (Wheel Housing, Shaft)

- Shaft must have an interference fit with the wheel so that it rotates along with it
- Safety factor must be higher than 2
- Shaft must have a clearance fit with the wheel housing to allow rotation
- Shaft must be lubricated with suitable lubricant to minimise friction

d) Mechanical Rotary Velocity encoder

- Must be able to perform at 11000 RPM
- Must be able to fit within the suspension system

2.3.1.2 Description of design process taken.

Some limitations to the design process were encountered due to the absence of technical details on shocks available from manufacturers. The main data available is the spring rate. Since the primary source of concern to the functionality is the

maximum deflection for a given loading, damping coefficient has been ignored in the design process. The selected shocks facilitate the smooth ride of the pod and their specification and manufacturer are provided in the following sections, and the 'FDD Hyperlink 2022' folder.

The design process taken is completed for an assumed pod mass of 150kg.

2.3.1.2.1 Shock Absorbers

The softer the shocks, the better they perform under uneven terrains. They minimise the spring's reaction force that is transmitted onto the pod. Stiffer shocks provide the best performance under external loading on the pod. Since bike shocks are heavy duty, the lowest spring rate was taken into consideration and its performance was studied. The design process has been completed for an assumed pod mass of 150kg.
Spring Rate of Mountain Bike Rear Shock Absorber = 148 N/mm
Deflections affect a single wheel at a time while external loadings transmit forces directly onto all the pod shocks.

Under lateral deflection of 3mm, $F = 148 * 3 = 444N$. Under vertical deflection of 2mm, $F = 148 * 2 = 296N$.

Since these forces are insignificant against the 1471N weight of the pod, the selected shocks offer a smooth ride. This shock absorber should be able to tolerate the minor deflections of the track. Parallel springs have their spring constant added up while series springs give a lower spring rate than its individual components.

Vertically, four shocks are connected in parallel. Under a vertical deflection of 6mm due to external loading, $F = 4 * 148 * 6 = 3552N$.

Horizontally, four shocks constrain the pod. These four shocks are made up of two parallel and two series springs. However, under vertical deflection, only two parallel shocks act together to resist the disturbance (based on direction of disturbance).

$$F = 2 * 148 * 6 = 1776N$$

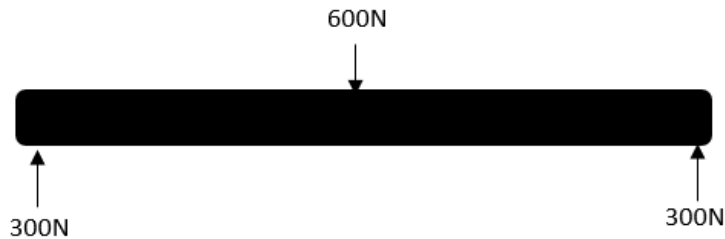
Compared to the propulsion force, both these forces are significant. Minor misalignments result in insignificant forces with deflections well within bounds. Since the pod shell is symmetrical, aerodynamic loads will not produce any significant horizontal loadings.

The spring determines the maximum deflection under disturbances. The damper will only reduce the amplitude thus allowing us to ensure shocks have been selected reasonably.

2.3.1.2.2 Wheel and Shaft

Being a major weight bearing component, it is necessary to have pod wheels that are able to bear loads larger than 60kg each. A safety factor 2.5 is applied onto the wheels, as one wheel is able to withstand the load of 160kg (manufacturer's data). Moreover, being a point of contact on the I beam, wheels are required to be made of a material softer than Aluminium 6061 T6, in order not to damage the I-beam during the run. Therefore, rubber coated aluminium wheels from RS pro with a max load capacity of 160kg and an aluminium hub are sufficient for the pod's performance requirements. A high load capacity indicates it is able to perform well at high friction forces (due to the high normal reaction force) making it suitable for the velocity we are working at. The selected wheels are also abrasion resistant indicating they are not to be damaged by track.

The shaft is designed with a material that provides a safety factor higher than 2. Considering the shaft is a simple beam problem, solid mechanics is used to determine its performance. Assuming a shaft with 12 mm diameter (which is equal to the hub diameter of the selected wheel) and steel as material, we can define a simple beam problem as follows:



For a cylindrical shaft with 6mm radius, the second moment of inertia is given by

$$I_{zz} = \frac{1}{2} \pi R^4 = \frac{1}{2} \pi * 0.006^4 = 2.035 * 10^{-9} m^4$$

The maximum bending moment acts at the centre which is given by

$$M - 300 * 0.054 = 0$$

$$M = 16.2 Nm$$

Since stress is maximum close to the surface, $y = 0.006m$ which gives,

$$\sigma_x = \frac{My}{I_{zz}} = \frac{16.2 * 0.006}{2.035 * 10^{-9}} * 10^{-6} = 47.7 MPa$$

Considering stainless steel has a yield stress of 257MPa, it gives a safety factor of

$$n = \frac{257}{47.7} = 5.38 > 2$$

2.3.1.2.3 Wheel housing and Fixtures

The wheel housing is the one of the main structural components that connects the wheel to the shock absorber. It consists of a rod on the top along with holes for the shaft at the bottom. Fixtures ensure that the shock absorbers are held rigidly in their intended place. Using reasonable understanding of structural mechanics and performance requirements, an initial design of the housing and fixture are simulated structurally. Based on analysis of results, modifications are made to increase the safety factor to 13. The design is developed through several iterations of simulations (Abaqus). Further information on performance and safety factors is provided in the simulations section.

2.3.1.3 Free Body Diagrams

Structural simulations are performed on all load bearing components that have been designed by the suspension team. Components such as shock absorber and wheel are excluded as they are off the shelf.

This section defines the load cases for simulations. Each component is tested with a 60kg load on it (in the real case, it only experiences a maximum of 40kg but a higher loading has been considered for reliability).

Wheel Housing

The 60 kg load has been distributed across the four upper shaft placeholders for the simulation.

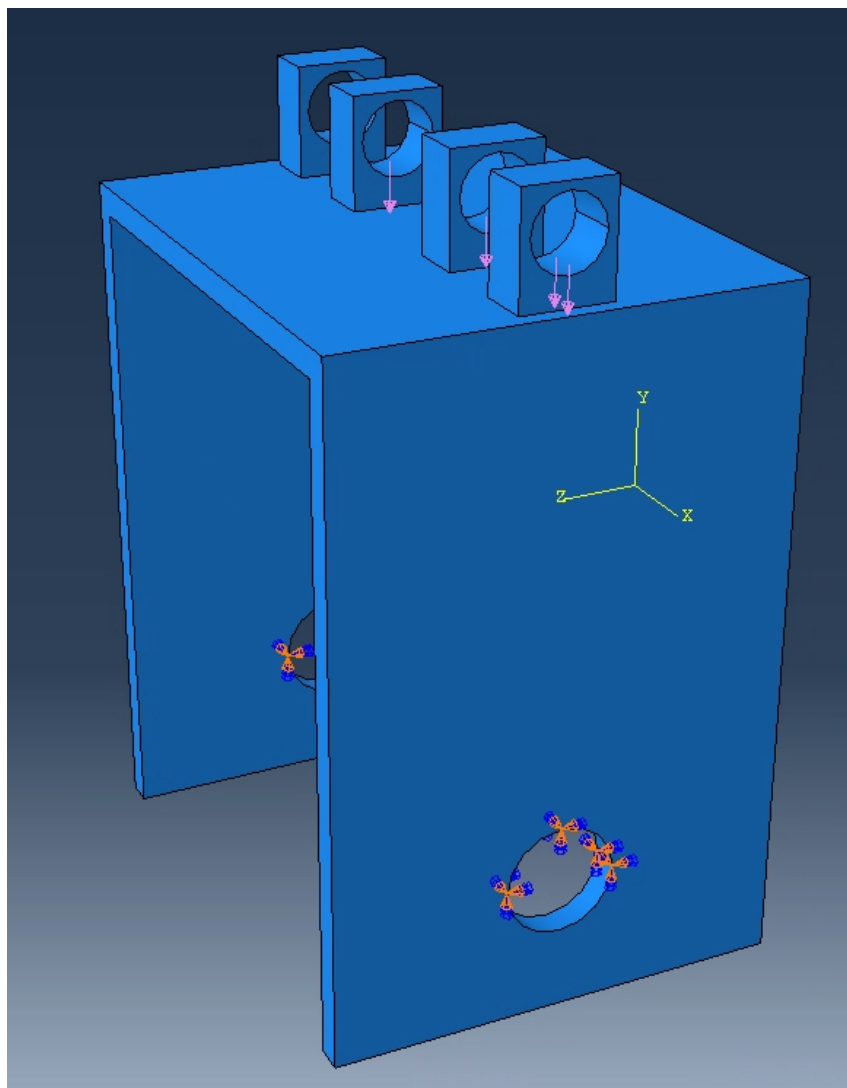


Figure 2.3.1.2.3.1 Wheel housing CAD

Upper housing shaft

The upper housing shaft secures the shock absorber with the wheel housing. A boundary condition has been applied wherever the shaft is secured within the shaft placeholders. A 60kg load has been applied at the centre of the shaft where the shock absorber is expected to be attached.

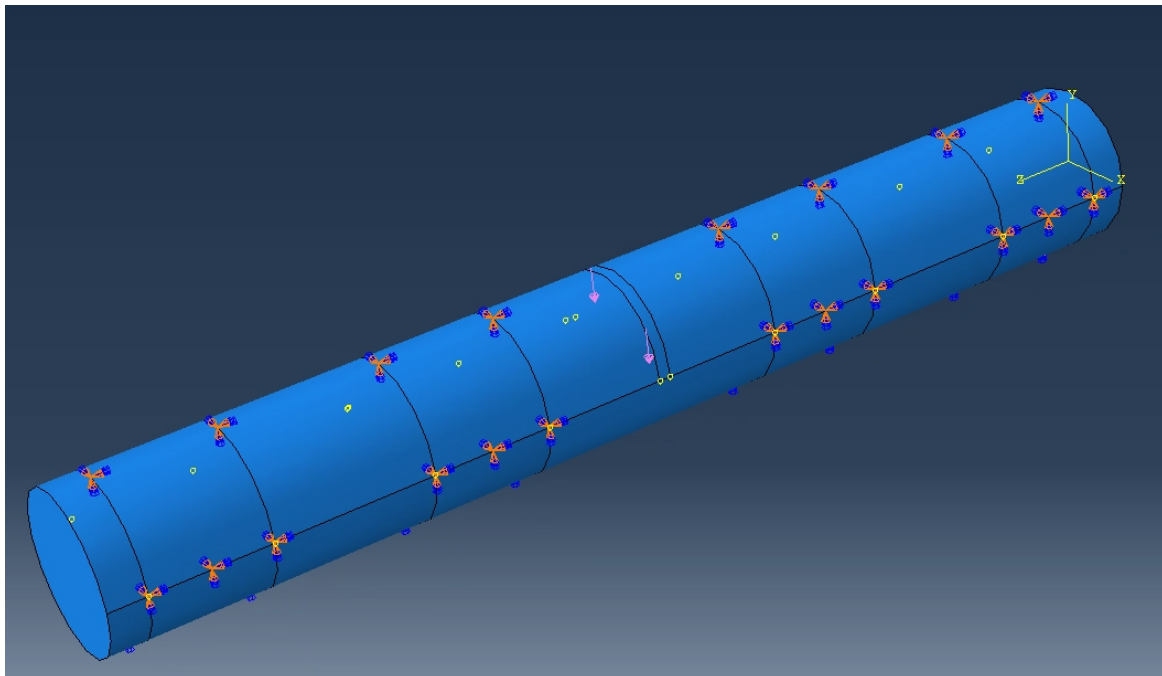


Figure 2.3.1.2.3.2 Upper housing CAD

Mounting Fixture

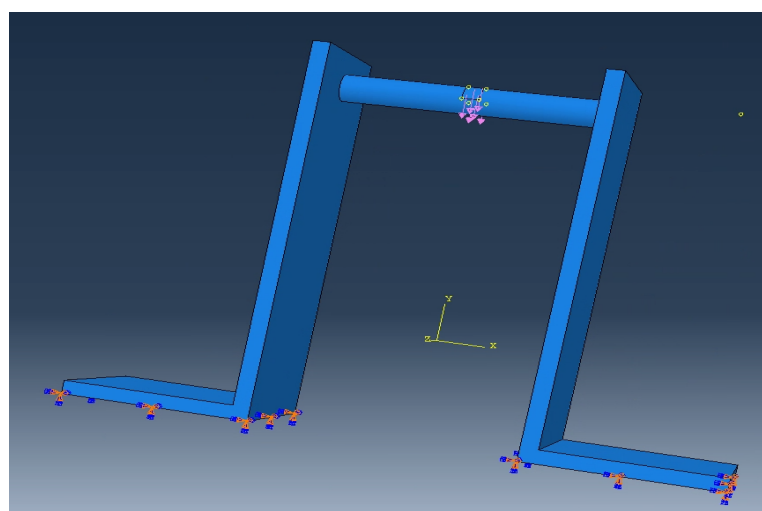


Figure 2.3.1.2.3.3 Mounting fixture CAD

2.3.1.4 Evidence of simulations

The primary focus of simulations was to improve on the design until the safety factor goes above 2. This was achieved by varying dimensions such as thickness or number of supports until the best possible safety factor was achieved. Considering the complex nature of the geometry, a tetrahedral mesh is used with a quadratic basis function for all simulations. The simulations have been conducted on Abaqus software.

Wheel Housing

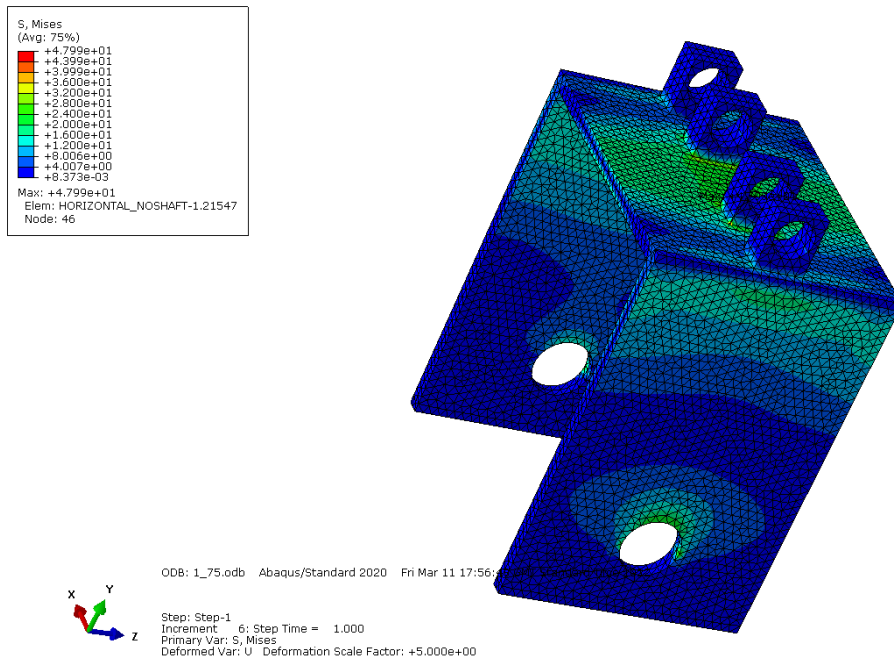


Figure 2.3.1.2.3.4 Wheel Housing

The image above is the final design iteration of the wheel housing. The mesh size was halved until the maximum stress was reasonably converged. The material used was stainless steel which has a tensile strength of 510MPa. Using simulations, maximum stress of 47.99MPa was determined within the housing. This gives a safety factor of 10.6 which is well above the required safety factor of 2.

Upper Wheel Housing Shaft

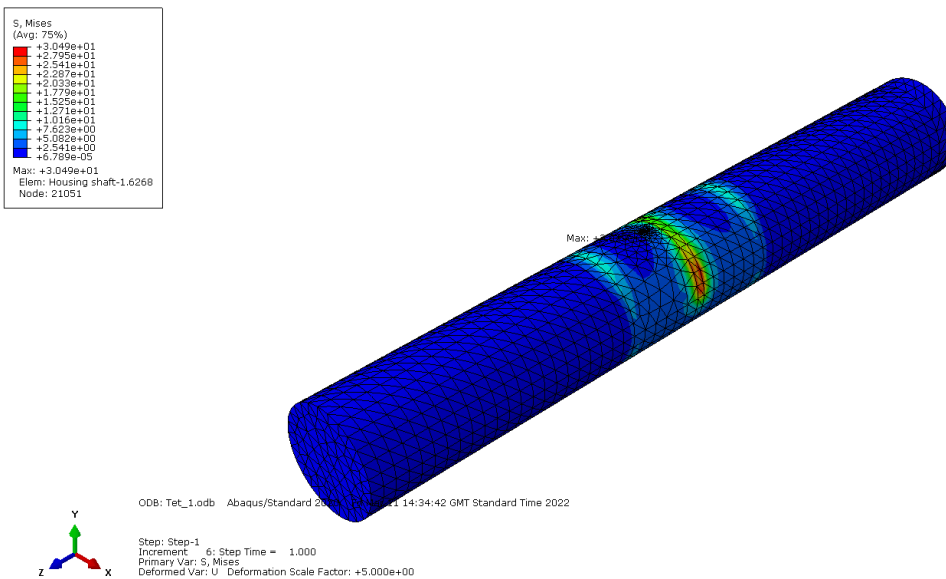
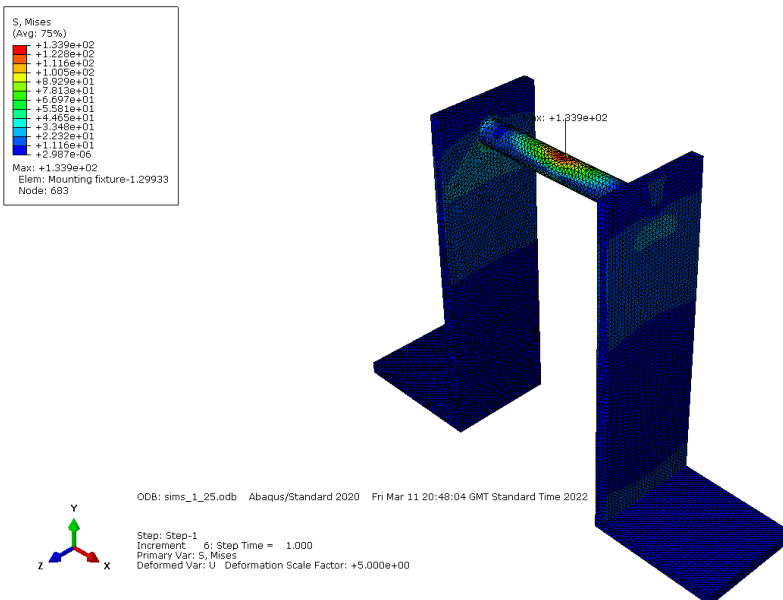


Figure 2.3.1.2.3.4 Upper Wheel Housing Shaft

The maximum stress within the upper wheel housing shaft converged to a value of 36.5MPa. Stainless steel has been used for the rod which has a yield strength of 510MPa. This gives a safety factor of 14.0 which is well above the performance criteria of 2.

Mounting Fixture



A safety factor of 5 was obtained through simulations.

2.3.1.5 Description of the manufacturing processes.

All the suspension parts are customised to fulfil all the requirements, and to facilitate the assembly of the system in the MakerSpace laboratory at Queen Mary University of London. The shaft on top of the wheel housing (the upper housing assembly shaft) is designed to be removable to allow for an easy slide in the shock absorber eye mount.

The first step in the manufacturing process is fixing the shock absorber onto the housing assembly. Jam nuts are used to hold the shock absorber in place and prevent it from turning. The eye mount, jam nuts, and housing assembly holes are aligned to allow the upper housing shaft to be inserted through. This is secured by the screws that pass through the top of the upper housing shaft placeholders.

The wheel of the system system is aligned with the lower wheel housing holes and the wheel shaft is inserted through it. The holes are lubricated to ensure smooth travel, providing the security to either side of the shaft. This step completes the assembly of a single suspension unit. Overall, the whole pod is equipped with 8 suspension units. Three suspension units (1 vertical wheel, 2 horizontal wheels) create a set of suspension that is implemented at the front and rear of the pod. Then, two (horizontal) suspension units are above LIM for additional support of structures.

Each shock absorber is mounted onto the frame by an L-bracket. The L brackets of the shock fixture are screwed into the frame facing the appropriate direction. Through a premade hole within the frame, the shocks are inserted, while keeping the wheel housing still attached. The top eye mount of the shock is aligned with the holes in the L brackets so that a rod can be inserted through. This rod is then further secured with jam nuts to prevent any unnecessary rotation. Thus, either side of the rod is completely secured with simple plates with three screws (2 in the L bracket and 1 in the rod).

2.3.2 Size, Components, Appearance

2.3.2.1 Evidence of CAD models

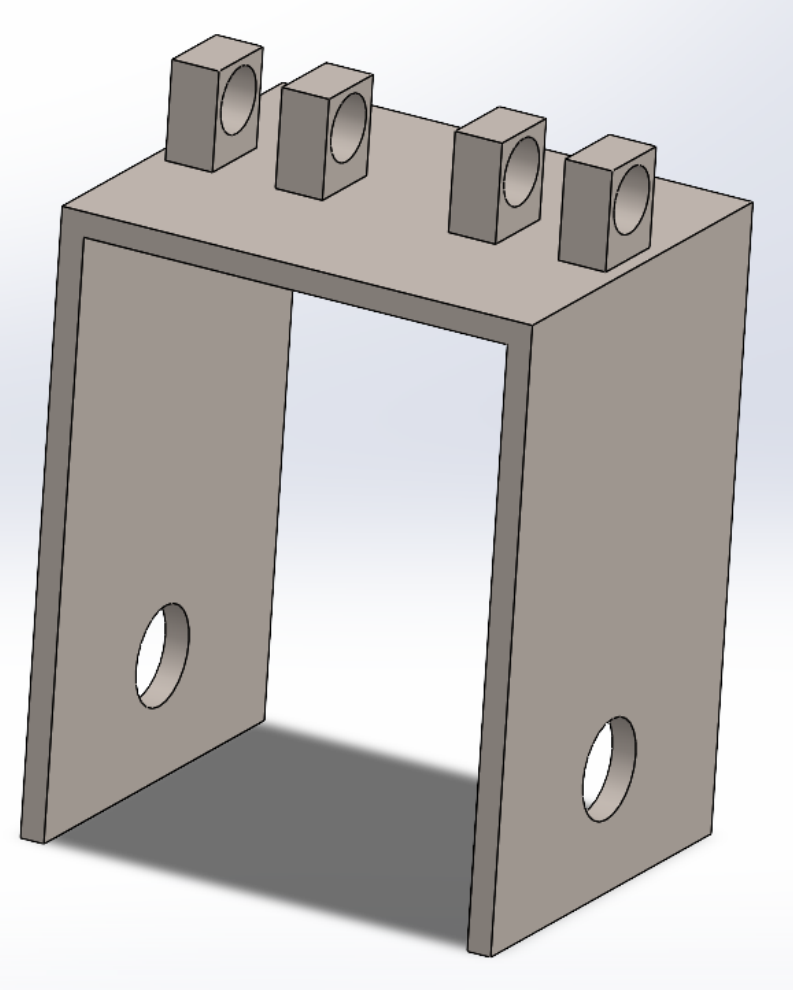


Figure 2.3.2.1.1 housing CAD

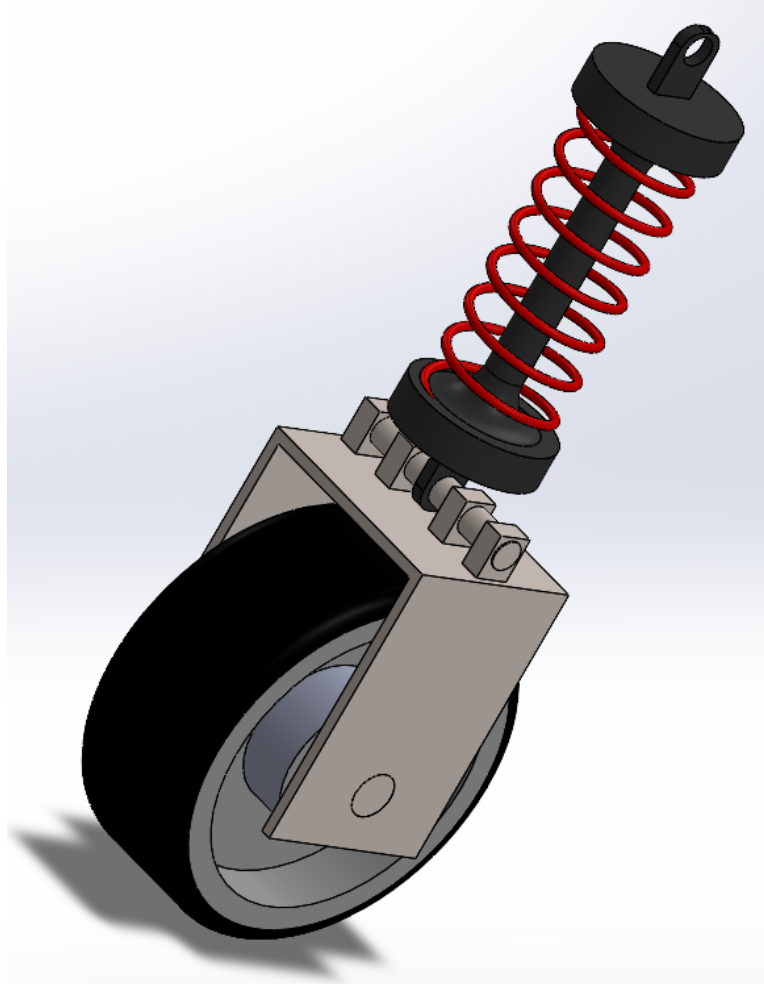


Figure 2.3.2.1.2 Wheel CAD

2.3.3 Integration into a Subordinate Structure/System

A special mounting fixture is designed on which the six suspension systems can be safely attached and then bolted into the top and sides of the frame of the pod. These fixtures are made of Aluminium and have been subjected to simulations to ensure the motors stay in their expected positions at all times while also being light, simple and easy to manufacture.

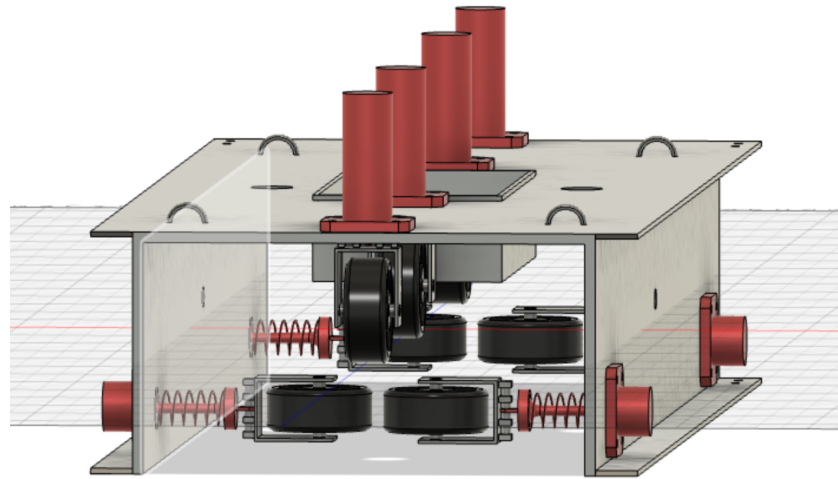


Figure 2.3.3.1. Suspension mounted on the frame

2.3.4 Demonstration Plan

2.3.4.1 Parts List

Table 2.3.4.1.1. Parts Lift of Suspension

Component	Quantity	Mass	Created
Shock Absorber	16	0.5kg	Splumzer
Wheel Housing	16	0.2kg	Slovas
Wheel Shaft	16	0.2kg	Slovas
Lock Nuts	32	0.1kg	RS Pro components
Upper Wheel Housing Shaft	16	0.2kg	Slovas

Shock Absorber Fixture	16	0.2kg	Slovas
Mechanical encoder	Rotary	2	0.3kg Broadcom
Wheel	16	0.5kg	RS Pro components

2.4 Structures

2.4.1 Technical Description of the System

2.4.1.1 Theory and principle physics of desired functionality

Structural integrity is of great importance to ensure the pod can perform its runs successfully, for this reason both the frame and the shell of the vehicle must be built and designed according to the highest engineering standards and with proper understanding of the physics involved in constructing such structural components. Given that the purpose and functionality of the frame and the shell are considerably different, the theory and physics applied to each part are to be described separately:

2.4.1.1 Frame

The frame is the skeleton of the pod, and components such as propulsion, suspension and braking fit inside it in such a manner that they can perform their tasks without interfering with each other, all while still being held in a compact, easily accessible form. Therefore, for the frame to function properly, it is required for it to withstand the loads exercised by all the subsystems inside the pod. Moreover, it is also required to withstand all external forces due to movement of the pod. The frame needs to be as light and as easily assembled as possible, to facilitate transportation of the pod and its maintenance.

For the frame to work as expected, the concepts of stress and strain must be properly understood, as they are essential when designing such structural components. Stress can be described as the force per unit of area of a material subjected from an external load:

$$\sigma = \frac{F}{A}$$

Strain on the other hand is an indicator of stretching deformation experienced by a material under stress, it is commonly represented as the change in length divided by the original length of the object:

$$\epsilon = \frac{\Delta L}{L}$$

The simulations verify the structural integrity and resistance to both expected and unexpected loads. Due to implementation of safety factors of higher order than 2, forces of even larger than expected values can be exerted on the frame, without it experiencing a structural failure. Having performed the initial simulations, and proving that the frame is structurally solid, the topology optimization was conducted to determine the structural redundancy in the design. The simulations allowed for decreasing the overall weight of the structures, and for the optimal distribution of the material within the frame.

2.4.1.1.2 Shell

The shell is a structural part of the pod required to protect both the frame and all the internal subsystems from the external environmental influence during the demonstration. The shell is designed to be both aerodynamically and structurally efficient. It also needs to be able to withstand the forces exerted on it during the pod's run. The movement of the shell is restricted to the maximum as it is not allowed to displace during the demonstration. Hence, it is structurally secured to prevent it from sliding, and then bolted onto the frame.

The aerodynamic concern during the design of the shell is the drag generated due to its shape. The drag force applied on an object can be calculated through the following formula:

$$D = C_D \cdot A \cdot V^2 \cdot \rho/2$$

Where D is drag, A is the area of the surface, V is velocity and ρ is the density of the fluid on which the object flows. As can be seen in the equation, the higher the velocity and density, the larger the drag force. Given that the planned maximum velocity of the pod is of 50km/h, the drag on the pod is too small to have a considerable impact and is therefore not taken into account.

Whether the airflow around the shell is laminar or turbulent can also have a great impact on the drag generated by the pod, this can be studied by analysing the formation of boundary layers around the shell and whether they eventually separate

from the surface of the shell leaving a turbulent wake behind them. The behaviour boundary layers is also greatly influenced by the Reynold's number of the airflow which can be calculated with the following formula:

$$Re = \frac{\rho \cdot v \cdot l}{\mu}$$

Where μ is the dynamic viscosity of the fluid, l is the length of the object, v is the velocity of the fluid and ρ is the density of the fluid. The following image provides a clear explanation on how air flow around an object can change at increasing Reynold number values ([source](#)):

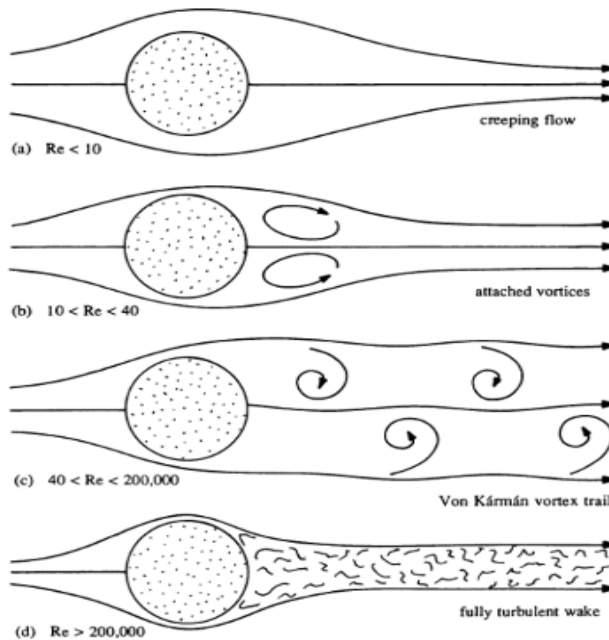


Figure 2.4.1.1.2.1 shows the airflow around the cylinder at different Reynolds numbers

Again, the Reynolds number is directly proportional to the speed of the object and the density of the air around it, and while very high Reynolds numbers are still achievable under these conditions, the effects of a turbulent wake around the pod are considered negligible.

Taking into account the rather small impact of aerodynamic forces on the shell, it is decided to give priority to aesthetic appeal when designing the shell. Although in future cases where the pod might be expected to move at much higher speeds (perhaps even supersonic speeds), all design choices will be subjected to CFD simulations to ensure they can handle the aerodynamic forces applied on them.

2.4.1.2 Design process

The initial design process required a setup of certain requirements for both structural parts. The requirements represent not only the Hyperlink's design philosophy of this year's project but also the team's design vision of the hyperloop. The main requirements and assumptions, identified as a design priority, are presented below.

2.4.1.2.1 Shell

The main design requirements for the structural shell are the following

- Good aerodynamic performance
- Easy access to all subsystems: achieved by an easily removable shell (the process of mounting and unmounting the shell should take less than 2 minutes)
- Subsystems protection: the shell must provide an adequate shielding for all instruments inside the pod
- Air inlet: a small amount of air should be allowed to flow inside the shell to provide additional cooling to the internal subsystems
- Structural Integrity
- Structural Resistance to all the Loads and Forces

The shape of the shell was primarily determined by its function which is to cover all the internal subsystems of the pod. Therefore, the shape is similar to a droplet, with a few bulks on top, to allow for accommodation of air reservoirs and batteries. The shell is designed to be equipped with an inlet at the front of the nose, to allow the air to freely travel through the system and efficiently cool it. The back of the shell is open to the environment, to allow the air to escape.

The shell needs to be strong enough to withstand all the loads exerted during the demonstration. However, it is required to be of a relatively light structure, so it does not add unnecessary weight to the pod. Therefore, the weight and structural resistance ratio had to be balanced, and it was achieved by selecting the material and the manufacturing technique for the shell. The material chosen for the shell is PA 2200 Nylon and the shell's manufacturing method is further described in detail in section 2.4.1.6 *Manufacturing Process*. The CAD model of the shell is presented below.



Figure 2.4.1.2.2. Rendering of the pod's shell

2.4.1.2.2 Frame

The main objectives of the frame are the following

- Structural Integrity
- Structural Resistance to all the Loads and Forces
- Subsystems accommodation
- Easy accessibility to subsystems
- Deformations, bending, fractures resistance

As the frame is required to cover all the internal subsystems, an inverted U-shape equipped with extensions at the top and bottom was selected. The initial design of the frame was presented in the Intend to Demonstrate Documentation (ITD). The following CAD image illustrates the initial design of the frame.

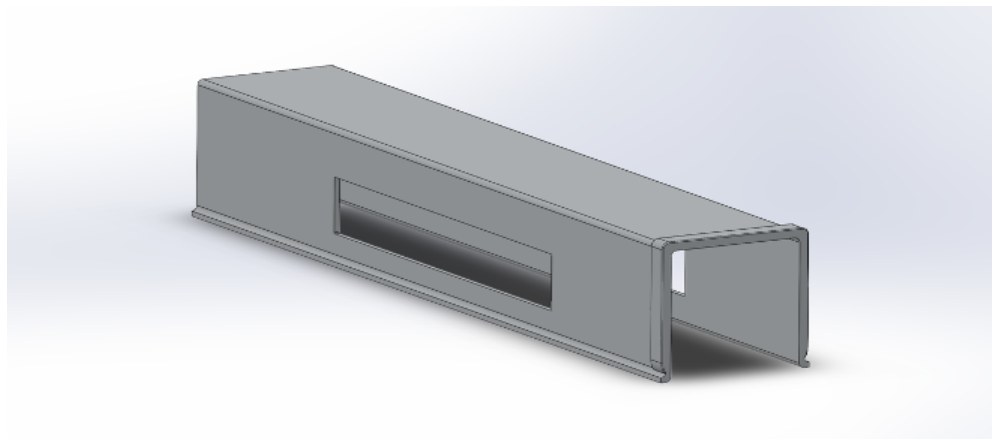


Figure 2.4.1.2.2.1. Initial Design of the Frame

The design of the frame was adjusted according to each subsystem, to accommodate all the systems while maintaining good structural integrity. The final design of the frame is presented below.

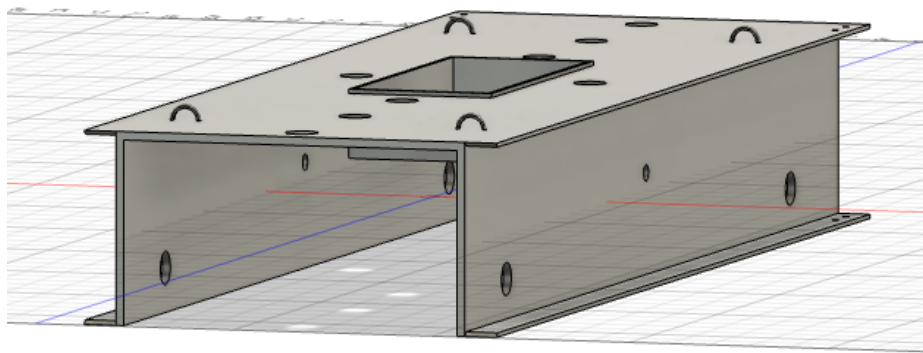


Figure 2.4.1.2.2.2. Final CAD Design for the Frame.

Structural FEA simulations were performed on the frame in Fusion360 software to predict its stress capacity and to ensure no bending and failure occurs under the loads of the subsystem. The factor of safety higher than 2 was applied and structural simulations are presented in section 2.4.1.4 *Simulations*.

The frame also has to provide attachment points for the shell to stand firmly in its position, this is achieved by making the shell slide into position, to that end, four extensions have been added on the sides of the frame which will act as a rail on which the shell can slide. Once placed in position, the shell will then be bolted into the frame. The following CAD images provides a clear view on the updated frame design and on how the sliding mechanism is meant to work:

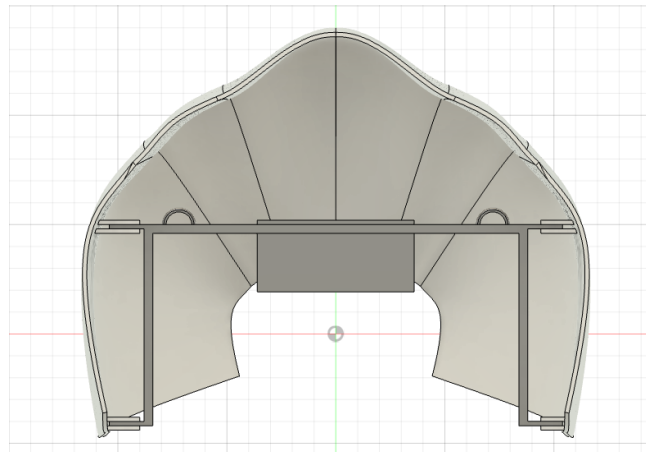


Figure 2.4.1.2.2.3 Rear view of the shell mounted on the frame, notice how the extensions are used as a guide to slide the shell into place.

2.4.1.3 Free Body Diagrams to define load cases for simulations.

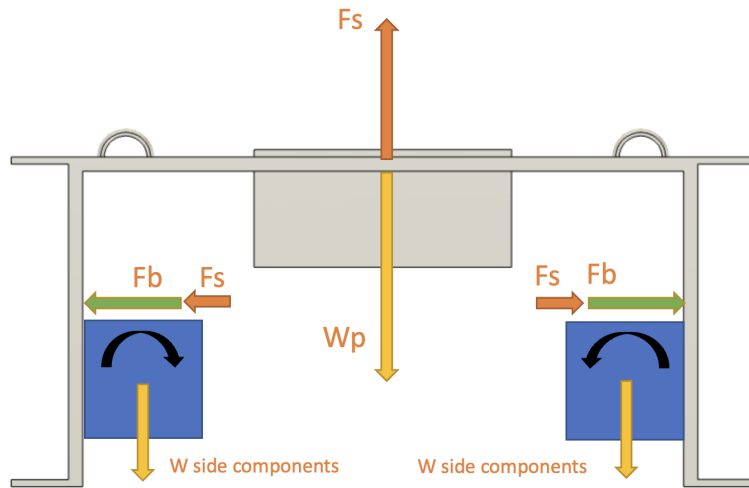


Figure 2.4.1.2.2.4 :Free body diagram of forces acting on the frame

This Free Body Diagram indicates the distribution of loads on the frame, where W_p is the weight of the pod itself, F_s is the balancing force of suspension, W_{prop} is the weight of propulsion and the bending moment it generates, and F_b is the reaction force generated when the brakes are engaged.

2.4.1.4 Evidence of simulations validating the theory, and detailed analysis of results.

Before running any simulations, the different conditions for structures are determined. Three different scenarios exist when the loads and forces applied on the structure would vary: The static operation (the pod standing on its own with no movement), the dynamic operation (pod standing on its own and with activated propulsion), and the braking operation (where the linear induction motor is stopped and the brakes are engaged). Having specified these conditions, the normal and expected loads for each scenario based on the calculations of each team are applied on the CAD model of the frame, and using the Fusion 360 simulation software the following results were obtained:

2.4.1.4.1 Static Operation

For the static simulation, loads are applied to allow for simulating the weight of each component in its corresponding position on the frame. For increased reliability and in order to maintain the specified safety factor above 2, the applied loads are two times greater. The following images showcase the stress, displacement and strain exercised on the frame when handling the weight of the hyperloop pod itself.

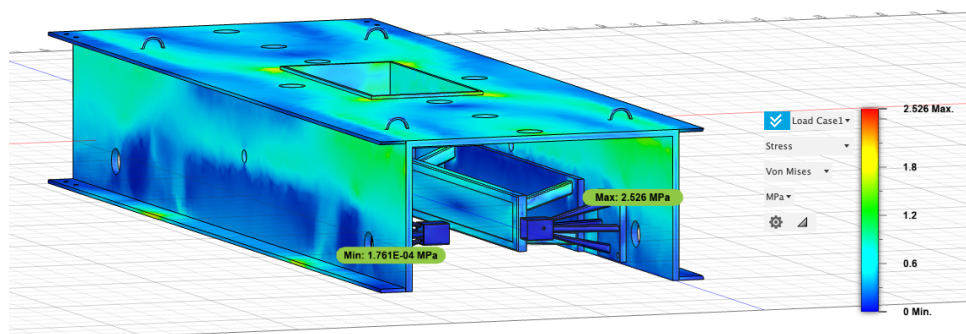


Figure 2.4.1.4.2 Stress experienced by the frame (MPa)

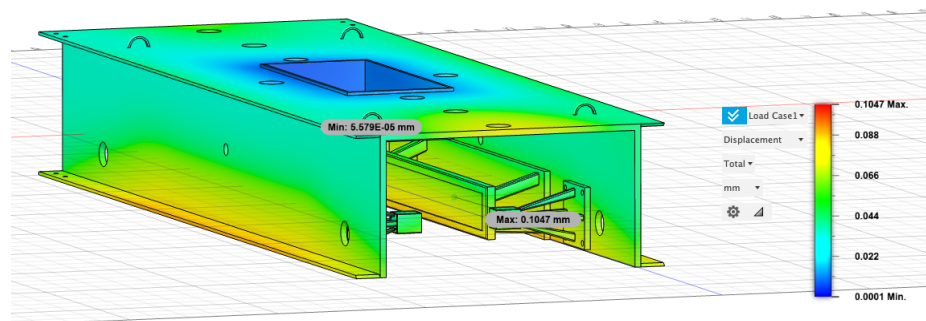


Figure 2.4.1.4.3 Displacement on the frame (mm)

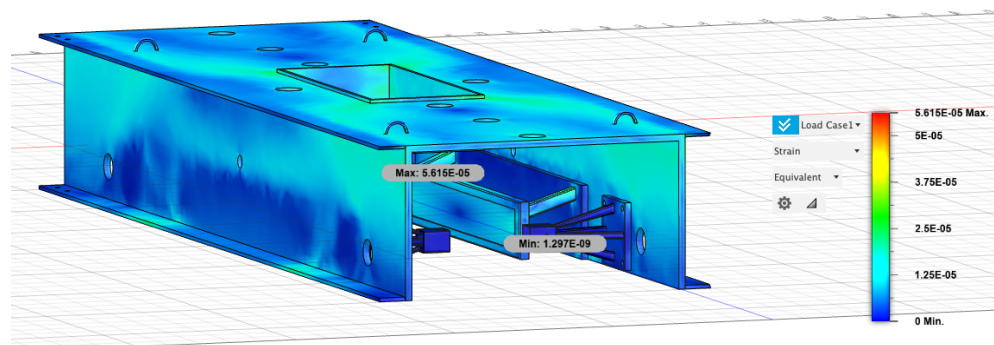


Figure 2.4.1.4.4 Strain on the frame

As seen in the simulations, the amount of stress and strain on the frame is minimal and well within the tensile strength of aluminium 6061 T6. There is however some very minor deflection on the lower part of the frame, but at fractions of a millimetre it can be considered to be negligible, and the structure is assumed to maintain its structural integrity during the static operation.

2.4.1.4.2 Dynamic Operation

As part of the second round of simulations, loads were applied to understand how both the frame and the mounting supports for the linear induction motor would handle the effects of propulsion. These loads, alongside the loads studied previously resulted in the following images:

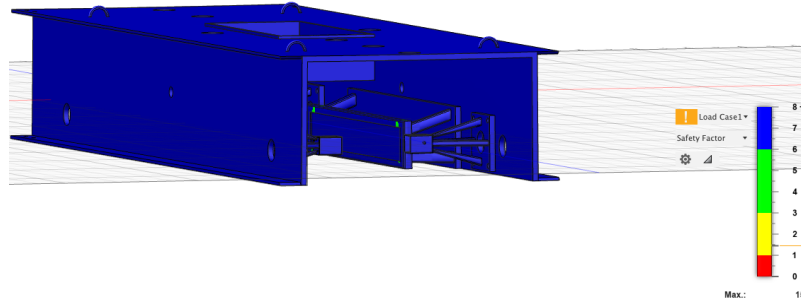


Figure 2.4.1.4.2.1 Safety factor on the frame (notice the change of colour in the mounting supports)

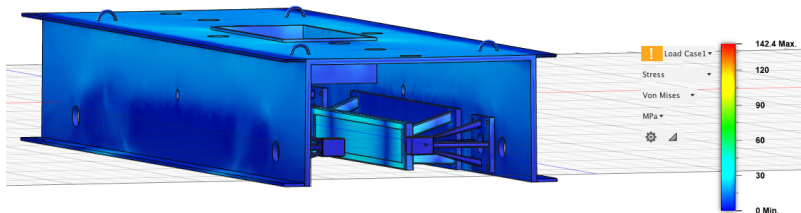


Figure 2.4.1.4.2.2 Stress experienced by the frame (MPa)

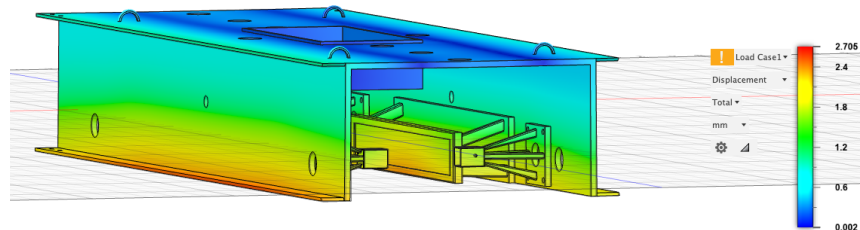


Figure 2.4.1.4.2.3 Displacement on the frame (mm)

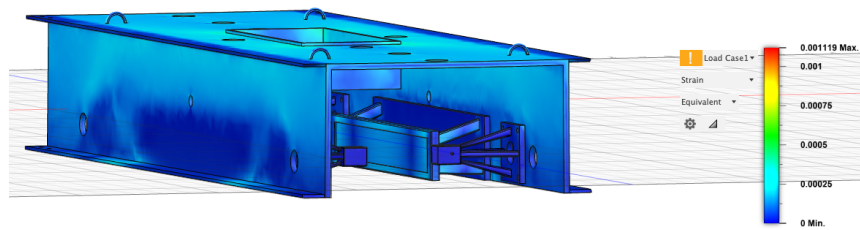


Figure 2.4.1.4.2.4 Strain on the frame

Activating the motors results in greater loads applied on the frame. As can be seen in the simulation stress and strain are highest on the mounting fixtures for the LIM,

reaching a maximum stress of 142MPa, on the corners of said fixtures the safety factor is at its lowest reaching a minimum of 2.5, some increased deflection can be seen again on the lower part of the frame, but again it can be considered minimal.

2.4.1.4.3 Braking Operation

Perhaps the most dangerous of the three scenarios, the frame must be able to resist the large forces generated once two braking systems are engaged (braking scenario II, emergency procedure). Again, the frame and mounting fixtures for the brakes are being tested to their limits, and it is therefore crucial that all components remain within the specified safety factor. In this case, the loads are applied to simulate the emergency scenario where both braking systems are activated at once, therefore generating double the force expected in a normal run. The following images indicate the simulation results for activated breaking.

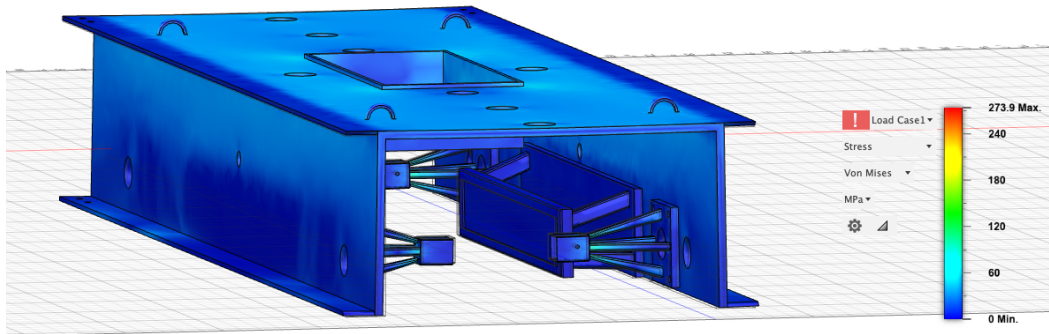


Figure 2.4.1.4.3.1 Stress experienced by the frame (MPa)

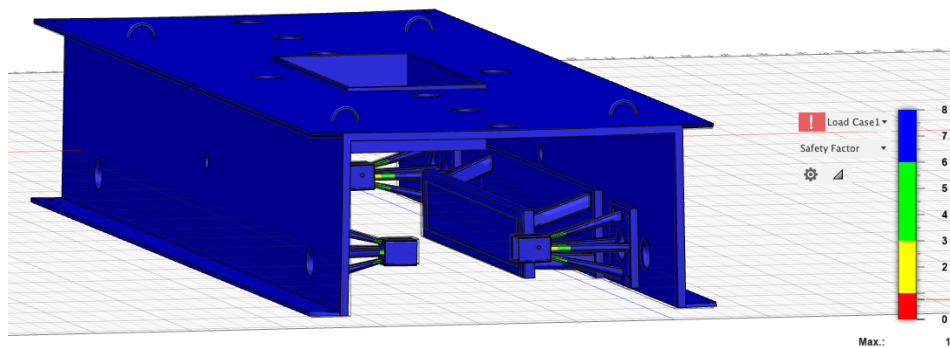


Figure 2.4.1.4.3.2 Safety factor on the frame (notice the change of colour in the braking supports)

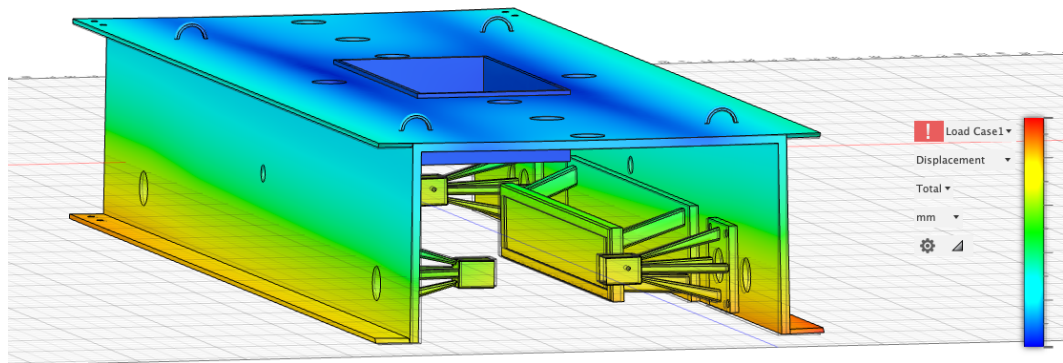


Figure 2.4.1.4.3.3 Displacement on the frame (mm)

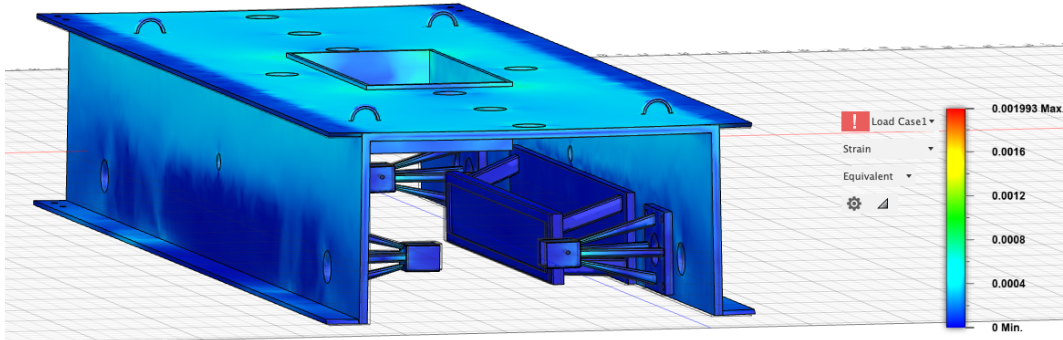
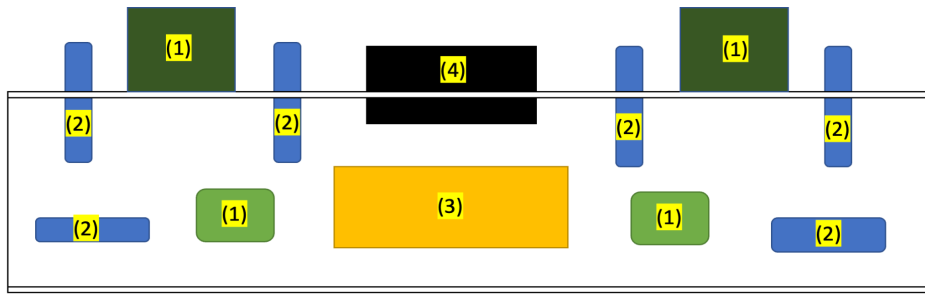


Figure 2.4.1.4.3.4 Strain on the frame

As can be seen in the pictures, stress and strain are highest at the mounting points for the brakes, and the safety factor is also lower at that point. An increased deflection of over 1mm can now be seen on the lower part of the frame, but considering this is an emergency scenario such relatively small displacements are deemed acceptable when security is paramount and stopping the pod as fast as possible is necessary.

2.4.1.5 Dimensioning process

The dimensioning process of the structure is directly related to the design process, as the shape and dimensions of the structural components are dependent on the size and requirements of all the different instruments inside the pod. Therefore, the dimensions of the frame and pod iterated as other teams made progress towards finalising their designs. Once each team had provided the dimensions and requirements for their components, it was agreed to organise all machinery inside the frame the following way:



(1): Braking and Air reservoirs

(2): Suspension

(3): Propulsion

(4): Battery

Figure 2.4.1.5.1: Distribution of components inside the frame

Based on this distribution, and knowing the size and dimensions of each component, the following dimensions were chosen for the frame:

Table 2.4.1.5.1: Dimensions of the frame

Height	230mm
Length	1500mm
Width	420mm
Thickness	10mm (5mm for the shell aligning rails)
Weight	38.7Kg

It must be noted that the thickness of the frame is chosen based on extensive simulations which were made to ensure the pod was capable of operating with no significant deflections or fractures. Regarding the choice of material, several factors had to be taken into account: tensile strength, heat capacity, weight, ease of manufacturing, and price. After extensive research and analysis, the best available options were carbon fibre and aluminium 6061, both of these materials provide great structural integrity, and while the 800J/g K heat capacity and 228 GPa tensile strength of carbon fibre is much higher than that of aluminium (0.896J/g K and 290MPa), it was finally decided to use aluminium due to the fact that the far superior ease of manufacture and manipulation, alongside its light weight, make aluminium 6061 a good choice in terms of safety and ease of use.

Having specified the dimensions of the frame, deciding on the size of the shell proved to be relatively straight-forward, the shape already designed was adjusted to fit around the frame and simulations were run to ensure its structural stability, resulting in the following measurements:

Table 2.4.1.5.1: Dimensions of the shell

Height	456mm
Length	2100mm
Width	577.3mm
Thickness	5mm
Weight	16.20Kg

Choice of materials for the shell proved to be relatively easier, given that the aerodynamic forces at 50km/h are close to negligible, it was decided to use the lightest possible material that would also remain structurally stable. After careful consideration PA 2200 Nylon was chosen, which can be used on 3D printing devices, therefore simplifying the manufacturing process, and after testing the shell on simulations it also proves to be structurally stable and capable of providing adequate cover for the pod.

2.4.1.6 Manufacturing Processes

The manufacturing of all structural components of the pod is to be outsourced in order to ensure the final product is of the highest possible quality and guaranteed to perform successfully.

As previously mentioned, the shell will be produced by a 3D printing company specialised in large and complex shapes such as the shell. The material used will be PA 2200 Nylon, and the 3D printing technique used will be Fused Deposition Modelling (FDM). One great benefit of using 3D printing for the shell is the ability to change the infill density wherever more strength is needed, this means that certain structural weaknesses can be easily solved by printing more material around those areas to ensure greater strength and stability.

Regarding the frame and the mounting supports for propulsion, braking and suspension, those will be manufactured externally by Slovas and will arrive ready to

use after being constructed. Some minor adjustments will have to be made at the maker space lab in Queen Mary University, where the mounting fixtures will be welded and bolted and specific gaps will be made on the frame to allow passage for cables and pipes.

2.4.2 Size, Components, Appearance

2.4.2.1 Evidence of CAD models

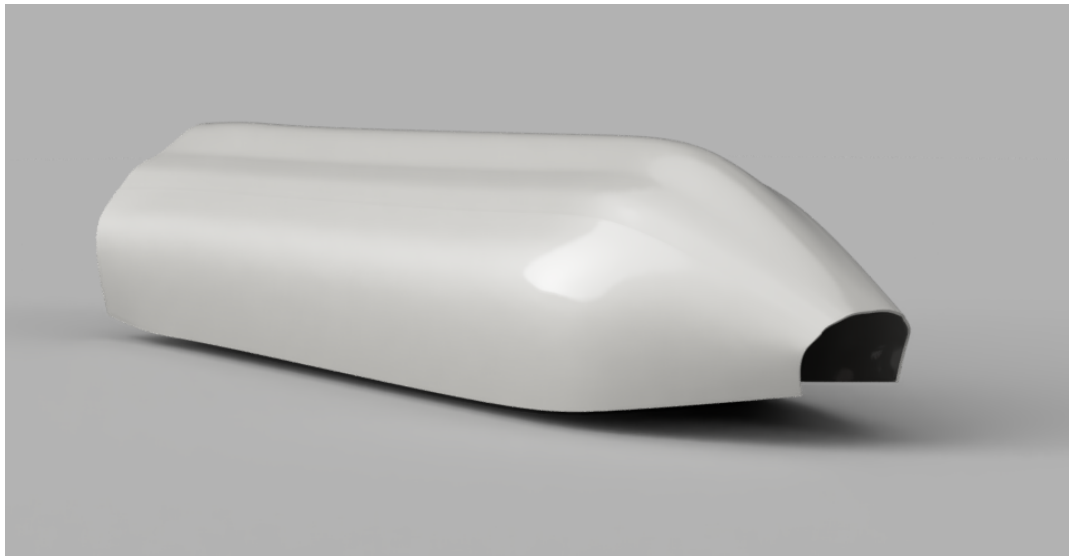


Figure 2.4.2.1.1: CAD of the shell



Figure 2.4.2.1.2: CAD of the shell



Figure 2.4.2.1.3: CAD of the frame with mounting fixtures inside

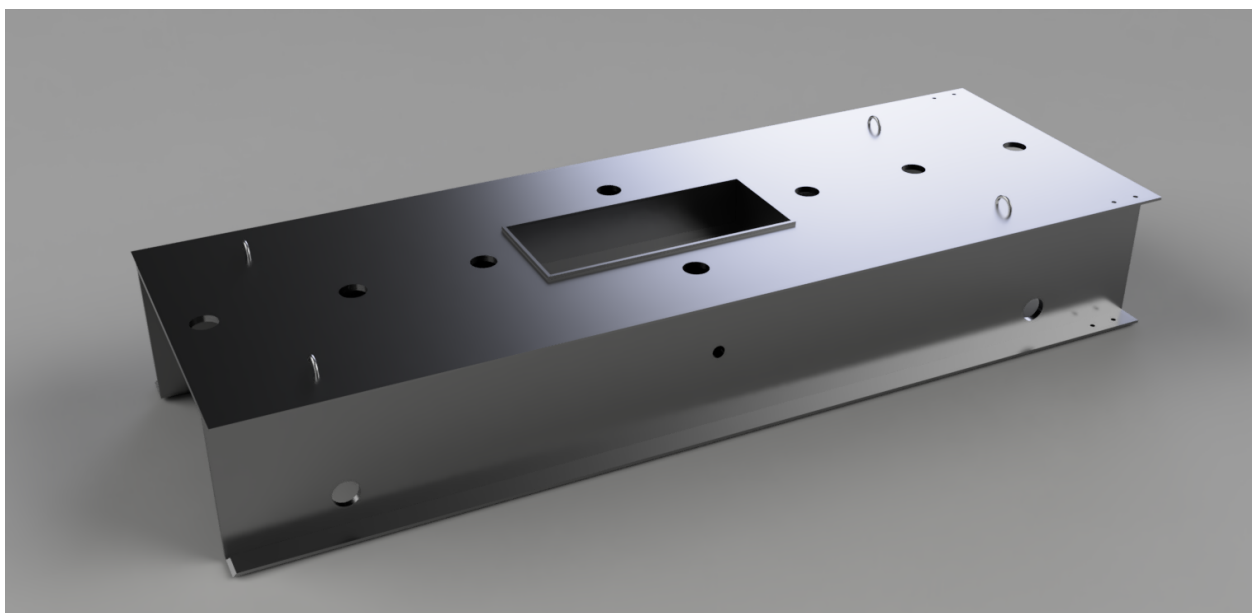


Figure 2.4.2.1.4: CAD of the frame

2.4.2.2 Technical drawings

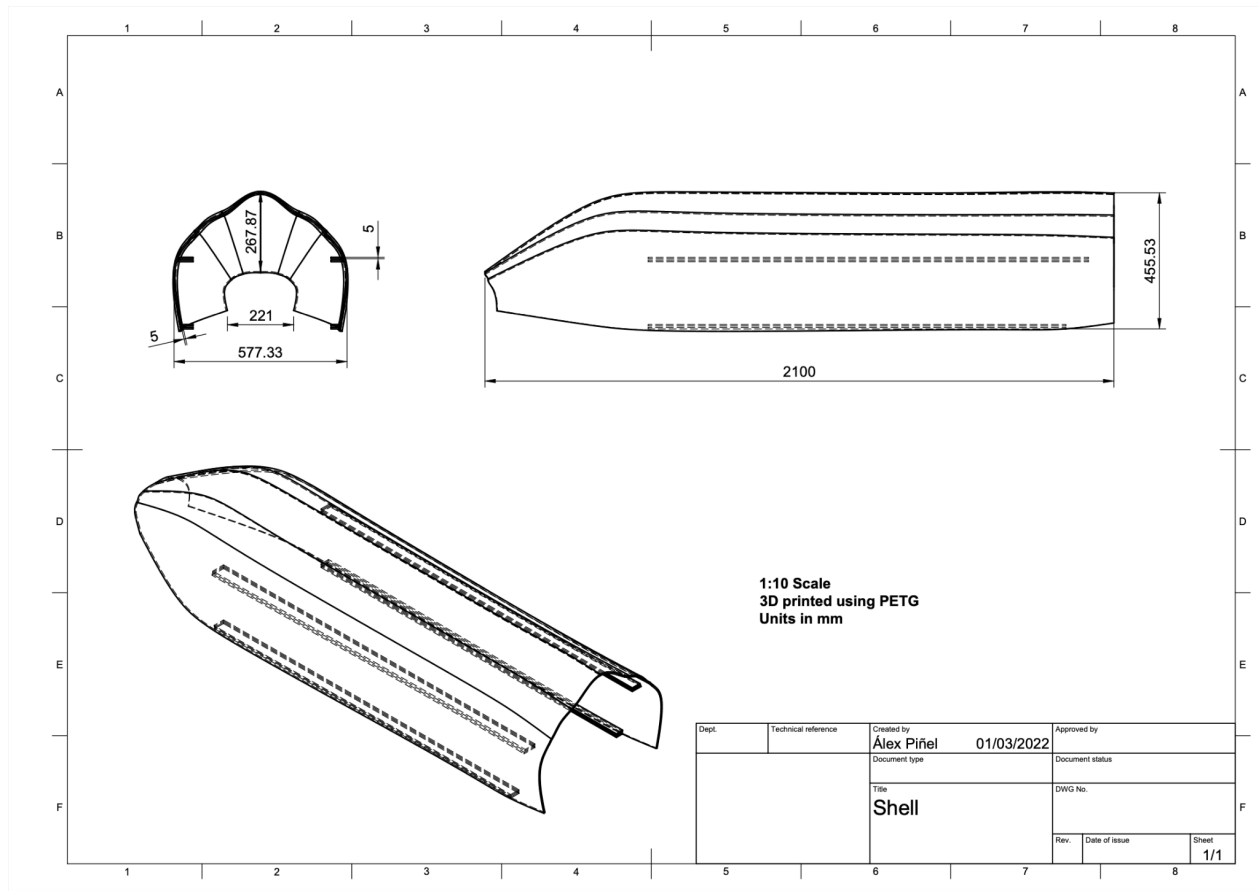


Figure 2.4.2.2.1: Technical drawing of the shell

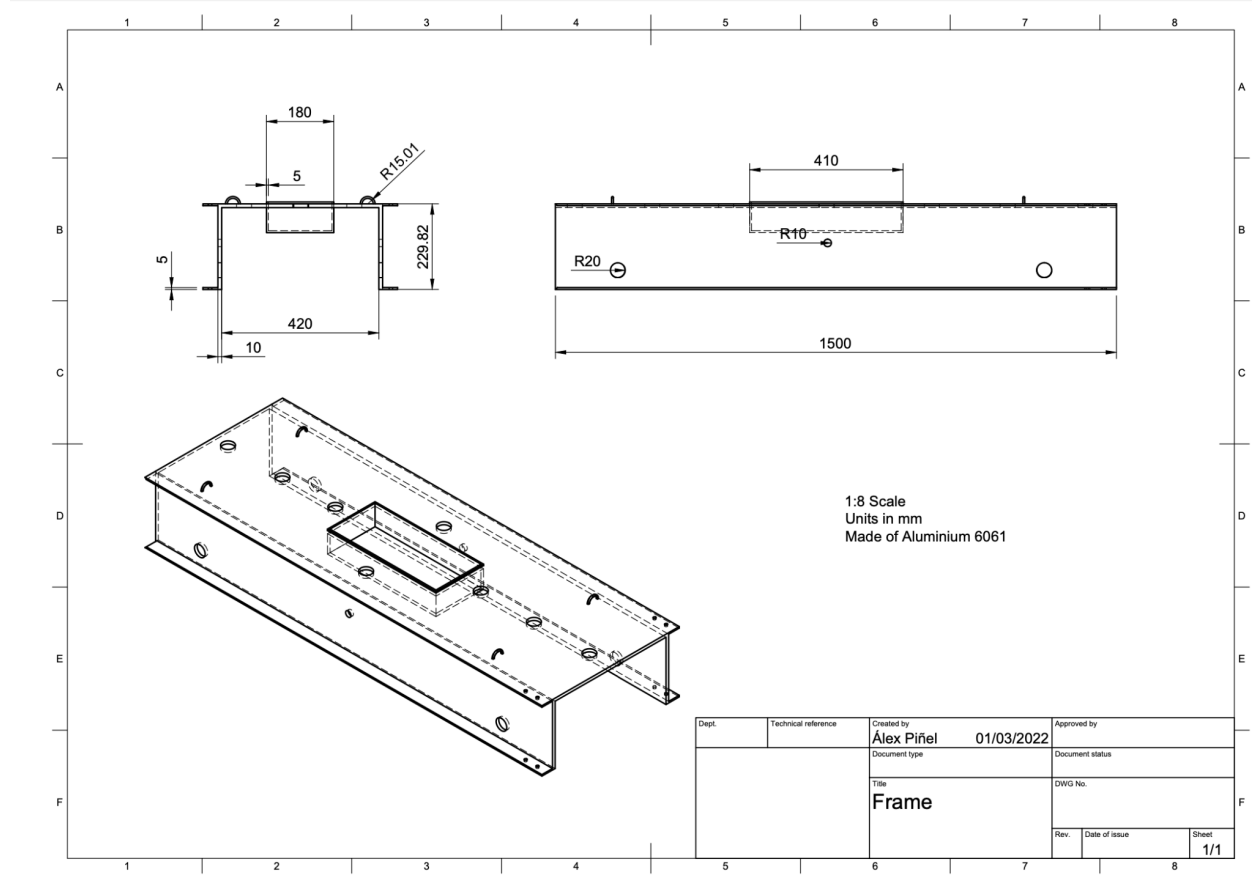


Figure 2.4.2.2.2: Technical drawing of the frame

2.4.3 Integration into a Subordinate Structure/System

The frame is the skeleton on which all components are integrated, all information on how these components are attached to the frame can be found in parts 2.1.3, 2.2.3, 2.3.3, and 2.5.3. The sliding mechanism through which the shell is attached is also described in part 2.4.1.2.

2.4.4 Demonstration Plan

2.4.4.1 Parts List

Table 2.4.4.1.1. Parts List of Structures

Component	Quantity	Dimensions	Mass	Created
Shell	1	2100x458x578mm	16.2kg	Outsourced
Frame	1	1500x420x230mm	38.7kg	Outsourced

Propulsion mounting	2	600x130x110mm	3kg	Outsourced
Braking mounting	4	100x100x200mm	1kg	Outsourced

2.5 Electronics & Power

2.5.1 Technical Description of the System

2.5.1.1 Theory and principle physics of desired functionality

The *Electronics and Power* team is responsible for delivering a highly-efficient and reliable power and control system. By integrating a Lithium-Ion battery, with electrical actuators and custom-built electronic subsystems a comprehensive arrangement capable of steering a complete Hyperloop Pod can be obtained. By an efficient application of a system-approach and decomposing the design into individual subparts, a maximum security and operation predictability is achieved.

It was decided to isolate each particular subsystem of the pod (Braking, Propulsion, Motherboard, Power) into an individual electronic module. All of these are securely interconnected with each other via an automotive-grade *Controller Area Network* (CAN) bus. Thus, by not implementing a centralised master unit, a communication system is highly secure. In addition, the Motherboard, serving as an interface between the vehicle and the control station, is capable of communicating via Ethernet (Wi-Fi), by utilising an on-board TCP/IP stack. This allows for a seamless integration with a control station, uninterrupted commands, and diagnostic data exchange.

2.5.1.2 Description of design process taken.

Research completed on electrical components and the related circuit designs used in practice. Manufacturers' data sheets and evaluation boards were used extensively. Conceptual designs for circuits for each board were drawn up using box diagrams. Specific functions of each board and the required components were listed. Each board was designed individually around the STM32 microcontroller in *Altium Designer*. A common input voltage of 24V was selected based on the power consumption evaluation. Circuit designs were transferred into the component placement system. CAD and GERBER files were generated for manufacturing. Several quality assurance steps were implemented for the final design.

Motherboard is designed to establish communication between the boards and with the outside (L6360 IO link, W6100 Ethernet module), as well as to collect data (FXOS8 Accelerometer). Braking operates motor drivers responsible for operation of the braking system (DRV8871) and collects data from optical encoders for telemetry purposes. Propulsion controls a 3-phase motor using STMicroelectronics STDRIVE components. It has a separate power source, independent from the low-voltage logic power supply, drawn directly from the battery.

A 47V Li-ion battery (LiTech Power 13S10P) was selected as the main power source. Integrated Battery Management System (BMS) board implements several safety systems including over charge/discharge protection, short circuit protection, overcurrent protection and temperature control. All the subsystems are grounded appropriately to the chassis to make sure that the ground potential level is always maintained at 0V in the circuit. The internal power structure Power is responsible for distributing battery charge throughout the system as well as providing additional safety systems for the battery. Step down circuitry was designed to provide 24V for each board. A smaller startup battery (24V, max discharge current 2A) is attached only during the initial deployment on the I-beam and the stationary test. It is used to power the system during the testing to avoid using the high capacity battery for safety. Highest safety measures are in place when the main battery unit is connected, including suitable PPE equipment for the system operator.

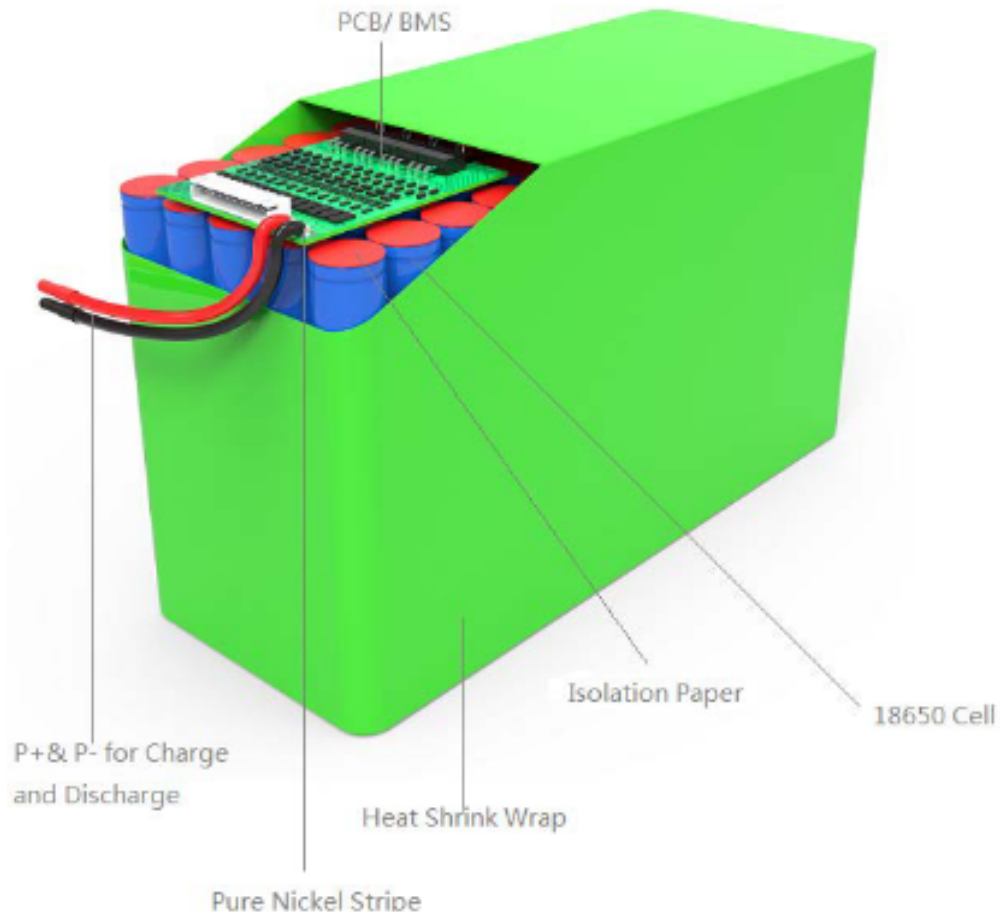


Figure 2.5.1.2.1 47V battery with integrated BMS

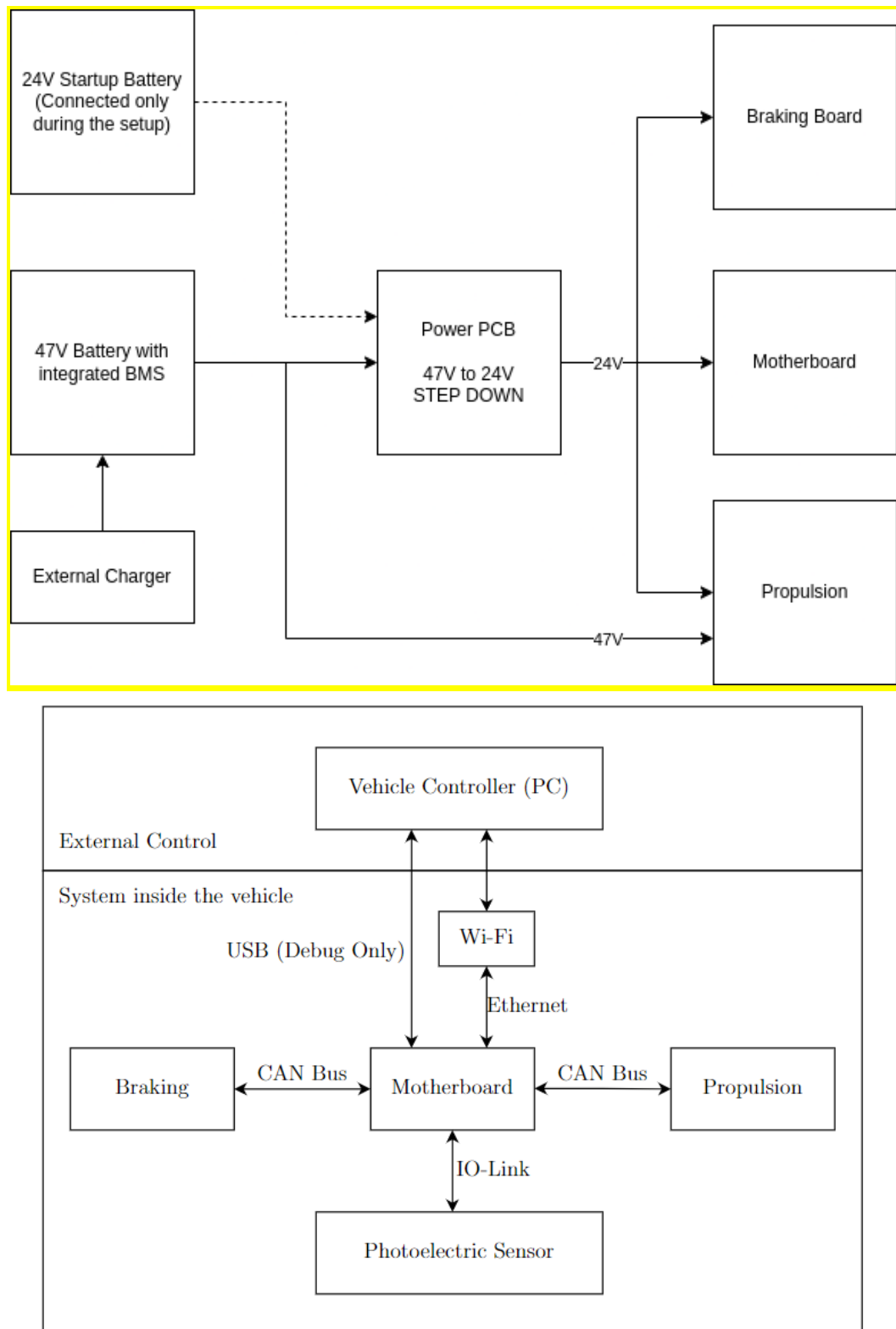


Figure 2.5.1.2.2 Diagram of the electronics subsystem interconnection

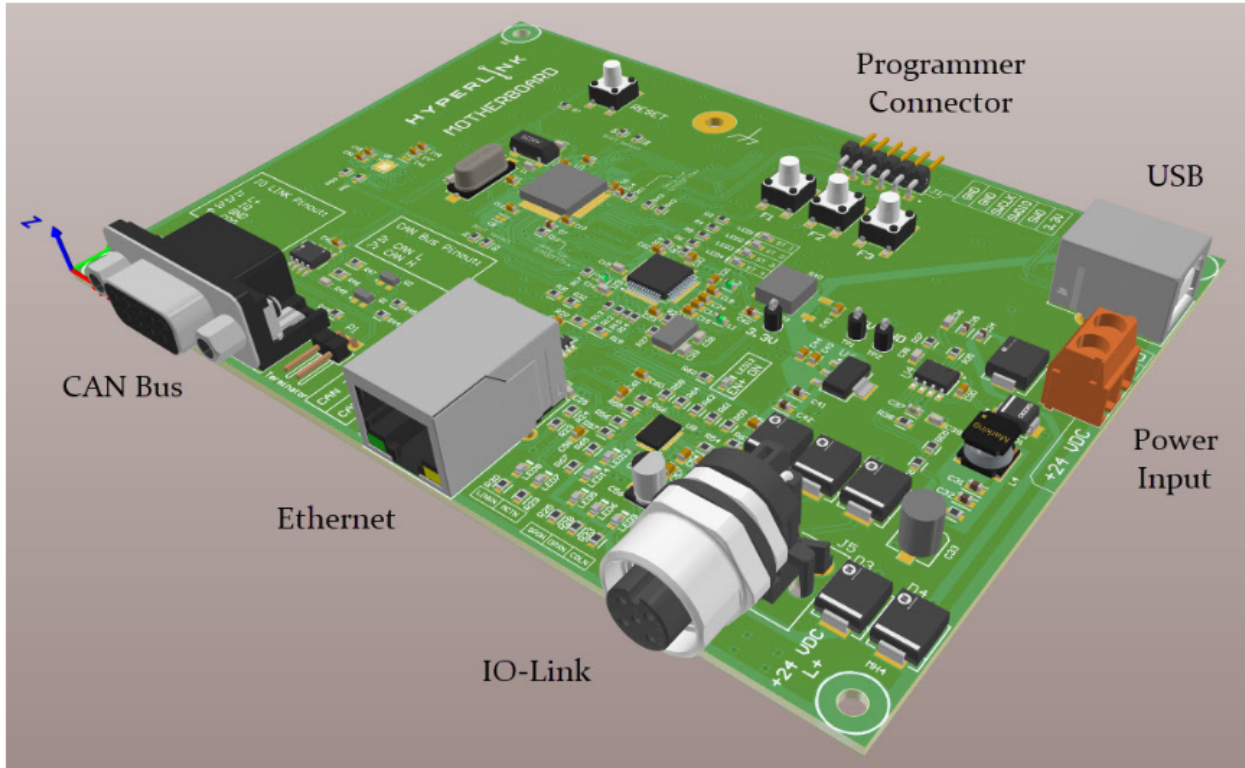


Figure 2.5.1.2.3 3D model of the motherboard

2.5.1.4 Description of the manufacturing processes.

Batteries are ordered as off-the-shelf products and are manufactured by the *Li-Tech* company which is also responsible for embedding safety-related circuitry within the integrated battery management system. On the other hand, all the PCB boards are manufactured and assembled by a PCB manufacturer. All the physical tests related to the PCB electrical performances are performed in the assembly house.

2.5.2 Size, Components, Appearance

2.5.2.1 Evidence of CAD models

Relevant evidence of the manufactured PCB boards is presented throughout this subsection. This also outlines the environment in which all the preliminary electrical tests take place, before mounting them into the Hyperloop pod structure.

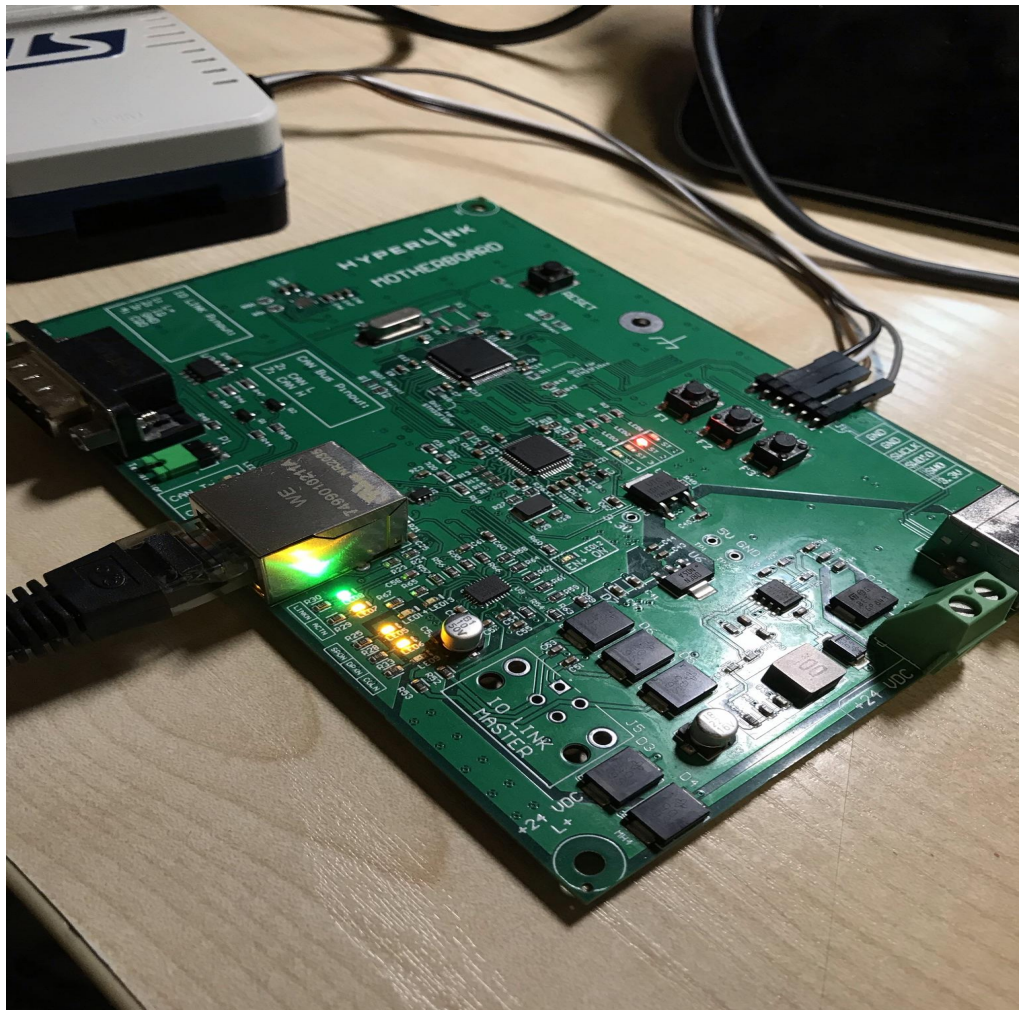


Figure 2.5.2.1.1 Assembled Motherboard

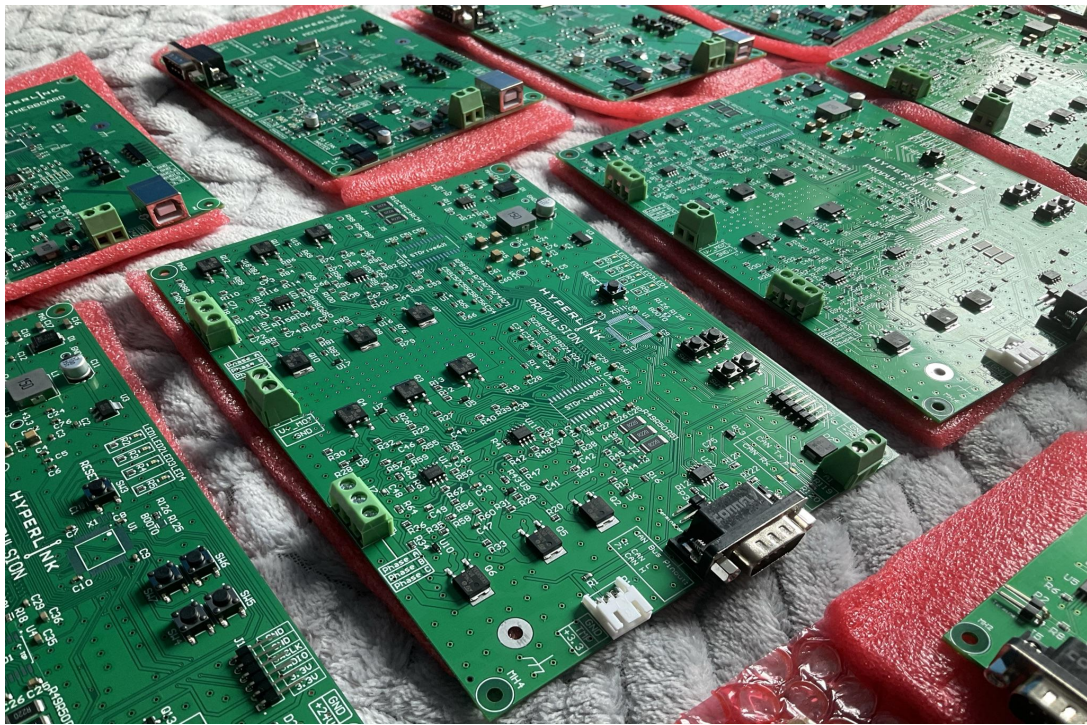


Figure 2.5.2.1.2 Assembled Propulsion boards

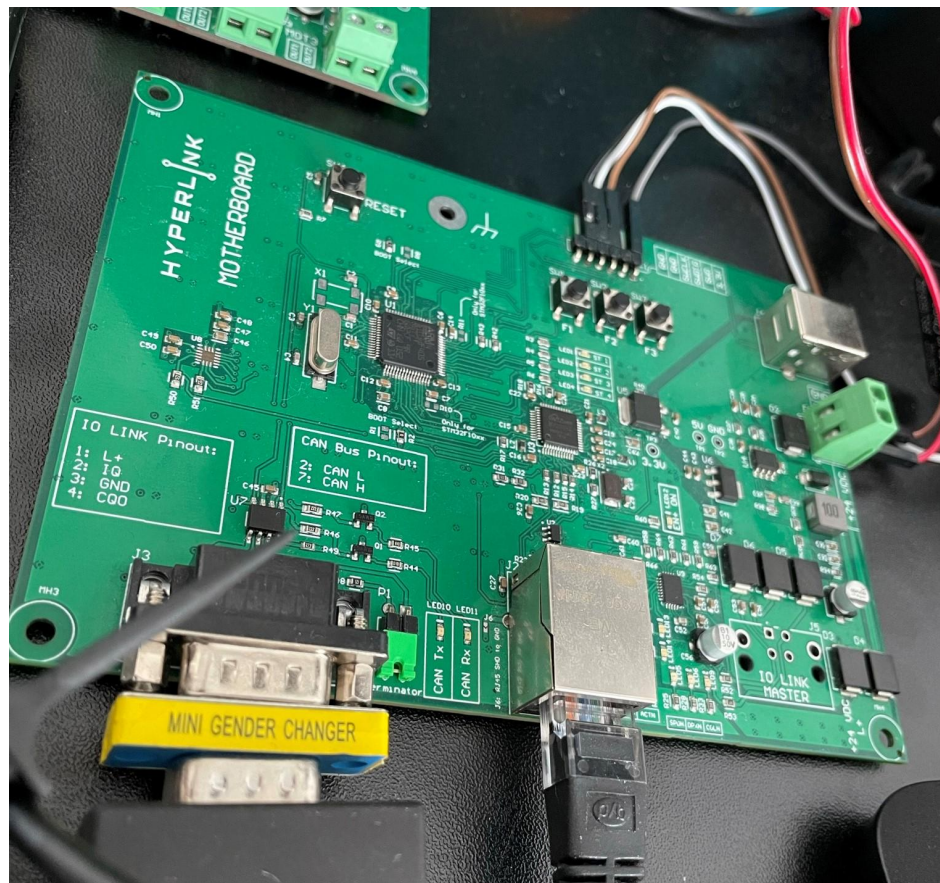


Figure 2.5.2.1.3 Assembled Braking board

2.5.2.2 Technical drawings

HYPERNLINK MOTHERBOARD

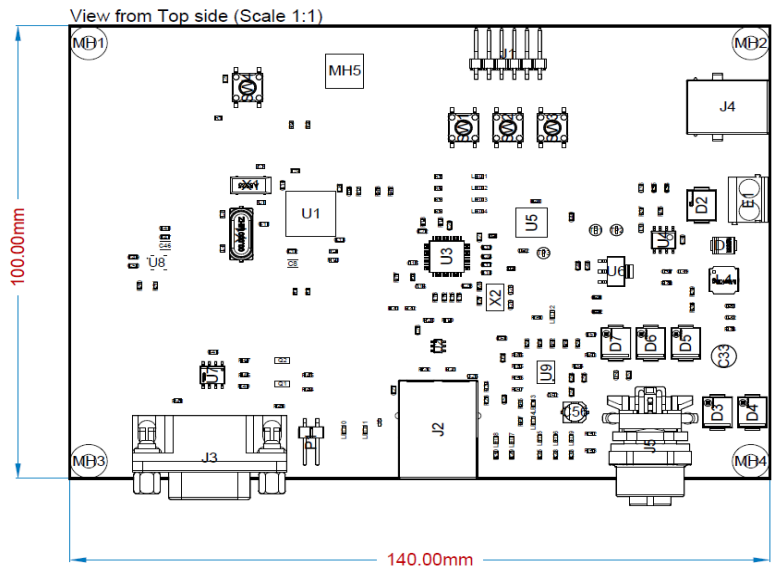


Figure 2.5.2.2.1 Motherboard mechanical drawing top view

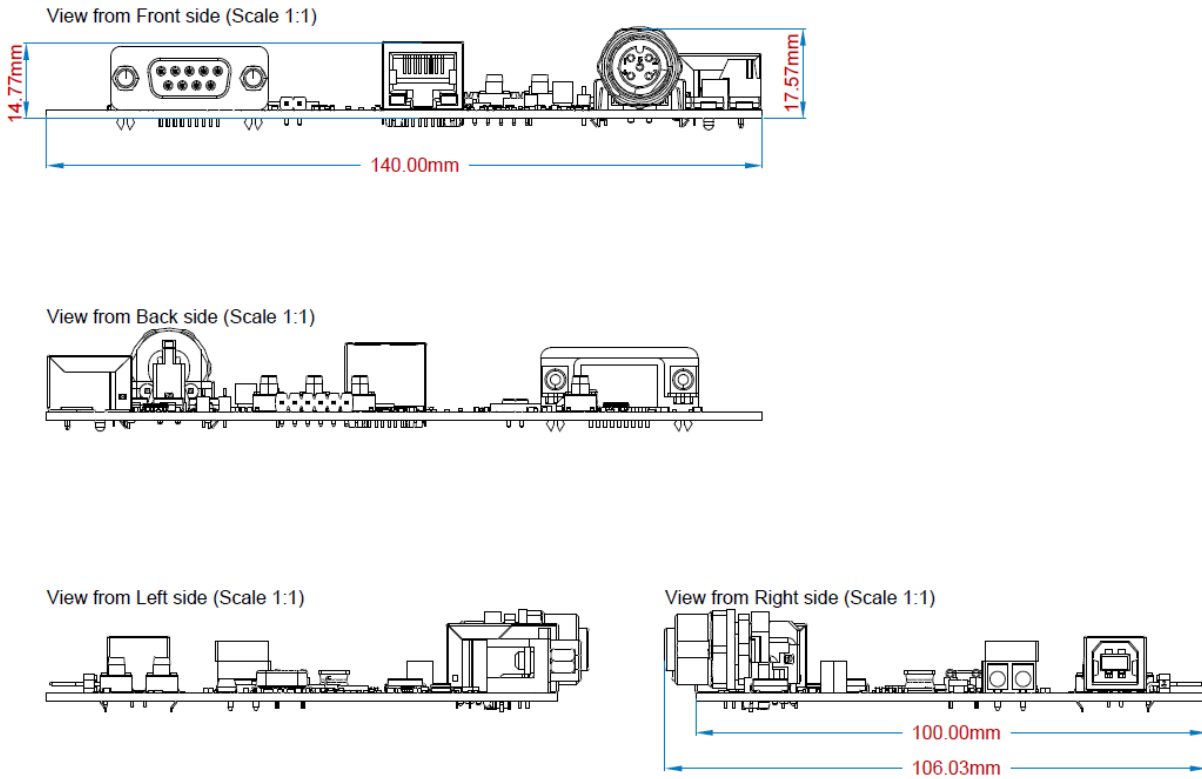


Figure 2.5.2.2.2 Motherboard mechanical drawing side view

Hyperlink Propulsion

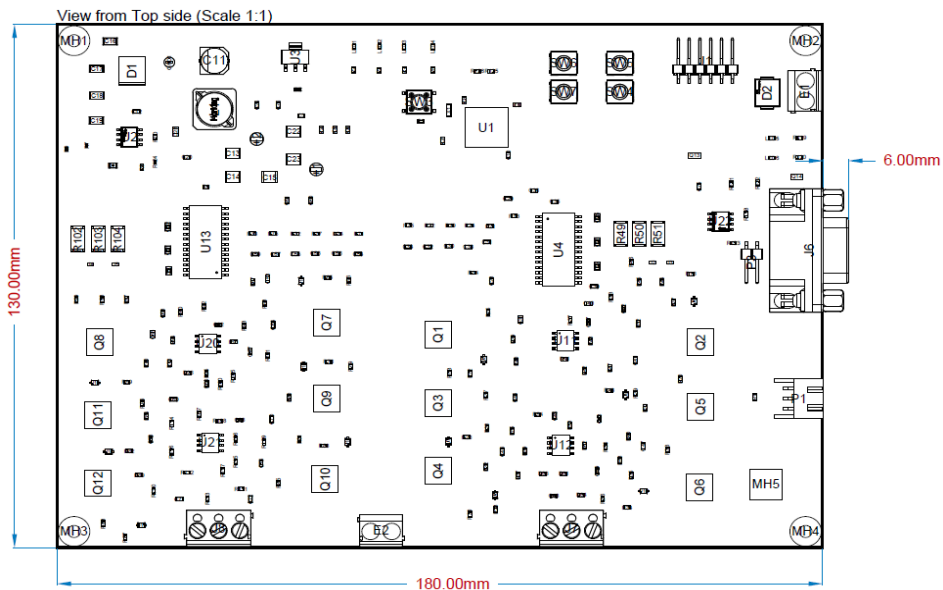


Figure 2.5.2.2.3 Propulsion mechanical drawing top view

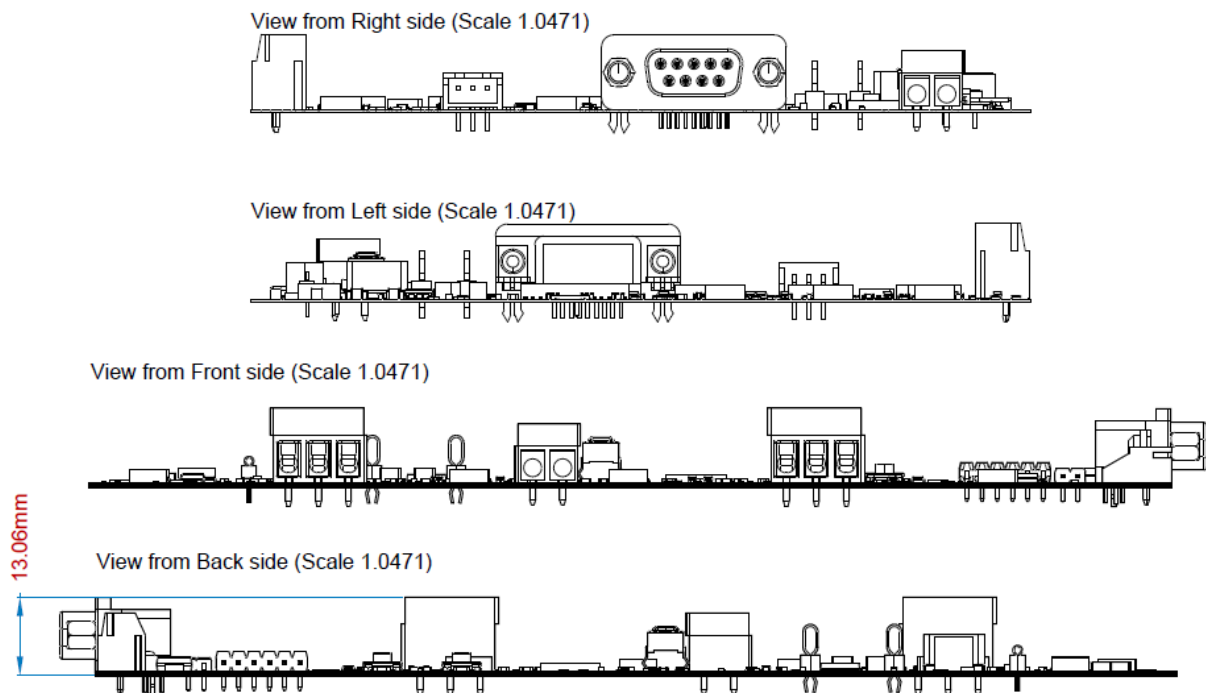


Figure 2.5.2.2.4 Propulsion mechanical drawing side view

Hyperlink Braking

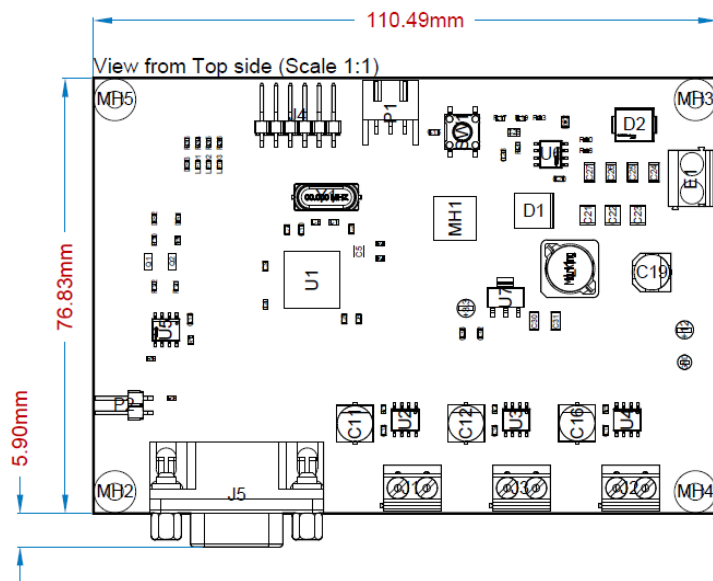


Figure 2.5.2.2.5 Braking mechanical drawing top view

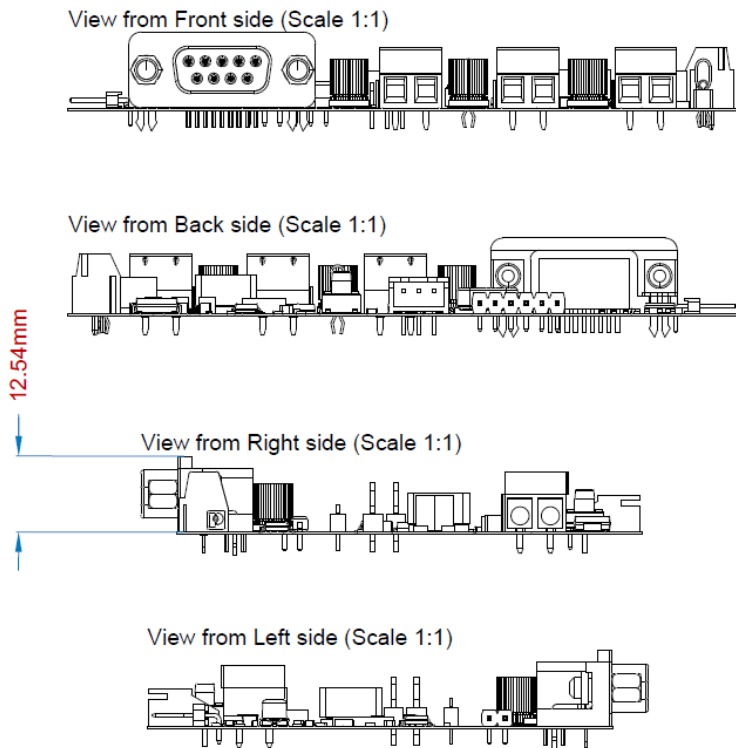


Figure 2.5.2.2.6 Braking mechanical drawing side view

2.5.3 Integration into a Subordinate Structure/System

All electronics PCBs are bolted onto the top of the structural frame of the pod. This assured the boards to keep a constant position and to maintain it at all times. The location of electronic boards is not directly near the propulsion, to avoid any possible overheating from the LIM. The battery is fixed by the battery housing and bolted onto the top part of the frame. The battery pack is placed centrally, above propulsion, to maintain the centre of gravity at the central location in the pod, equally distanced from both, front, rear, and both sides. Such a symmetrical arrangement also allows to achieve more stability which has crucial benefits for both structures and suspension systems.

2.5.4 Demonstration Plan

In addition to the components specified in section 2.5.4.1 *Parts List*, to prepare Hyperloop pod for demonstration it is required to charge the main battery through a dedicated charging circuitry. Also, to activate logic systems on the board **before** the main battery is physically connected to the circuit via a protection switch, a low-power startup battery is to be connected to the *Power PCB* only for the time of

positioning the pod on the test track and performing all the stationary tests. This is to increase the safety of the entire system, and make sure that the subsystems can be fully operated during the setup procedure. The same will be applied for the process of removing the pod from the test track, after the demonstration and disabling the main battery from the internal vehicle network.

2.5.4.1 Parts List

Table 2.5.4.1 Parts Lift of Electronics & Power

Component	Quantity	Dimensions	Mass	Created
Battery (47VDC)	1	400 x 170 x 170 mm	10kg	Outsourced
Low power startup battery (24VDC)	1 (only used during setup procedure)	TBC	TBC	Outsourced
Wifi Module	1	224 x 82 x 48mm	0.4kg	Outsourced
Propulsion Board	1	180 x 130 x 13.06mm	0.1kg	Custom-designed, Manufacturing outsourced
Braking Board	1	110.49 x 76.83 x 12.53mm	0.1kg	Custom-designed, Manufacturing outsourced
Motherboard	1	140 x 100 x 17.57mm	0.1kg	Custom-designed, Manufacturing outsourced
Power Board	1	TBC	0.1kg	Custom-designed, Manufacturing outsourced
Encoders	3	TBC		Outsourced

Photo Reflective Sensor (RSPRO 729-5195)	1	12 mm x 31.5 mm x 21 mm	0.05	Outsourced
Temperature Sensor (DS18B20 on a flywire)	5	5 mm x 10 mm x 2 mm	0.01	Outsourced
Pressure Sensor	6	TBC	TBC	Outsourced

2.6 Software

2.6.1 Environments and packages

The Software team is responsible for ensuring all the electronics hardware and software components work simultaneously and function with each other safely. The main task for software is to control the subsystems and gather all the data received from them. The data log of information from subsystems is essential to assure the health of the pod at all times. Software and Electronics is the logical unit and is responsible for controlling the subsystems as intended in 3 main stages at EHW: pre-demonstration, demonstration, post-demonstration.

2.6.1.1 STM32CubeIDE

STM32CubeIDE is an all-in-one multi-OS development tool, which is part of the STM32Cube software ecosystem. This is the software used to compile and load the written software system onto the boards described in the prior 2.5 *Electronics & Power* subsection.

2.6.1.2 TouchGFX

We are using TouchGFX to implement a user interface which is going to be installed on the remote computer. This user interface is going to be used to monitor, configure and control the pod all remotely from the computer. TouchGFX is a graphic software framework optimised for STM32 microcontrollers. The boards that have been designed for the pod have been based on STM32 microcontrollers making the library ideal for the application. TouchGFX offers useful components like dials and visual

elements allowing changes in position, speed and other variables to be as clear as possible.

2.6.1.3 HAL

In order to program the boards, the HAL (Hardware Abstraction Layer) is used. It allows the user to manipulate and control pins / LEDs inputs and outputs on the electronic boards within the pod. HAL provides a consistent set of middleware components such as TCP/IP. HAL helps the software engineering team focus on ensuring the functionality and safety of the pod be tested in a manner which is clear and simple.

2.6.2 System Software Flowcharts

2.6.2.1 System Flow Diagram

This diagram below represents the states of the pod and how the transitions/ conditions incur a change in state.

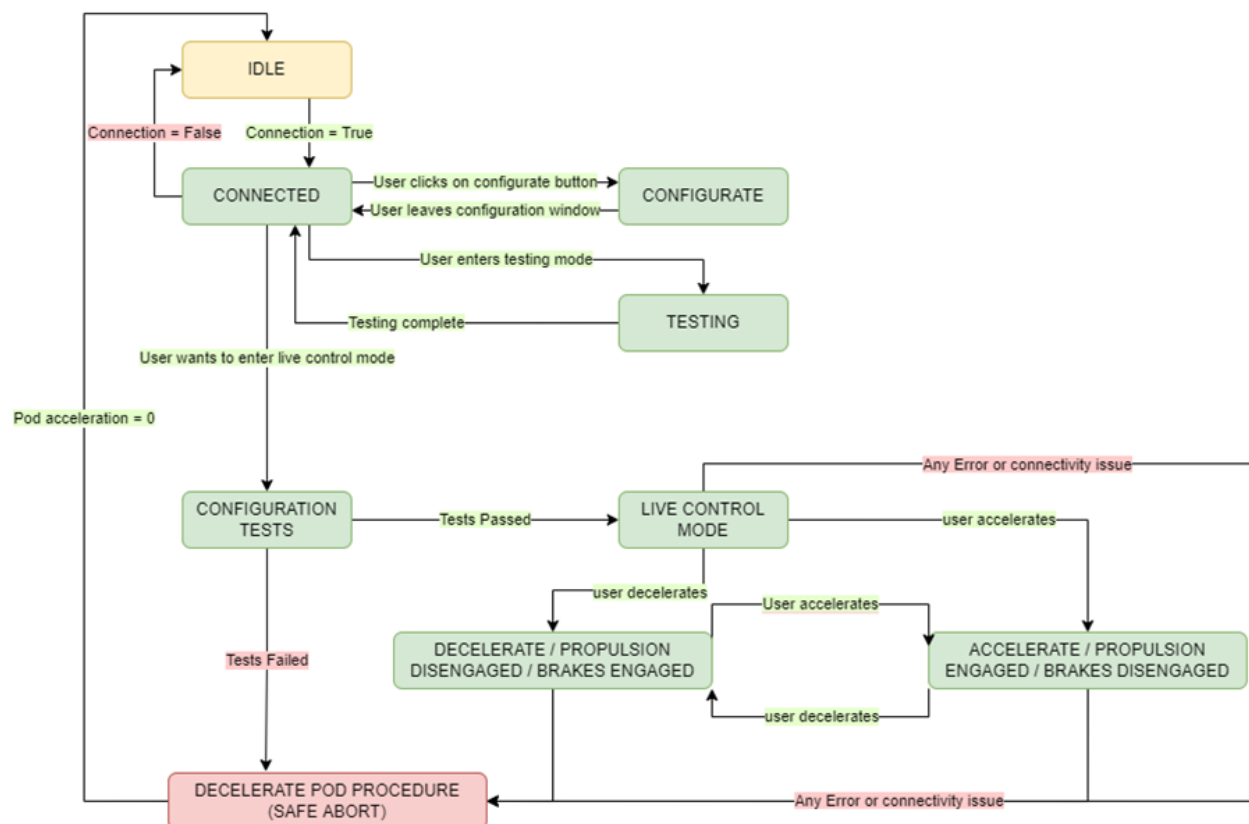


Figure 2.6.2.1.1 - State Diagram representing states in pod

2.6.2.2 Further description of flow states

IDLE - Pod is powered on and working only via internal communication. No connection has been established with the computer and the brakes are engaged by default. In this state it should be impossible for propulsion to activate.

CONNECTED - Pod is powered and connected to the remote PC. The PC at this point is loaded with the software and can communicate signals with the pod. The initial interface shown to the user is the menu interface allowing them to select from a variety of different interfaces. During connection the pod is stationary and the brakes are activated.

CONFIGURE - User interface switched to configuration page. The requirements for each test are set in this page and run during testing. Pod is stationary and brakes are engaged.

TESTING- Pod is stationary and both braking systems are engaged. Data is being live fed from the pod into the remote computer. Here is an opportunity to manually identify any erroneous data or statistics.

LIVE CONTROL MODE - At this point the Pod has completed and passed all tests and it is believed that the Pod is technically safe to run. If connection is lost for any reason past this point, SAFE ABORT will be activated and the Pod will be returned to IDLE. In this state the pod can now accelerate and brake with user input. Data is being fed live from the pod to the remote computer at the same time.

DECELERATE - When decelerating the main Brakes system is activated following the decelerating protocol. The propulsion system is currently inactive in this state. If the acceleration state is what we wish to transition to, we must first disengage braking. Once the pod has come to a standstill it returns to the idle state.

ACCELERATE - When accelerating the propulsion system is activated and both the brake systems are disengaged. The only other state it can transition to now is safe abort or DECELERATE. Before moving to any of these states, acceleration must be disengaged.

CONFIGURATION TESTS - This is executed as soon as the user wants to enter live control mode. All tests must pass before the pod transitions to LIVE CONTROL MODE.. If one or more tests fail the user will be returned to the CONNECTED state.

SAFE ABORT - This state attempts to activate both the mainBrake system and the secondaryBrake system. This is our fastest way of decelerating the system. Once the system returns being stationary it goes to the IDLE state.

Important information:

Once the pod has reached either half the distance of the track or the maximum speed of 50km/h we activate the deceleration protocol.

mainbrake system is the brake we use during regular deceleration.

secondaryBrake system is the brake we use if mainBrake fails or SAFE ABORT is activated.

Propulsion system cannot be activated until the configuration test has been succesful.



2.6.2.3 Protocol for decelerating pod (flowchart)

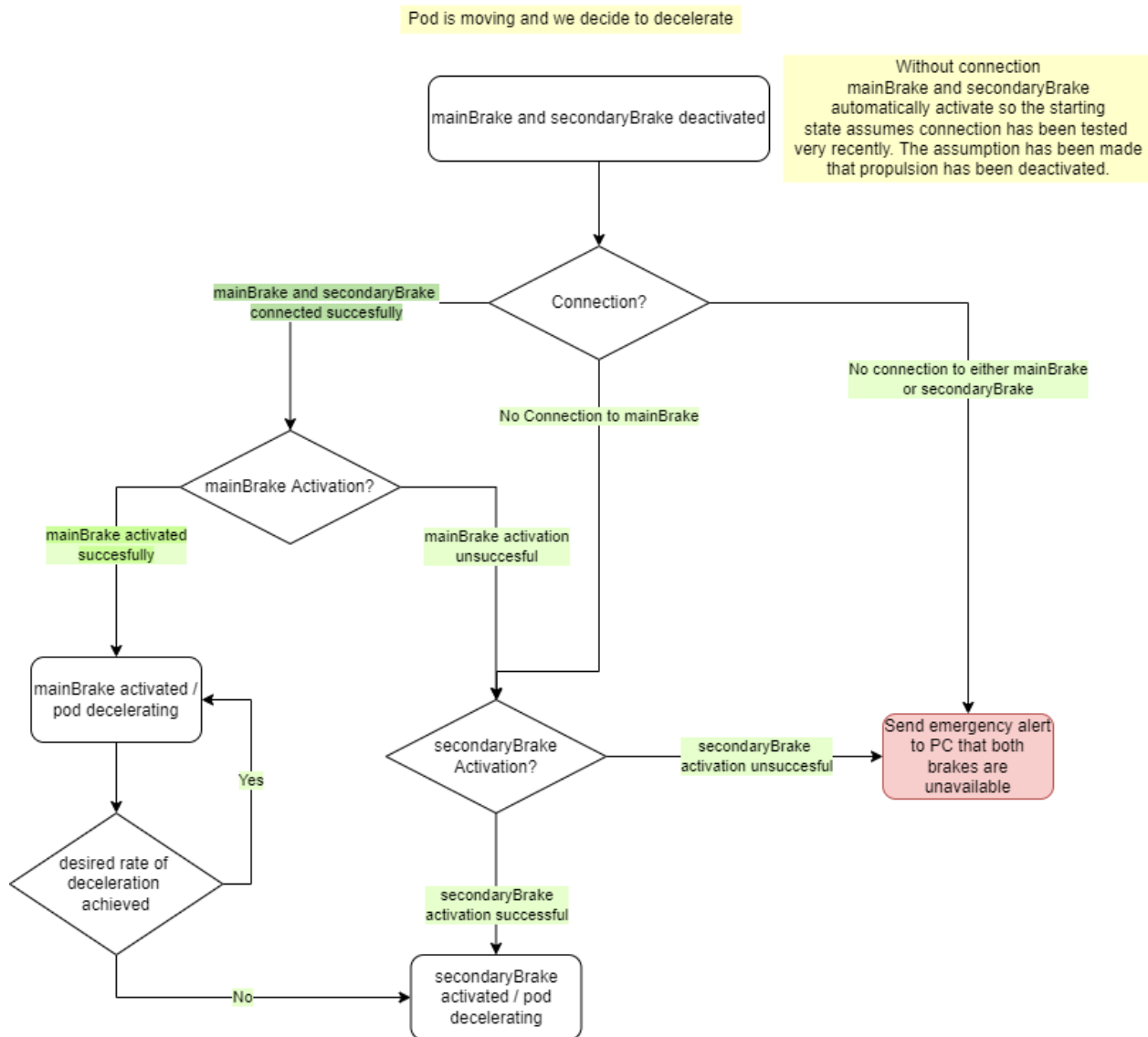


Figure 2.6.2.3 - State Diagram representing the main brake and secondary brake during an attempt to decelerate the pod.

The procedure shown above is executed as soon as we wish to decelerate. The 4 moments where we want to decelerate are once we have reached a specific distance, once we have reached our target speed, an error occurs or we activate emergency braking. We have two brakes which are connected to the braking board in parallel ensuring redundancy and allowing one connection to exist if another fails. In an emergency we would activate

2.6.3 Graphical User Interface

2.6.3.1 Initial Menu Interface (concept)

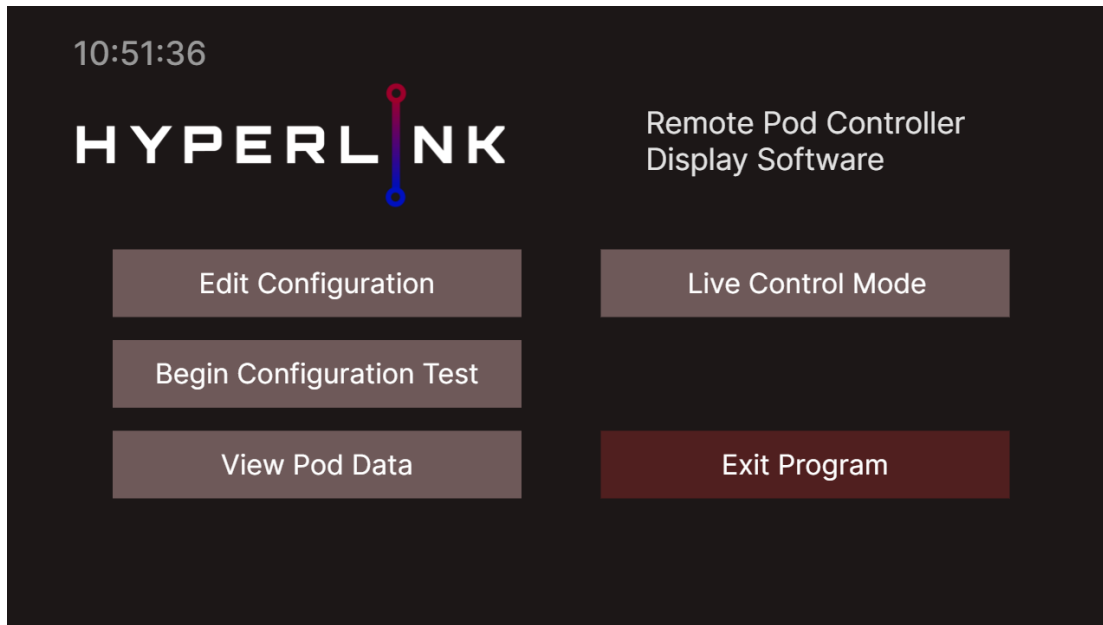


Figure 2.6.3.1.1 - Concept design for initial menu interface

When the program is launched the user is presented with the following screen. Clicking on “Edit Configuration”, “Begin Configuration Test”, “View Pod Data” or “Live Control Mode” will lead to a different window. “Exit Program” will close the program.

2.6.3.2 Configuration and testing interface (concept)

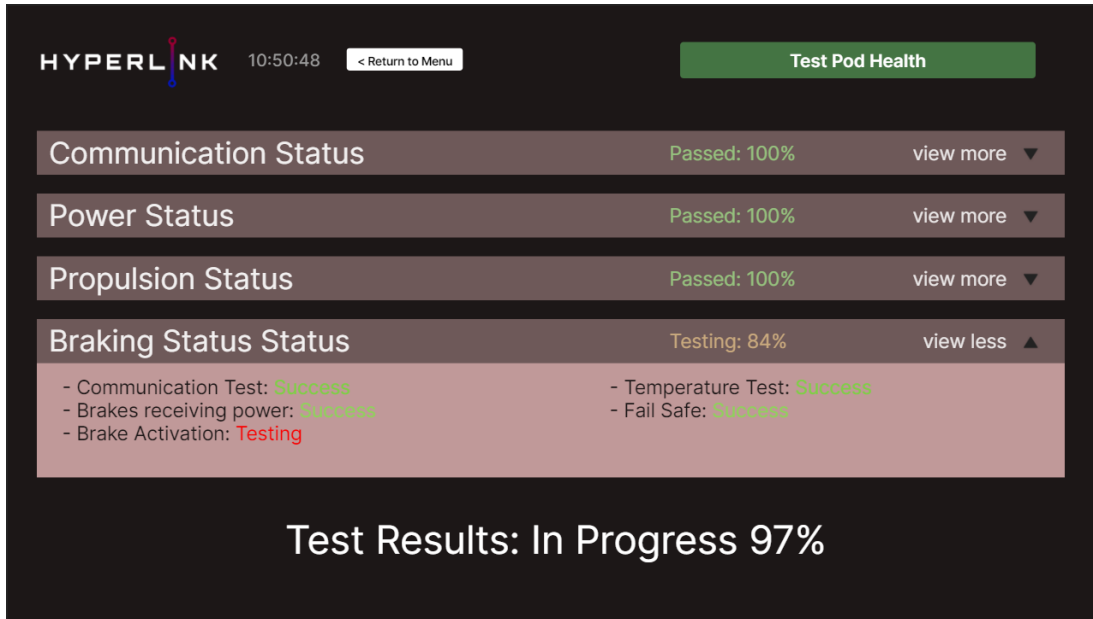


Figure 2.6.3.2.1 - Concept design for configuration test interface.

Pressing on the “begin configuration test” button will open the following window. If “test pod health” is pressed a program will run a set of pre-made tests testing all components of the pod. The user will be able to see exactly which part of the pod has failed and why.

2.6.3.3 View Pod Data Page (concept)

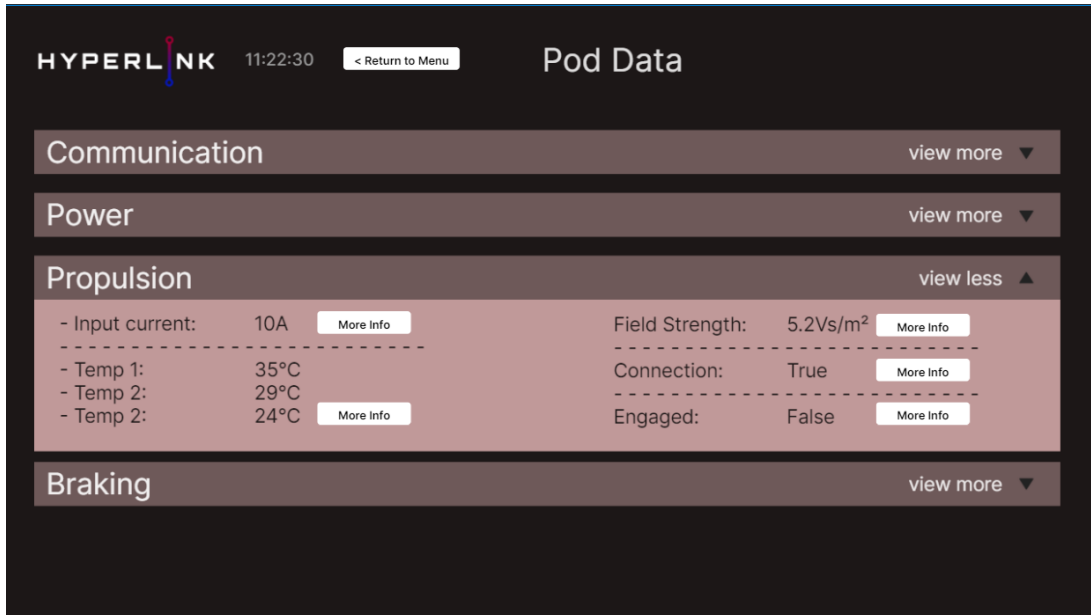


Figure 2.6.3.3.1 - Concept design for pod data page. Pod is assumed to be running in this screenshot and delivering the data via connection to the remote PC.

Here live data is being fed from the pod to the remote computer and displayed in a neat format allowing the user to see data categorised into different areas of the pod.

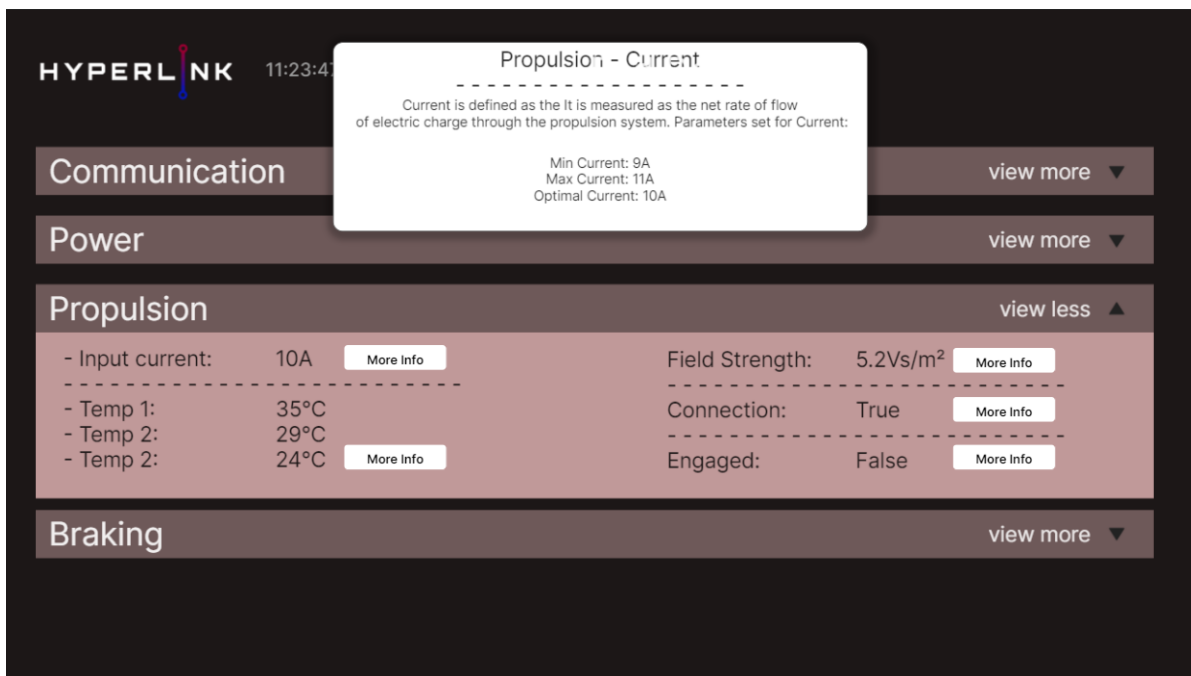


Figure 2.6.3.3.2- Concept design for pod data page. A modal which has appeared at the top of the page as a consequence of the user clicking more info next to current.

Depending on the component or piece of data being presented, clicking on more info will present information about the data being fed and its current parameters and minimum / maximum limits.

2.6.3.4 Configure Pod Page (concept)

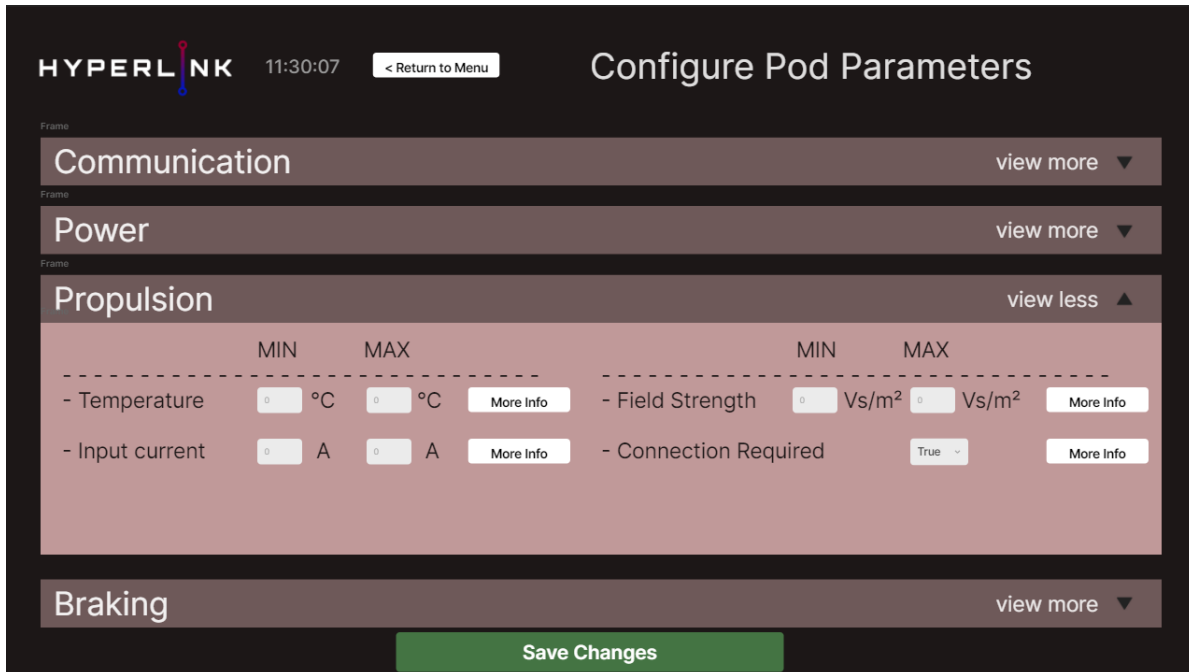


Figure 2.6.3.4.1- Concept design for Configure pod parameters page.

In the configure pod parameters page we are able to set minimum and maximum values for all of the values which are being tested in the Pod on the “configuration pod test” page. The more info buttons here allow for

2.6.3.5 Live running interface (implemented using TouchGFX)

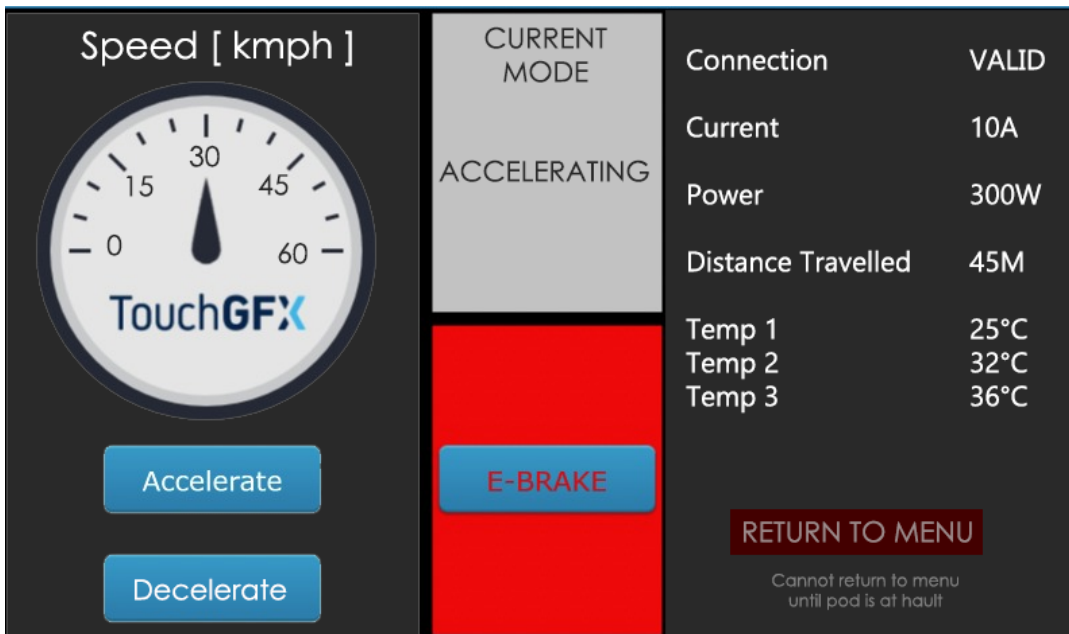


Figure 2.6.3.5.1 Currently implemented user interface which is shown when the Pod is actually moving.

This user interface has been implemented using touchGFX. We have some sample data on the screen but are prepared to update with further display components depending on the pod's requirements. E-brake engages emergency brake procedure and is accessible by a person at the remote computer via clicking on it.

The sample data visualisation on the right of the GUI is used to represent the current state of the Pod whilst in motion during the circuit it is travelling in. Whilst in operation, the GUI will provide live feedback of connectivity between the Pod and the remote computer, as well as the Pods statistics in terms of remaining power, temperature of the Pod and the speed in which the Pod is travelling at.

2.6.4 UML Diagrams

2.6.4.1 Class Diagrams

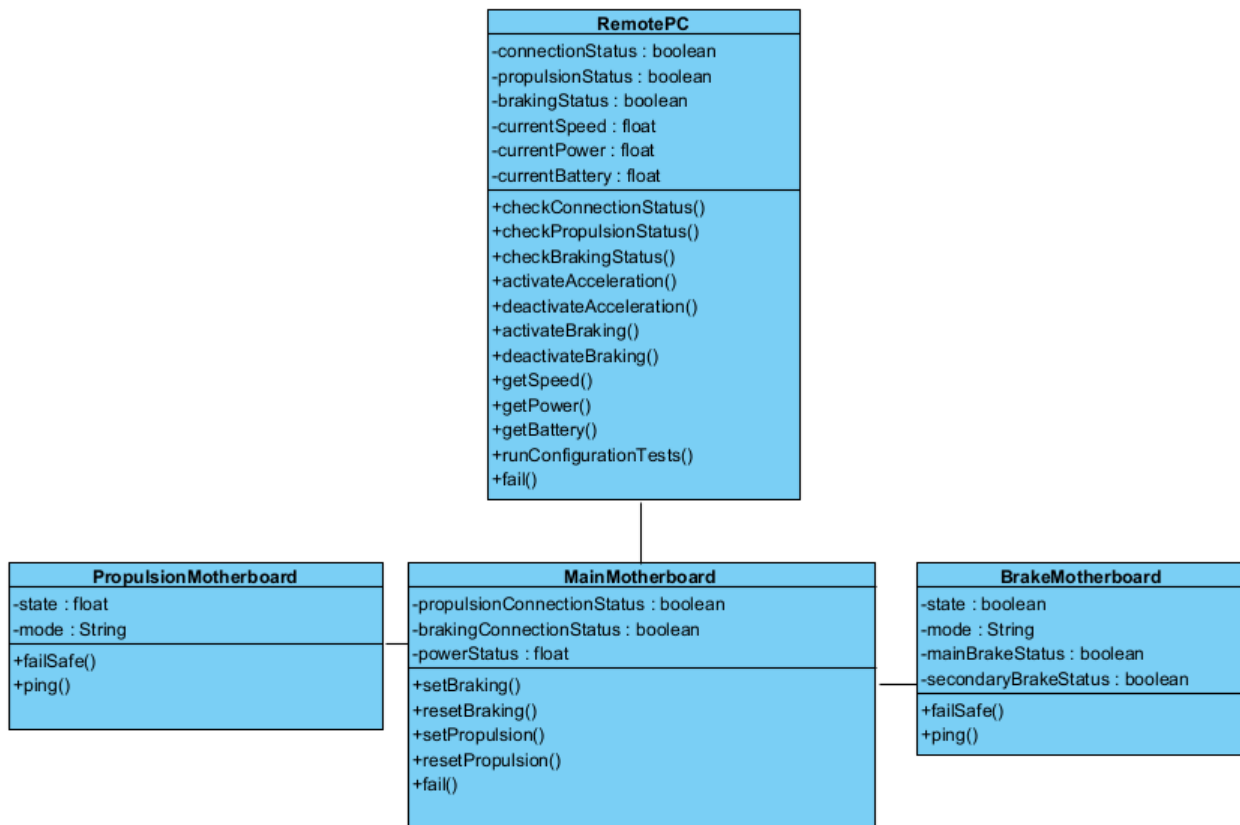


Figure 2.6.4.1.1 - Class Diagram showing how different boards communicate with each other

The remote PC here represents the logic which lies and operates under the developed user interface. The remote PC communicates directly with the main motherboard and the main motherboard is responsible for communicating data between the braking board and propulsion board.

2.6.4.2 Class Diagram: Key Methods and variables

Methods:

- **fail**: This method can be called from any board in the system. If one board loses connection from its closest component, a failure is called which deactivates the acceleration and activates both mainBrake & secondaryBrake.

- **checkConnectionStatus:** This method pings the main motherboard to see if the connection is still alive. The connection status Boolean value will rely on this method. If connection is unavailable, a fail method is called on the main board causing brakes to activate and propulsion to deactivate.
- **checkPropulsionStatus:** Same as above but checks the propulsion board. As no direct means of communication is available from remote PC to propulsion board, we check the propulsionConnectionStatus variable on the main motherboard. If connection is unavailable, a fail method is called on the main board causing brakes to activate and propulsion to deactivate.
- **checkBrakingStatus:** Same as above but checks the braking board. As no direct means of communication is available from remote PC to propulsion board, we check the brakingConnectionStatus variable on the main motherboard. If connection is unavailable, a fail method is called on the main board causing brakes to activate and propulsion to deactivate.
- **runConfigurationTests:** This method is used on the configuration testing window and verifies all the connections and power inputs match values which we expect.
- **ping:** This sends an update to the parent board stating that connection is still present. This will then update the according variable.

Variables:

- **mode:** This variable is on both the propulsion and braking board. This has three modes at the moment: "idle", "active", "fail". "Idle" means that nothing yet should be activated. Active means that it is now possible to change the status of these boards. Failure means permanently activating brakes and permanently disabling the propulsion mechanism.
- **State:** This variable is also on the propulsion and braking board. True means that braking / propulsion would be currently active and False would mean the opposite.
- **mainBrakeStatus:** Using the ping function the mainBrakes connection status will be tested and updated frequently to ensure mainBrakes are connected. If they are not, the failSafe will be called and the secondaryBrake will be engaged.
- **secondaryBrakeStatus:** Using the ping function the secondaryBrakes connection status will be tested and updated frequently to ensure secondaryBrakes are connected. If they are not, the failSafe will be called and the secondaryBrake will be engaged.
- **currentPower:** This is the amount of power being used through all 3 boards
- **currentBattery:** This is the remaining amount of battery on the Pod

2.6.5 Hardware and their application

2.6.5.1 Photoelectric reflective sensor

We are using the photoelectric sensor alongside the reflective strips which are at the side of the track to measure distance and speed. This is being used alongside both encoders to provide us with 3 sources of position, which then can be used to calculate velocity.

2.6.5.2 Encoders

We are using two encoders which are placed on the shaft to calculate velocity and also give us an idea of distance. This will provide greater reliability than the photoelectric sensor but both will be monitored. Encoders will be used as the primary source of distance and velocity and the photoelectric reflective sensor will be used as the secondary source.

2.6.5.3 Temperature Sensor:

This sensor is placed near propulsion and is tested during configuration tests but also output onto the screen during live control mode. If any one of the temperature sensors records a temperature outside of our range, the system will enter SAFE ABORT mode.

2.6.5.4 Pressure Sensor:

This pressure sensor is placed so it can read the pressure from the air reservoir and the two cylinders. Using the data that is being fed here we are able to detect pressure leaks. Some of this data will be appropriately manipulated to show concise and important information on the LIVE CONTROL MODE interface. If any detection of pressure leak is detected then the pod will enter SAFE ABORT mode.

2.6.5 Demonstration Plan

From a software point of view we assume that all prior checks have been completed and passed before executing software. The majority of components that are used are mentioned in the electronic engineering parts subsection.

2.6.5.1 Demonstration Setup

The demonstration setup will include a remote pod control station that will consist of a laptop computer and monitors to control the run and operation of the pod during demonstration. Connectivity will be established through a wifi module.

2.6.6 Equipment & Infrastructure

The following list states the required components for software to run:

- Main motherboard - this is connected to the main computer via the wireless adaptor
- Wireless adaptor - this will be plugged into the main motherboards ethernet port for connectivity reasons.
- Braking board - This is connected to the main motherboard and will contain internal logic relating to braking
- Propulsion board - This is connected to the main motherboard and will contain internal logic relating to propulsion.
- Computer- It is important to ensure that the laptop or computer we use has CubeIDE installed to ensure we can execute and load the programs we have developed.
- Table - This is to place the laptop or computer on so the user on the computer does not injure back during use.
- Jumper wiring - to connect all of the boards together correctly and to their respective components.

3. Safety

Table 3.4.1. Transportation and lifting risk mitigation measures

Potential Failure Mode	Severity	Occurrence	Score	Causes	Risk Mitigation	New Severity	New Occurrence	New Score	Procedure if it happens
Pod suffers damage during transport to Delft	7	3	21	Not secured properly with packaging filling, placement of the pod crate not strong enough, improper placement in the van	The security of packaging will be checked thoroughly before the pod is shipped. Significant amount of filling will be used. A designated duty-cargo crate will be used. The correct placement of the pod in the van will be ensured through multiple checks.	7	1	7	Fix any loose parts or tighten screws. A thorough inspection will be implemented to ensure no damage goes unnoticed and the procedures for fixing all the components will be followed depending on what got damaged.
Pod falls from the crane during lifting	9	3	27	The crane is not strong enough. The lifting fixtures are not secured properly. The	Lifting procedure will be followed every time, with at least 2 team members ensuring	9	1	9	Fix any loose parts or tighten screws. A thorough inspection will be implemented to ensure no damage

				lifting procedure is not followed.	that it's followed correctly every time.				goes unnoticed and the procedures for fixing all the components will be followed depending on what got damaged.
Pod falls during the attempt to lift it	4	4	16	The lifting procedure is not followed.	Lifting procedure will be followed every time, with at least 2 team members ensuring that it's followed correctly every time.	4	2	8	Fix any loose parts or tighten screws. A thorough inspection will be implemented to ensure no damage goes unnoticed and the procedures for fixing all the components will be followed depending on what got damaged.
Pod suffers damage during transport to Delft	7	3	21	Not secured properly with packaging filling, crate not strong enough, improper placement in the van	The security of packaging will be checked thoroughly before the pod is shipped. Significant amount of filling will be used. A designated duty-cargo crate will be used. The correct placement of the pod in the van will be ensured through multiple checks.	7	1	7	Fix any loose parts or tighten screws. A thorough inspection will be implemented to ensure no damage goes unnoticed and the procedures for fixing all the components will be followed depending on what got damaged.

3.1 Propulsion

3.4.1 FMEA & Risk Mitigation

Table 3.4.1. FMEA & Risk Mitigation for Propulsion

Potential Failure Mode	Severity	Occurrence	Score	Causes	Risk Mitigation	New Severity	New Occurrence	New Score	Procedure if it happens
Current overload	5	4	20	Failure in control board. Capacitor holds charge too long and discharges in one go.	Software systems will maintain the current input below the	1	4	4	System is fused so the fuse will break disabling propulsion

				Problem when converting DC to AC with inverter	maximum current load of the wire				all together. This is reported to UI
Short Circuit	6	6	36	Failure in the wire terminals are screwed configuration , like down and connections snapping or tearing, are secured. Check may result in the system has continuity current taking the path of least resistance through the stator core.	Check that all terminals are screwed down and connections are secured. Check the insulation rating between windings and stator.	6	2	12	Ground the stator
Magnetic field damages other components	6	2	12	LIM relies on using strong magnetic fields to generate force	Will be tested once the pod is complete. If still problematic a shield will be made. Simulations indicate the field is equivalent to 0.100mm from LIM.	4	2	8	Stop the motor, cut off the power supply, emergency brake
Linear Induction Motor Overheating	8	5	40	Natural caused currents by heating eddy	Have thermal sensors that disable the propulsion system if temperature is too great	8	2	16	Brake instantaneously, use laser thermometer to wait until at acceptable temperature, wait until cooled completely, check all operations are functioning

3.4.2 Procedure in case of Failure

- In case of any form of failure turn motor off
- Overheating
- Short Circuit
- Current overload
- Magnetic interference

3.4.3 Energy Storage

The propulsion of the pod when the battery is switched off has no energy storage, apart from its own potential energy due to LIM's mass.

3.4.4 Special Transport, Storage and Lifting Requirements

- Switched off battery during storage and during transport
- Storage need to keep the wires secured
- Gloves and disinfection
- Keep upright to avoid exerting forces on the epoxy
- Keep wires well insulated and way from moist environments/ hot areas

3.2 Braking

3.4.1 FMEA & Risk Mitigation

Table 3.4.1.1. FMEA & Risk Mitigation for Braking

Potential Failure Mode	Severity	Occurrence	Score	Causes	Risk Mitigation	New Severity	New Occurrence	New Score	Procedure if it happens
Air leakage in air reservoir	1	2	2	Bad manufacturing of the air reservoir or bad sealing	Choice of high quality and better reservoirs, proper mounting to the frame	1	2	2	Engage the emergency braking
Over Pressurised air reservoir	3	4	12	Over compressing the air inside reservoir	Monitoring and measuring amount of compressed air using external compressor inside the reservoir	3	4	12	Open the valves that have one side connection to atmosphere to reduce pressure immediately
Explosion of air reservoir	1	1	1	Due to amount overpressurization	Inspection of pressure difference inside the air reservoir	1	1	1	Engage the emergency braking
Clog of the external compressor	2	3	6	Build up of dirt or mistake in manufacturing	Selection of new good quality external compressor	2	3	6	Use the reserve external compressor
Jammed spring	4	5	20	Fatigue and brittleness of material due to constant tension and compression	Usage of spring with higher Young's modulus to prevent fatigue failure	4	5	20	Engage emergency braking

Leakage of air in fittings	6	6	36	Improper sealing fittings	Sealing of the off fittings with better equipment	6	6	36	Engage braking	emergency
Tubing falling off	2	2	4	Assembling error	Correct sealing of the tubes to the fittings	2	2	4	Engage braking	the emergency
Bad sealing of the valves	5	6	30	Mounting error	Assembling the valves to the frame properly	5	6	30	Engage braking	emergency
Resistment of valve turning	3	4	12	Buildup of dirt and sediment	Utilising new and high quality valves bought from good manufacturer	3	4	12	Engage braking	emergency
Wear of elastic for sealing the ball valve	1	5	5	Gas getting pushed through elastic of the valve	Sealing the valve properly do the gas doesn't go through elastic	1	5	5	Engage braking	emergency
Leakage in bolts and nuts	6	7	42	Loose nuts and bad connector alignment	Align the connector correctly to the tubes and tighten the bolts and nuts efficiently	6	7	42	Engage braking	emergency
Leakage within the ball valve	4	5	20	Using valve after some inactive period	Implication of unused new valve	4	5	20	Engage braking	emergency
Friction wear of brake pad	7	8	56	Cased by heat generated from a friction force	Choice of right material for brake pad with proper Young's modulus, as well as uniform application of brake force	7	8	56	Engage braking	emergency
Brake pad edge lift	2	3	6	Improper brake-in procedure	Mounting of brake pad properly to the rod and I-beam	2	3	6	Engage braking	emergency
Explosion of brake pad	1	1	1	Due to high heat caused by friction	Controlling of the system properly so it doesn't causes explosion	1	1	1	Engage braking	emergency
Over Pressurised	4	5	20	Inlet pressure higher than the pressure	Controlling the valve openings	4	5	20	Open the valves that have one side connection to	

pneumatic cylinder				range of cylinder					atmosphere to reduce pressure immediately
Jammed piston	3	5	15	Bad lubrication of the cylinder walls	Using lubrication on pneumatic cylinder walls	3	5	15	Engage braking emergency
Failure of whole braking system	1	1	1	Failure of every component of the system	Test the system beforehand	1	1	1	Engage braking emergency
Failure of emergency braking system	1	1	1	Failure of every component of the system	Test the system beforehand	1	1	1	N/A

3.4.2 Procedure in case of Failure

There is a spring that is constantly engaged in the brake cylinder for safety purposes. If the power cuts off from the system, the spring remains engaged and exerts a force in the opposite direction to motion by extending and will therefore slow the system down to a stop. Furthermore, there is an emergency system that can be engaged within the propulsion system. In the coding of the propulsion system, a line can be included which flips the magnetic field of the system which will cause an opposing force to motion and slow the system down.

Another emergency brake occurs when the pod sets the pressure drop in the brake pipe to maximum. Air leaves the brake pipe until it reaches atmospheric pressure. The pressure in the brake pipe drops fast, which makes the control valve connect both reservoirs to the brake cylinder, reaching an equal pressure in the three volumes. The final pressure is higher than the maximum one provided in normal applications, leading to a higher brake force.

Emergency Brake:

It occurs when the pod sets the pressure drop in the brake pipe to maximum. Air leaves the brake pipe until it reaches atmospheric pressure. The pressure in the brake pipe drops fast, which makes the control valve connect both reservoirs to the brake cylinder, reaching an even pressure in the three volumes. The final pressure is higher than the maximum one provided in normal applications, leading to a higher brake force.

3.4.3 Energy Storage

Pneumatic hydraulic energy is the energy stored in the form of pressurised fluid, making it an application of fluid power. Fluid power is the use of pressurised fluids to generate, control, and transfer power. Fluid power can be divided into two parts: hydraulics, which stores energy in the gravitational potential energy of a liquid, typically water, and pneumatics, which stores energy in the compression and pressurisation of a gas.

Pneumatic energy has a variety of forms. One of the main forms we will be using is the form of pressurised gas (our case air). This energy is stored in compressed air and subsequently converted into mechanical energy when the gas is displaced to a lower pressure environment.

The energy stored in compressed air is equivalent to the work done to compress the air. This work is given by the equation:

$$W = RT \ln(P_p/P_a) \quad \text{when} \quad PV = \text{constant} \quad \text{for isothermal system}$$

where;

- W is the work done to compress the fluid (joules, J)
- V is the volume of the air reservoir the air is in (cubic metres, m³)
- P_p is the pressure of the compressed air (pascals, Pa)
- P_a is the pressure of the atmosphere (pascals, Pa)
- ln is the natural logarithm

The relationship between pressure and volume is given in the Fig 3.4.3.1 below

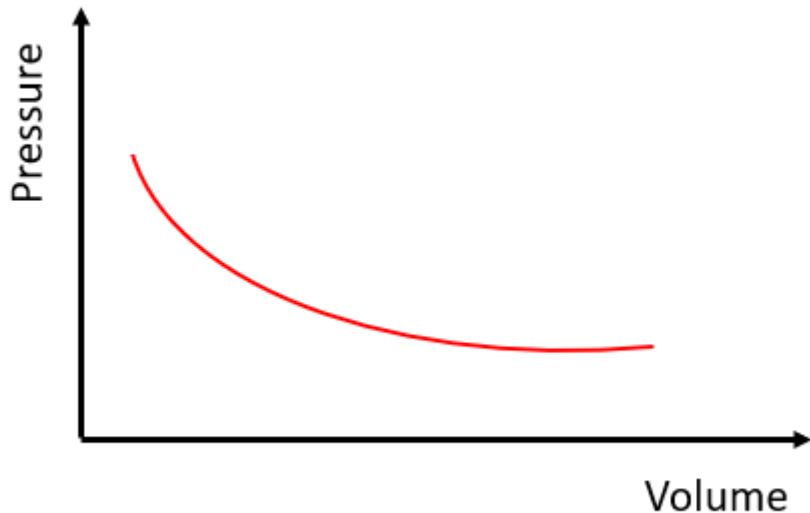


Figure 3.4.3.1 Pressure/Volume dependency graph

Compressed air energy storage (CAES) is a way of capturing energy for use at a later time by means of a compressor. The system uses the energy to be stored to drive the compressor. When the energy is needed, the pressurised air is released. That, in a nutshell, is how CAES works.

Pneumatic braking system is an efficient and reliable method of energy storage and easy to transport. This is one of the reasons as well why we have decided to use it.

One more form of energy storage is the storage of potential energy when it comes to spring. Due to the spring's altitude when it is loaded, the potential energy will occur, ensuring the spring has enough power to push the brake pads towards the I-beam when braking is applied.

3.3 Suspension

3.4.1 FMEA & Risk Mitigation

Potential	Severit	Occurre	Score	Causes	Risk Mitigation	New	New	New	Procedure if it
-----------	---------	---------	-------	--------	-----------------	-----	-----	-----	-----------------

Failure Mode	Severity	Occurrence	Score	What happens
Fracture of Wheel housing	8	2	16	High loading during operation Simulations have been used to ensure safety factor is above 2
Compression beyond shock's travel limit	5	5	25	High loading during operation Stiff springs are chosen with the ability to tolerate loads more than twice the expected loading and reasonable travel limit
Fracture of the shock fixture	6	4	24	High loading during operation Simulations have been used to ensure safety factor is above 2
Fracture of wheel shaft	8	4	32	High loading during operation Simulations have been used to ensure safety factor is above 2
Abrasion of wheel	3	2	6	High operational speeds Abrasion resistant wheels have been selected
Misalignment of wheel	5	4	20	Incorrect alignment of shock fixture (aligned at the wrong angle) Repeated check of all wheels for their angle against the I beam edge to ensure it is parallel
Rotation of the wheel housing	3	2	6	Not sufficient interference between shafts and eye mounts A torque load test will be done for the top and lower mount to ensure it is secured
Rotation of the wheel housing	3	2	6	Jam nuts are not torqued sufficiently A torque load test will be done for the top and lower mount to ensure it is secured

3.4.4 Special Transport, Storage and Lifting Requirements

The suspension, thus the pod, during transportation in a box is being transported on the I-beam with the braking system engaged (as it's engaged by default). It's because the suspension was designed to bear the whole weight of the pod when touching the I-beam. Therefore, taking the pod off the I-beam and placing it on the ground would result in the frame taking the whole weight of the pod, and it was not designed that way. Hence, during transportation is it safer for the pod to travel with the suspension system on an I-beam at most times.

3.4 Structures

3.4.1 FMEA & Risk Mitigation

Table 3.4.1.1. FMEA & Risk Mitigation for Structures

Potential Failure Mode	Severity	Occurrence	Score	Causes	Risk Mitigation	New Severity	New Occurrence	New Score	Procedure if it happens
Frame Bending	2	6	12	Excessive loads are applied on the frame	Run structural simulations ensuring the design and materials used are within a safety factor of at least 1.5	2	1	2	Abort the demonstration
Frame fracture	4	4	16	Excessive loads or accidental collisions	Run structural simulations ensuring the design and materials used are within a safety factor of at least 1.5	4	1	4	Replace the component with the new one or weld if fracture is minor
Shell fracture	1	5	5	Excessive aerodynamic loads or accidental collisions	Run CFD and structural simulations ensuring the design and materials used are within a safety factor of at least 1.5	1	2	2	Demonstration without the shell
Propulsion mounting fractures	4	5	20	Insecure attachment, Excessive loads, Poor quality materials, unexpected impacts	Run structural simulations ensuring the design and materials used are within a safety factor of at least 1.5. Ensure mounting is secure and well fixed when assembling the pod.	4	2	8	Replace the component with the new one
Braking mounting fractures	4	5	20	Insecure attachment, Excessive loads, Poor quality materials,	Run structural simulations ensuring the design and materials used are within a safety factor of at least 1.5. Ensure mounting is secure and	4	2	8	Replace the component with the new one

				unexpected impacts	well fixed when assembling the pod.				
Suspension mounting fractures	4	5	20	Insecure attachment, Excessive loads, Poor materials, unexpected impacts	Run structural simulations ensuring the design and materials used are within a safety factor of at least 1.5. Ensure mounting is secure and well fixed when assembling the pod.	4	2	8	Replace the component with the new one
Component detachment	5	3	15	Insecure attachment, Excessive loads, Poor materials, unexpected impacts	Run structural simulations ensuring the design and materials used are within a safety factor of at least 1.5. Ensure mounting is secure and well fixed when assembling the pod.	5	1	5	N/A

3.4.2 Procedure in case of Failure

As can be seen in the FMEA table, any failures that may happen before the pod is tested will result in either repairing or replacing the component at risk. If the failure happens while the pod is running, the procedure in all cases is to immediately activate the brakes and stop the pod as fast as possible to ensure the safety of all personnel and equipment that may be at risk.

3.4.3 Energy Storage

The structures of the pod have no energy storage, apart from its own internal energy due to the frame's and shell's mass and the kinetic energy of the whole pod when moving at a certain velocity. This kinetic energy can be calculated for when the pod is running at its maximum speed of 50km/h:

$$E_k = \frac{1}{2}mv^2$$

$$E_k = \frac{1}{2} \cdot 160\text{kg} \cdot (13.8\text{m/s})^2 = 15.24\text{kJ}$$

3.4.4 Special Transport, Storage and Lifting Requirements

For safety reasons, when transporting the pod at the EHW venue, the shell is removed to be transported separately from the rest of the pod. The reason is that the shell is one of the most fragile components of the system, and that during the transportation process it is crucial to identify if all the systems inside are in the

correct positions. Hence, removing the shell allows for visual control of the inner subsystems at all times during transportation. Moreover, the lifting procedure is done with a crane which is connected to the structural frame of the pod, hence the shell needs to be removed to mount the crane. Further details on the lifting procedure of the whole pod are presented in section 4. *Logistics*.

3.5 Electronics & Power & Software

3.5.1 FMEA & Risk Mitigation

Table 3.5.1.1. FMEA & Risk Mitigation for Electronics, Power, Software

Potential Failure Mode	Severity	Occurrence	Score	Causes	Risk Mitigation	New Severity	New Occurrence	New Score	Procedure if it happens
Loss of connection with propulsion	3	5	15	Wire is loose, board fails, electromagnetic interruption	Ping the motherboard frequently and test if the connection is still alive	3	1	3	deactivate propulsion on loss of connection and activate brakes. This should bring the pod to a halt
Loss of connection with braking	8	5	40	Wire is loose, board fails, electromagnetic interruption	Ping the motherboard frequently and test if the connection is still alive	8	1	8	The braking board understands that on loss of connection brakes are to be automatically activated (this is their standard state). This should bring the pod to a halt
Loss of connection with main motherboard	8	5	40	Wire is loose, board fails, electromagnetic interruption	Ping the remote computer frequently and test if the connection is still alive	8	1	8	The main motherboard understands that on loss of connection brakes are to be automatically activated (this is their standard state). This should bring the pod to a halt
Remote computer crashes	8	5	40	Operating system may have crashed, the laptop may have died.	The board has logic internally stored on chip where if it cannot detect a connection with the desktop application failSafe mode will activate	8	2	16	The main motherboard understands that on loss of connection brakes are to be automatically activated (this is their standard state). This

									should bring the pod to a halt
No power is being provided to the board	8	2	16	Battery fails, wire comes loose, board breaks.	Pre tests are ran on the computer and a live feed of information such as power input and current are displayed. Current will be monitored actively and any unexpected changes will lead to further inspection.	2	1	5	Emergency brakes are applied as default (in order to deactivate them we need power) so the pod will automatically come to a halt.
User does not activate pod deceleration at desired speed / distance	8	3	24	user not paying attention, signal does not send to pod	Once a specific target speed has been met or a maximum distance has been travelled, propulsion deactivates and brakes activate.	8	1	8	Pod stops after given speed or distance without user interaction
Exceeding electrical and physical battery ratings	8	3	24	Overheating, power surge, short circuit, unsuitable electrical load	Overcurrent, overvoltage, temperature, short circuit protections implemented on the embedded battery BMS. Power board incorporates fuses. Listed protections implemented in the individual subsystems.	8	1	8	Pod automatically stops using emergency braking. BMS disconnects the battery from the system.
Overheating of individual subsystems	6	3	18	Individual subsystem boards overheating causing component shutdown	Internal temperature sensors implanted in microcontrollers	6	1	6	Emergency brakes engaged, power to propulsion is shut down

3.4.2 Procedure in case of Failure

A number of spare replacement PCB boards will be available.

3.4.3 Special Transport, Storage and Lifting Requirements

Detailed FMEA and description of risk mitigation measures. During transportation the battery is switched and disconnected at all times, and braking is engaged (as it is engaged by default).

4. Logistics & Safety

4.1 Transport, Lifting & Lift Plan

The pod will be transported in one piece, on the designated display and lifting I-beam, in a designated shipping crate. A designated shipping van will be utilised, and this will be outsourced to a professional shipping company. Additionally, for the safety of the system, the crate will be filled with fill packaging, to prevent any damage during shipment. All other equipment, including the lifting crane, will be transported in separate, designated crates.

The hydraulic crane is used to lift and transport the pod around the demonstration and EHW venue. During the lifting procedure, the shell is dismantled and transported separately. The shell is lifted by 2 people, as it weighs approximately less than 40kg, maintaining a 25kg limit per person. The crane is designed to lift up to 1 tonne, therefore a factor of safety of 5.8 is maintained.



Figure 4.1.1. SwitZer 1 Ton Hydraulic Folding Engine Crane

{https://www.manomano.co.uk/p/switzer-1-ton-hydraulic-folding-engine-crane-grey-17702216?model_id=17700218}

The pod is equipped with U-fixtures welded onto the frame. The chain from the crane is attached to them in each corner of the frame and is lifted by the. The chain is designed to lift loads up to 1 tonnes, thus lifting the pod is within the predicted and safety limits. The forces while lifting are different than when the pod rests on the I-beam, therefore, additional stress simulations were performed to verify the safety and structural integrity during the lifting procedure.

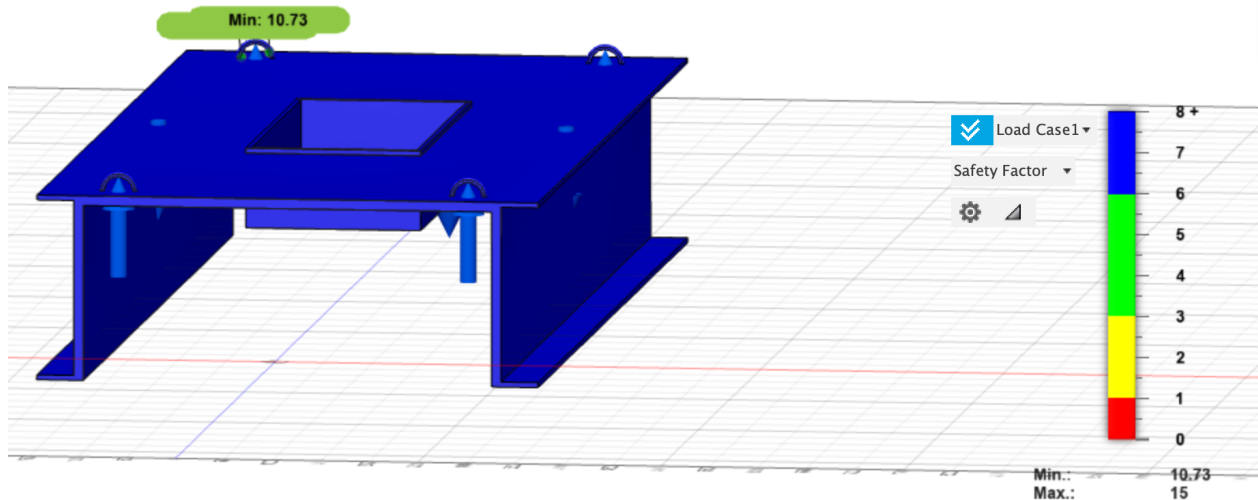


Figure 4.1.2. U-fixture simulation - safety factor

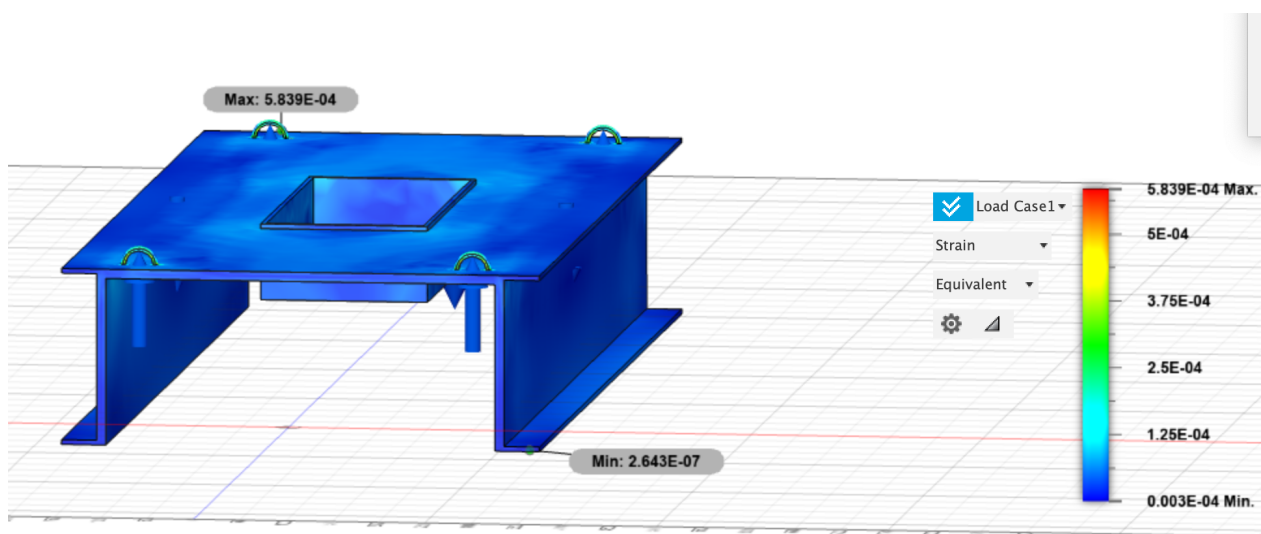


Figure 4.1.3. U-fixture simulation - strain

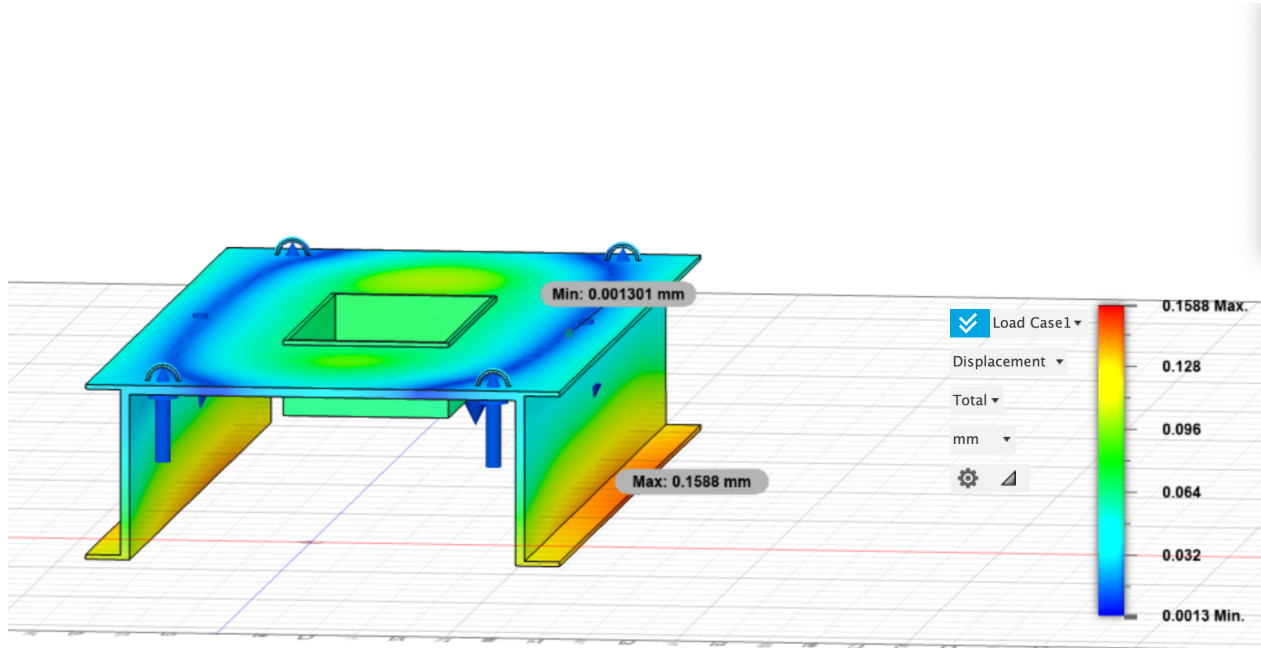
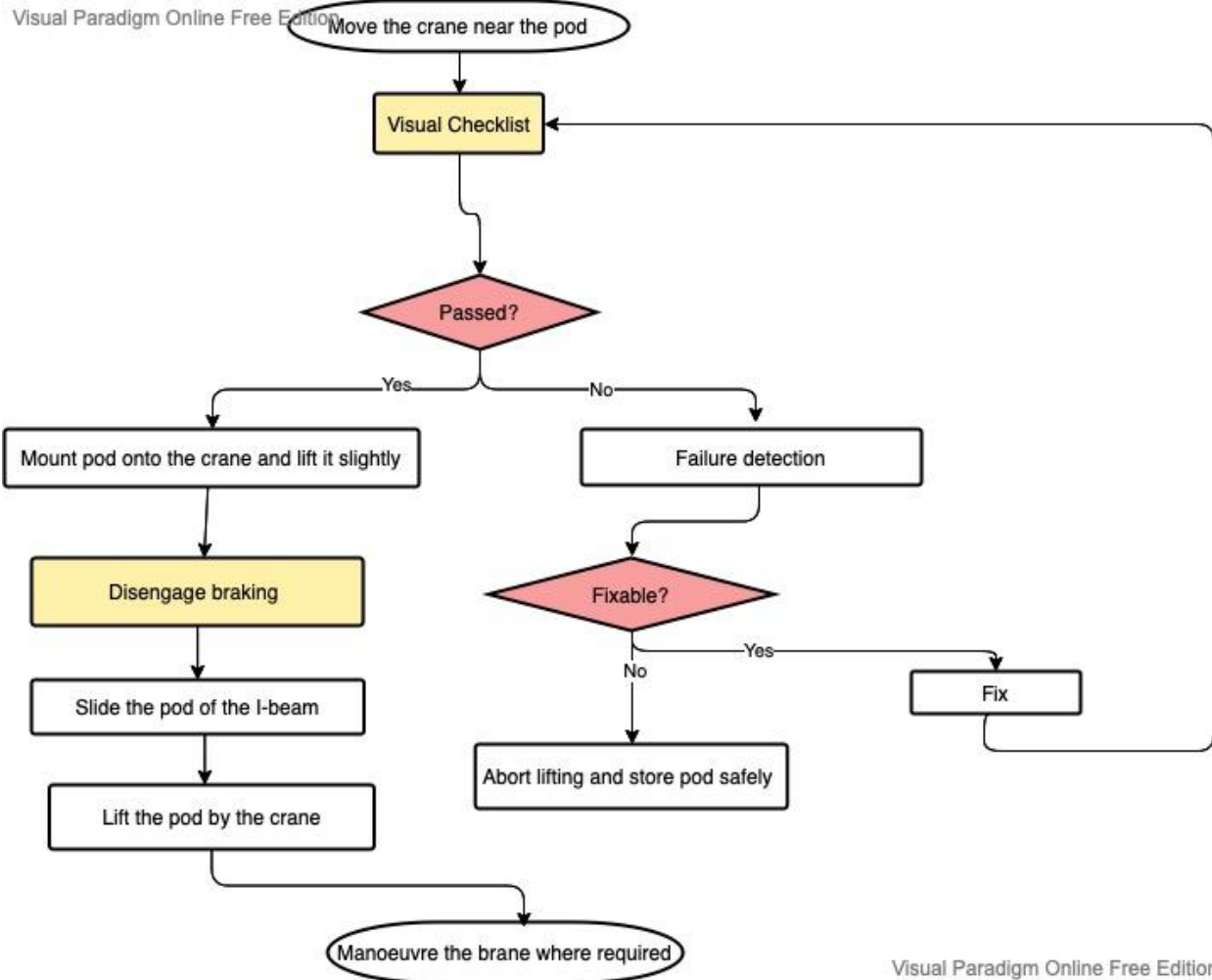


Figure 4.1.4. U-fixture simulation - displacement

The lifting procedure is represented as a flowchart and included below.



Visual Paradigm Online Free Edition

Figure 4.1.5. Lifting Procedure Flowchart

Visual Checklist is the procedure of visually examining the pod and determining its overall structural health. The purpose of this is to verify if all subsystems are in the correct place, there are no deformations of structure or mounting fixtures. It's further described in section 4.3 *Demonstration*. However, the procedure for lifting the pod also includes a general scan of the environment around the pod and assessment if it's safe to lift it i.e. no objects, people in the way or other potential risks that may cause damage to the pod or surroundings.

4.1.1 Specification of transportation procedures

4.1.1.1 Lifting the pod

The pod will only be lifted in designated, safe, and level areas. This will ensure full safety and ensure that the team fully controls the pod's movement. The pod will only be lifted when the crane is fully stationary. During the descending procedure, at least 5 team members will be present. Of the 5, 2 will be tasked with ensuring that the crane remains fully stationary, while 3 will ensure that there's no excess displacement when the pod is being lifted.

The pod will be lifted through the use of the crane presented on Figure 4.1.1.

4.1.1.2 Moving the crane around EHW premises

Once the pod is lifted by the crane, it will be moved around EHW premises. Extra care will be taken to move the crane slowly, with care and in a way which avoids any bumps or imperfections on the ground. At least 5 people will be involved in moving the crane at all times. From the 5, 3 will be responsible for pushing and manoeuvring the crane, while the remaining two will be responsible for clearing the path of any minor obstacles and securing the pod from moving to the sides.

4.1.1.3 Descending the pod at the storage area, demonstration area, or display area

The pod will only be descended in designated, safe and level areas. This will ensure full safety and ensure that the team remains in full control of the pod's movement. The pod will only be descended when the crane is fully stationary. During the descending procedure, at least 5 team members will be present. Of the 5, 2 will be tasked with ensuring that the crane remains fully stationary, while 3 will ensure that there's no excess displacement when the pod is being descended.

4.2 Storage

Safe storage will be ensured at all times, through ensuring that no sources of potential energy are present and that all other sources of energy are physically detached from the system.

4.2.1 Storage Procedure

Safe storage will be achieved through ensuring that the system is void of any potential energy and not subject to any unplanned-for external forces during storage. This will be ensured through placing the pod on the storage I-beam, while following the lifting procedure. Additionally, the below-described potential energy safe storage procedure will be followed to ensure the system is void of potential energy.

Additionally, it will be ensured that the pod remains stationary during storage, as the braking system is engaged by default, even with the power source being detached.

Throughout the storage procedure, PPE will be worn by all members coming in contact with the pod. This will include protective gloves and protective eyewear.

4.2.2 Potential Energy Safe Storage

The sources of potential energy present in the system are elastic potential energy, pressure and electric potential energy.

It will ensure that no elastic potential energy is present, through ensuring that all springs are in positions of zero displacement, where they're not compressed or elongated. This will be done through engaging the secondary braking system.

It will be made sure that there's no pressure build-up in the cylinders or pistons, through evacuating both systems. This will be done electronically, and checked through the sensors present onboard.

Electric potential energy will be physically detached from the system by detaching the battery and storing it separately from the pod, in a safe and dry environment. The battery will be manually turned off before being removed from the pod.

4.3 Demonstration procedures

Visual Checklist

The procedure of visually examining the pod and determining its overall structural health. The purpose of this is to verify if all subsystems are in the correct place, there are no deformations of structure or mounting fixtures. The Visual Checklist includes:

- Correct wheels orientation
- No structural failures (fracture, deflections, bending, fractures)
- No fixtures failures (bolting, screws, mounting fixtures)
- Correct position of subsystems
- Subsystems intact
- Tubing/wiring intact

Stationary test

The procedure is performed on a pod when the batteries and all subsystems are switched off. The only engaged system is braking, as it is designed to be engaged by default. The purpose of this test is to determine the stability and structural integrity of the pod before the demonstration. The stationary test examines the right placement of all subsystems with respect to the I-beam. This procedure includes checking:

- Propulsion alignment
- Braking system position
- Suspension orientation
- Battery placement
- Sensors placement

Software Testing: Connectivity Test

As a remote computer is being used to ensure completion of all the following tests, the first test we complete is the connectivity test. A ping will be sent from the remote computer to the main motherboard to see if a connection is present. If this is true, the same will be done from the main motherboard to the braking and propulsion board. It will be expected that all tests return a true boolean, and this will allow us to proceed with the following tests. This test will be considered failed otherwise.

Interconnection test

Now that we are confident that all of the boards are connected, the remote computer will test that all pins and wires are required to be accessible via the

software and that all states are currently set correctly. The board will manipulate any states that are incorrect and will not pass if any connections are not as expected.

Controllability Test

The brakes are deactivated for a short while and all operational components states are toggled to ensure that we have full control over the pod. If one component does not respond as expected this test will fail.

Sensor Test

We are already confident at this point that we are connected to the sensors. This part of testing just returns values and computes important statistics based on temperature, position, and pressure. If any one of these statistics is outside of the range set on the configuration menu on the remote computer then the test will fail and the erroneous data will be investigated.

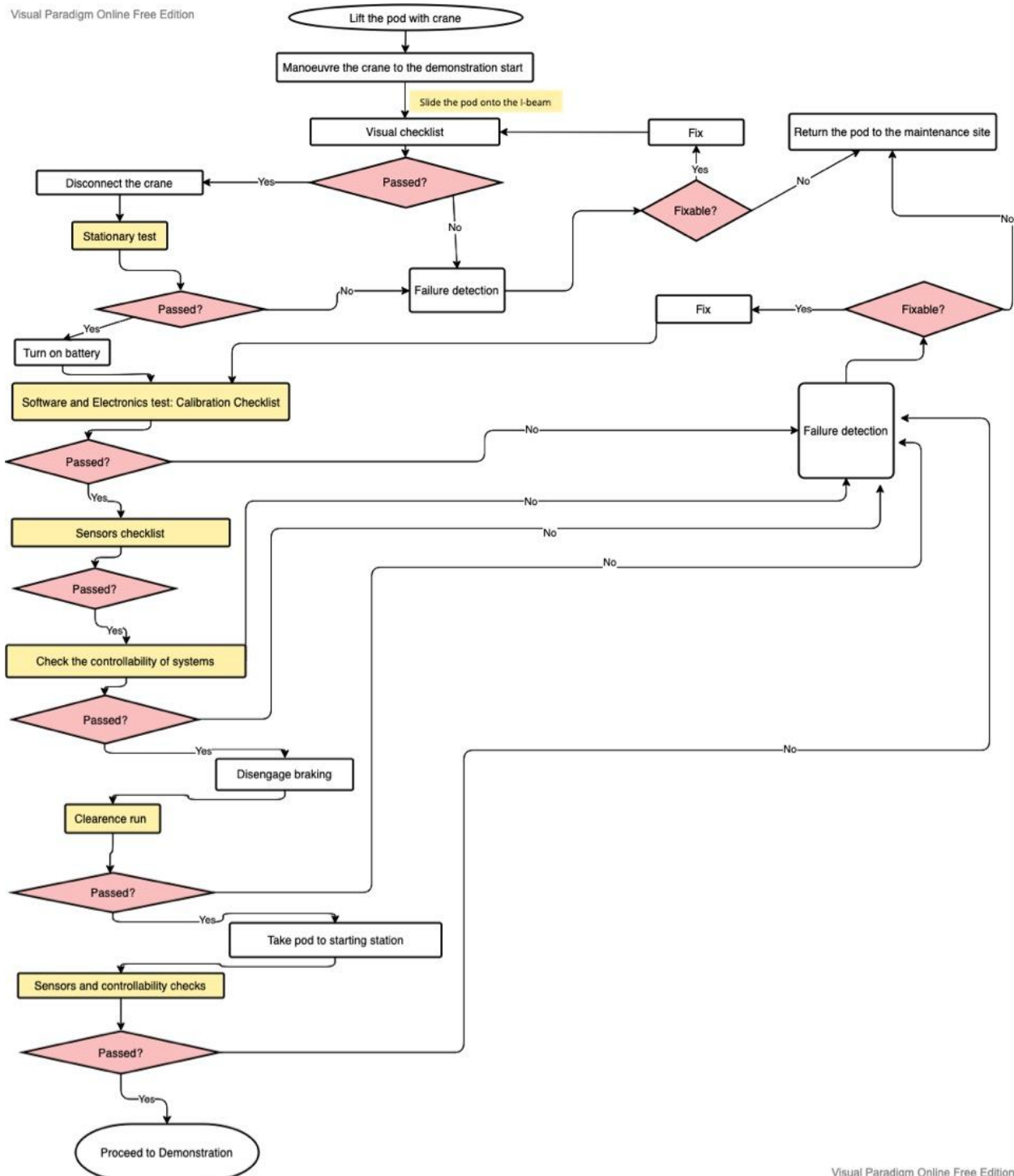
Clearance run

The test before the demonstration where the braking is disengaged, propulsion is not powered and the pod is pulled along a couple of metres along the I-beam through 2 team members pulling it through a band mounted to two front and back U-fixtures of the frame. The shell is detached at this stage to allow access to the internal components. The purpose of this test is to check the clearance of the subsystems and the I-beam, to make sure the track is not to be damaged during the demonstration.

The battery health assessment is the procedure of determining the condition of the battery. Its purpose is to state if the battery is safe to be used again and if the power cutoff is required.

4.3.1 Pre-demonstration procedure

Visual Paradigm Online Free Edition



Visual Paradigm Online Free Edition

Figure 4.3.1.1. Flowchart of pre-demonstration procedure

4.3.2 Demonstration procedure

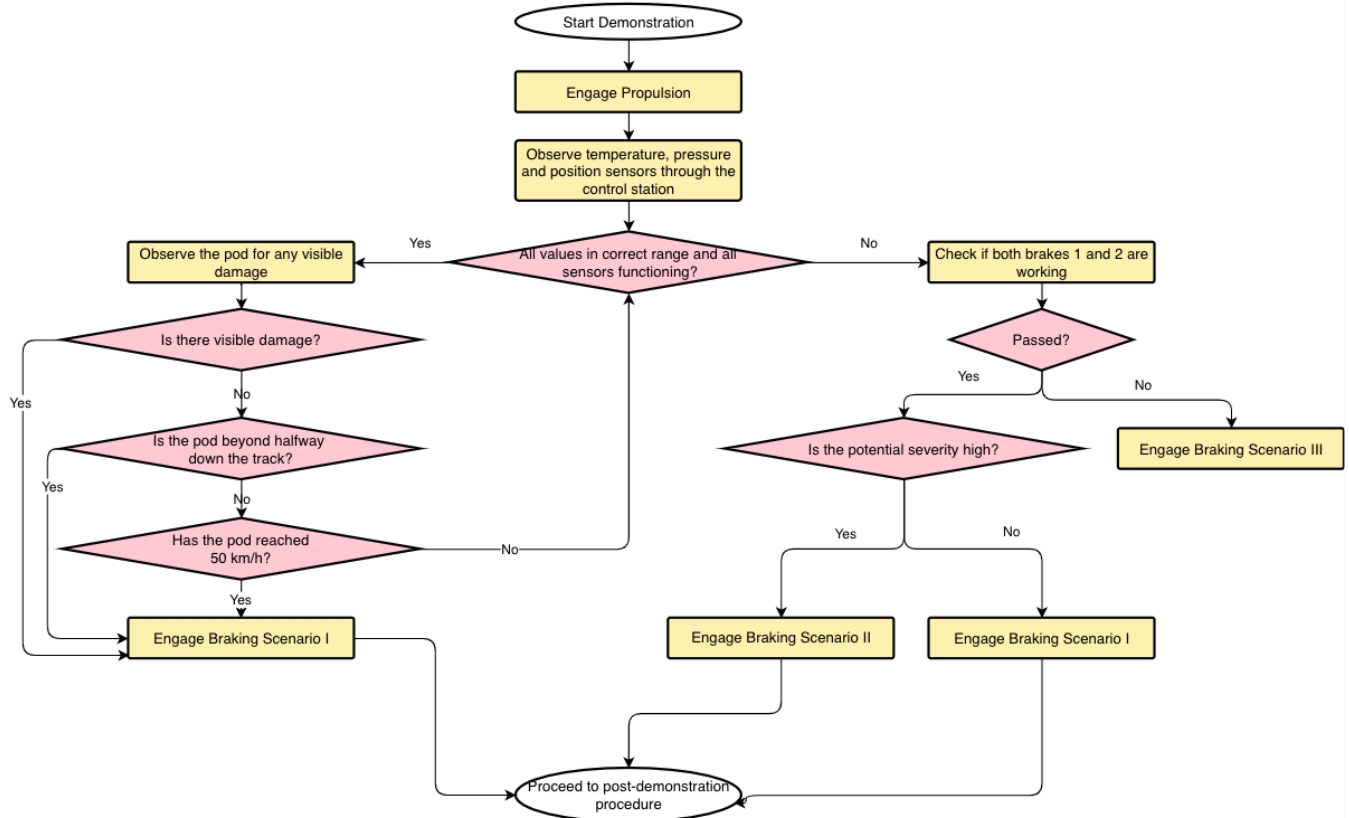


Figure 4.3.2.1. Flowchart of demonstration procedure

4.3.3 Post-demonstration procedure

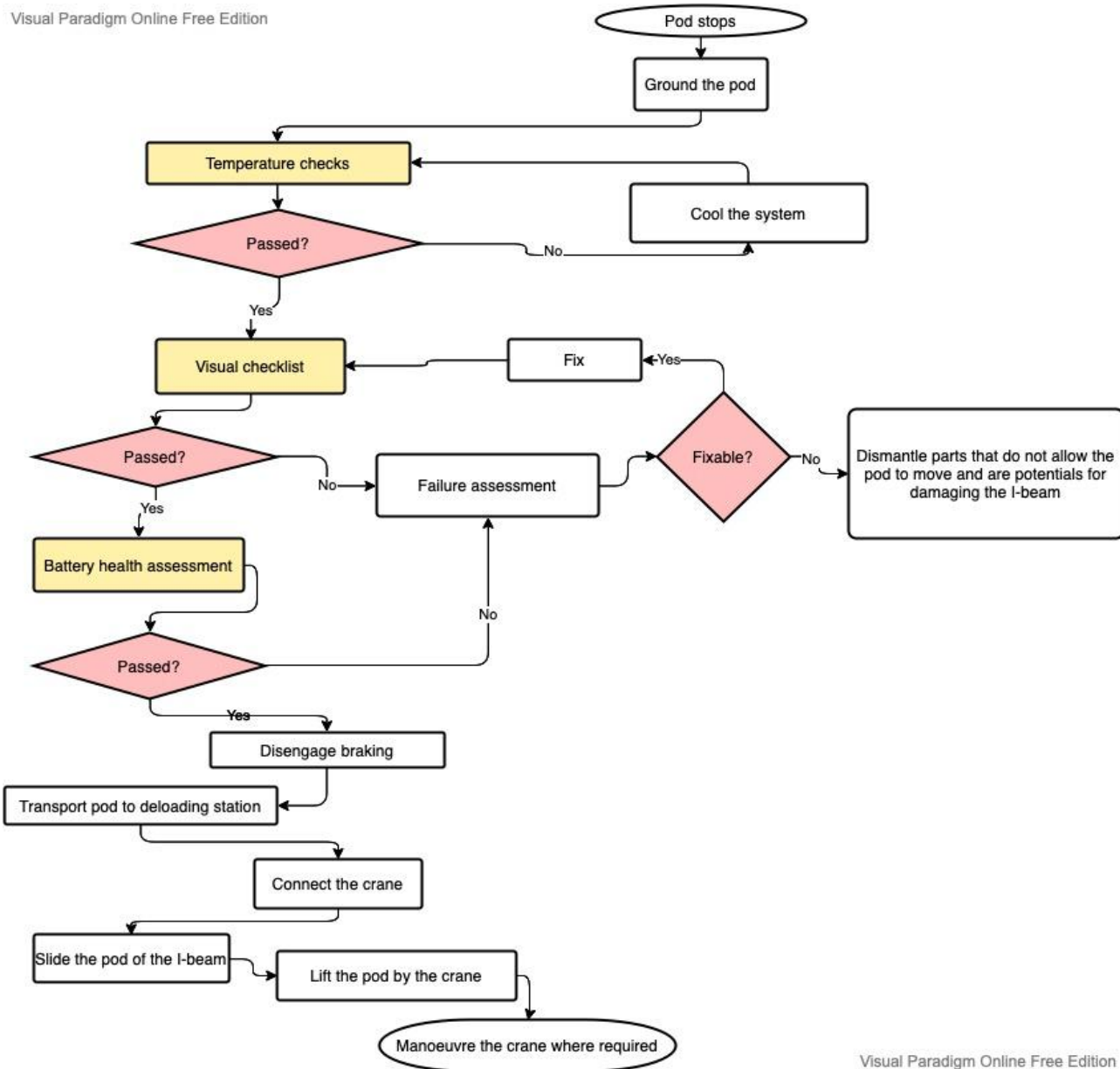


Figure 4.3.3.1. Flowchart of post-demonstration procedure

5. Testing

A general test of the whole system will be conducted to ensure that the run performed at EHW will be as safe as possible.

This test will be designed to mimic the EHW testing procedure as closely as possible. The pre-demonstration procedure, demonstration procedure, and post-demonstration procedures described in the above section will be followed to ensure that.

The test will be performed on an I-beam laid on the QMUL campus. The track will be approximately 40m long, and the goal of the test will be to reach a speed of 20 km/h.

The description of the testing facilities and the testing of all separate subsystems can be found below.

5.1 Testing Facility

All testing will be conducted at the QMUL university campus. This includes the below facilities:

- QMUL School of Engineering and Materials Science Maker Space
- QMUL Electronics School of Electronic Engineering and Computer Science Laboratory
- QMUL campus grounds

5.1.1 Propulsion

5.1.1.1 Manufacturing & Testing Procedures

The testing apparatus will be manufactured using the same method as outlined in 2.2.1.6 *Manufacturing processes*. Dual stators will be positioned parallel to each other with the I beam rotor in between them. The stators will be held together with a simple suspension structure, as seen in *Figure 2.1.3.1. LIM's mounted on the frame* and will be hooked by a force gauge, so that, as thrust is generated, the force is measured.

During this phase, the dimensioning of that stator itself will be fixed, so no property of the stator can be tested. The only thrust affecting parameters that can be tested are the voltage and current inputs, and the turn number.

These will be varied one by one, with other variables being set to control to ensure a fair test. The same values that were inputted for the simulation process will be used. The results of these tests should confirm the data that was obtained during the simulation process.

5.1.1.2 Testing Plan & Methodology

Voltage test

- 1) Set up the apparatus, conduct a visual and physical check to ensure the test will not fail. Check for potential points of failure, such as loose windings, structural failure etc.
- 2) Maintain constant current input of 10A and turn number of 35. Apply power with a voltage of 40 V.
- 3) Record the maximum thrust obtained from the force gauge.
- 4) Turn the system off and wait for a cooldown.
- 5) Repeat steps 1) through 4), increasing the voltage by a constant amount up to 80 V.
- 6) Collect the data and plot a graph of thrust force vs voltage input. Observe the trend.

Current test

- 1) Set up the apparatus, conduct a visual and physical check to ensure the test will not fail. Check for potential points of failure, such as loose windings, structural failure etc.
- 7) Maintain constant voltage input of 48V and turn number of 35. Apply power with a set current of 1A.
- 8) Record the maximum thrust obtained from the force gauge.
- 9) Turn the system off and wait for a cooldown.
- 10) Repeat steps 1) through 4), increasing the current by a constant amount up to 20A.
- 11) Collect the data and plot a graph of thrust force vs current input. Observe the trend.

Turn number test

- 12) Set up the apparatus, conduct a visual and physical check to ensure the test will not fail. Check for potential points of failure, such as loose windings, structural failure etc.
- 13) Maintain constant voltage input of 48V and current input of 10A. Apply power with a turn number of 10.
- 14) Record the maximum thrust obtained from the force gauge.
- 15) Turn the system off and wait for a cooldown.
- 16) Repeat steps 1) through 4), increasing the turn number each time by a constant interval up to 100.

17) Collect the data and plot a graph of thrust force vs turn. Observe the trend.

5.1.1.3 Expected Results

Voltage test:

- As voltage is increased, there will be an initial exponential increase in thrust, followed by a more linear relationship as more voltage is applied. With sufficiently high voltage, the gradient of linearity may start to decrease as the high power input results in increased heat, leading to an increase in resistance.

Current test:

- As current is increased, there will be an initial exponential increase in thrust, followed by a more linear relationship as more current is applied. With sufficiently high current, the gradient of linearity may start to decrease as the high power input results in increased heat, leading to an increase in resistance.

Turn number test:

- Very similar result to the current and voltage test. Initial exponentiality followed by linearity. The gradient of linearity may decrease with an increase in turn number, as the voltage supply may not be sufficient to match the induced voltage by the coils, reducing the rate of increase of thrust.

5.1.2 Braking

5.1.2.1 Manufacturing & Testing Procedures

Before testing takes place, certain procedures have to be satisfied.

- Safety procedure

When it comes to safety, our team will be following certain measurements. Since the testing will be done at Queen Mary University of London in the Makerspace SEMS lab, precautions will be taken as stated in the Makerspace rulebook. Lab coats, metal gloves, gum shoes and protective glasses will be used to ensure safety of all members of the team while demonstrating the experiment.

In order to be qualified to work in the lab, all team members of the team have obtained three certificates by completing Health & Safety as well as Fire safety module provided by SEMS.

- Assembling procedure

Assembling of the braking system will be completed once all the ordered components get delivered from the manufacturer as mentioned in Section 2.2.4.1. Parts List/BOM. Air reservoirs will be connected using tubes to pressure sensors that will measure pressure of reservoirs that get compressed from the external pump. The connection with the tubes will then continue to the solenoid valve that controls how much air will get in the next component which is the pneumatic cylinder. The cylinders piston will be connected to the rod with a spring around it. The rod will be connected from one side to the brake pad that will lie on the I-beam when braking force is being applied.

- Mounting procedure

The whole braking system except for the external compressor will be mounted on the frame of the pod. Air reservoir bottom legs will be connected to the frame using shafts and will be placed one behind another. Valve/tubing connections will be free inside the pod and a pneumatic cylinder will be placed on the small section on the frame in order for the brake pad to touch the I-beam.

5.1.2.2 Testing Plan & Methodology

Air reservoir:

The air stored in an air reservoir is kept at a high pressure and is compressed. Any faults with the tank pose a safety risk to the overall system and its surroundings. The risks can be mitigated by cleaning and examining the tank at regular intervals. Any faults found will subsequently improve.

Brake pads:

The brake pads will have to meet certain criteria for it to be suitable and safe to use. The testing of the brake pads was done by an experiment where the brake pad was dragged along a sheet of Aluminium 6061 T6 replicating the I-beam and brake pad interaction.

Control/ball valves:

The control valve was tested by a series of small experiments: flow test(leakage), function test and body test. These tested if the control valve

worked without any problems to its functionality and whether there was any leakage.

Spring:

A compression test was completed to determine whether the brake spring was fitting. The length of the spring was determined at low forces then compressed to known percentages of that length. The force was measured to reach those lengths.

Pneumatic cylinder:

The pneumatic cylinder will be subjected to a series of tests that will determine if there is leakage and tested for integrity. It will be tested at several known values of pressure for a specific period. This will determine if there is any failure to its structure and whether it will function at its desired purpose.

5.1.2.3 Expected Results

The components above will all be tested to determine their functionality and safety. The expected results are that the components will fulfil their necessary tasks. From these experiments we will obtain several parameters that describe the braking system. From the data obtained we will be able to improve and alter the design wherever it is necessary. If any faults or errors occur within the testing, we will be able to alter the experiments or the design. The data obtained will then allow us to test the braking system with the hyperloop pod.

5.1.3 Suspension

Two tests will be conducted on suspension before testing on complete pod assembly to ensure its safe and reliable performance. Both labs will be conducted in a MakerSpace at the Queen Mary University of London. A load test will be conducted to ensure all fixtures and housings are able support the load of the pod along with demonstration loads. A speed test will be conducted on a single suspension unit to ensure it is able to perform at high speeds.

5.1.3.1 Manufacturing & Testing Procedures

This section details how testing equipment will be manufactured and assembled.

5.1.3.1.1 Load Test

The load test involves installing all the vertical suspension units onto the empty pod frame (which would already have been load tested at this point).

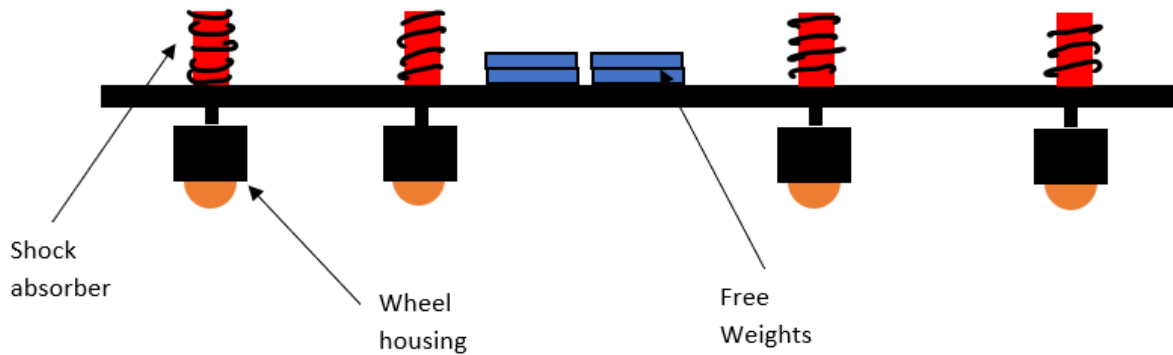


Figure 5.1.3.1.1.1 Load testing setup for the shock absorbers

The vertical suspension will be fully assembled as mentioned in the suspension manufacturing section.

5.1.3.1.1.2 Speed Test

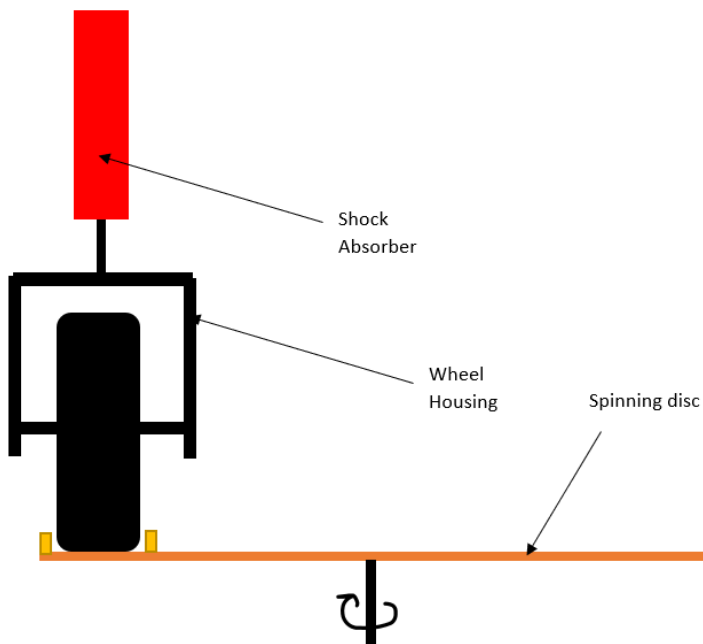


Figure 5.1.3.1.2.1 Load testing setup for the wheels

The speed test will be conducted on a single suspension unit. The top eye mount of the shock absorber will be secured by a stand available within the lab. The suspension unit will be assembled as mentioned under the “Description of Manufacturing process” subheading of suspension. The spinning disc will be custom made from the manufacturer for assembly.

5.1.3.1.3 Complete Test

A complete test of the suspension test will be performed once the full pod is assembled.

5.1.3.2 Testing Plan & Methodology.

A load test will be performed before the speed test for safety.

5.1.3.2.1 Load test

Free weights up to 150kg will be added onto the frame (as shown in the diagram) with 10kg increments. At each increment, the housing assembly and shafts are visually inspected for any major deflections. The distance of the base of the wheel housing will be measured relative to the test bench.

5.1.3.2.2 Speed Test

A single suspension unit will be tested for its performance under 50 km/h speeds. To simulate track conditions, an aluminium 6061 T6 disc with a 200mm diameter rotating at 1530 RPM can be used.. The disc is spun for thrice the duration of a single demonstration. Once the test is complete, the wheel, shaft, and housing are inspected for any kind of wear, tear, or microfractures. The disc is also inspected to ensure the wheels don't damage the track during demonstration.

5.1.3.2.3 Complete Test

Position sensors will be installed to provide the horizontal and vertical deflections of the pod during a test demonstration of the pod at Queen Mary University of London.

5.1.3.3 Expected Results

5.1.3.3.1 Load Test

The vertical suspension should be able to bear the compressive loads of the weight of the pod with minimum deflection. All measured deflections must be below 2mm.

5.1.3.3.2 Speed Test

No wear, tear, or microfractures detected within the suspension unit. No damage to the disc.

5.1.3.3.3 Complete Test

All data on horizontal and vertical deflections of the pod during a test demonstration are below 6mm.

5.1.4 Structures

5.1.4.1 Manufacturing & Testing Procedures

The manufacture of both the frame and its attachments will be outsourced, therefore a campaign of tests will begin as soon as the parts arrive in order to verify the quality of the parts and their performance in the hyperloop pod.

5.1.4.2 Testing Plan & Methodology

5.1.4.2.1 Load test

First, loads will be added to simulate the weight of all components on the pod, all deflections or deformations will be carefully measured and if required further supports will be added on the frame.

5.1.4.2.2 Mounting test

All mounting fixtures will be bolted in their corresponding position to test their rigidity and to ensure there is no wobbling or deformation on any of the parts.

5.1.4.2.3 Component test

Every component of the pod will then be attached in their assigned positions. Again, any potential deformation or wobbling will be measured and taken into account, and it will be ensured that all components are free to operate as designed from their positions in the frame.

5.1.4.2.4 Active test

The braking, propulsion and suspension of the pod will be activated to ensure their operation has no undesirable effects on the structure.

5.1.4.3 Expected Results

The expected results should be the same or very close to the simulations shown in part 2.4.1.4. All bending and displacements will be carefully compared to the simulations to ensure the results match and prove the structural integrity of the frame with a safety factor of 2 or more.

5.1.5 Electronics & Power

5.1.5.1 Manufacturing & Testing Procedures

All the PCB boards have been tested regarding, both, electrical compliance and logic behaviour by programming and observing the behaviour of the microcontroller. All the physical aspects of the PCB design have been tested by the manufacturer, as well as in the assembly house to maintain the highest level of safety and reliability.

5.1.5.2 Testing Plan & Methodology

After obtaining the PCB boards, all of them have positively passed the initial test based on:

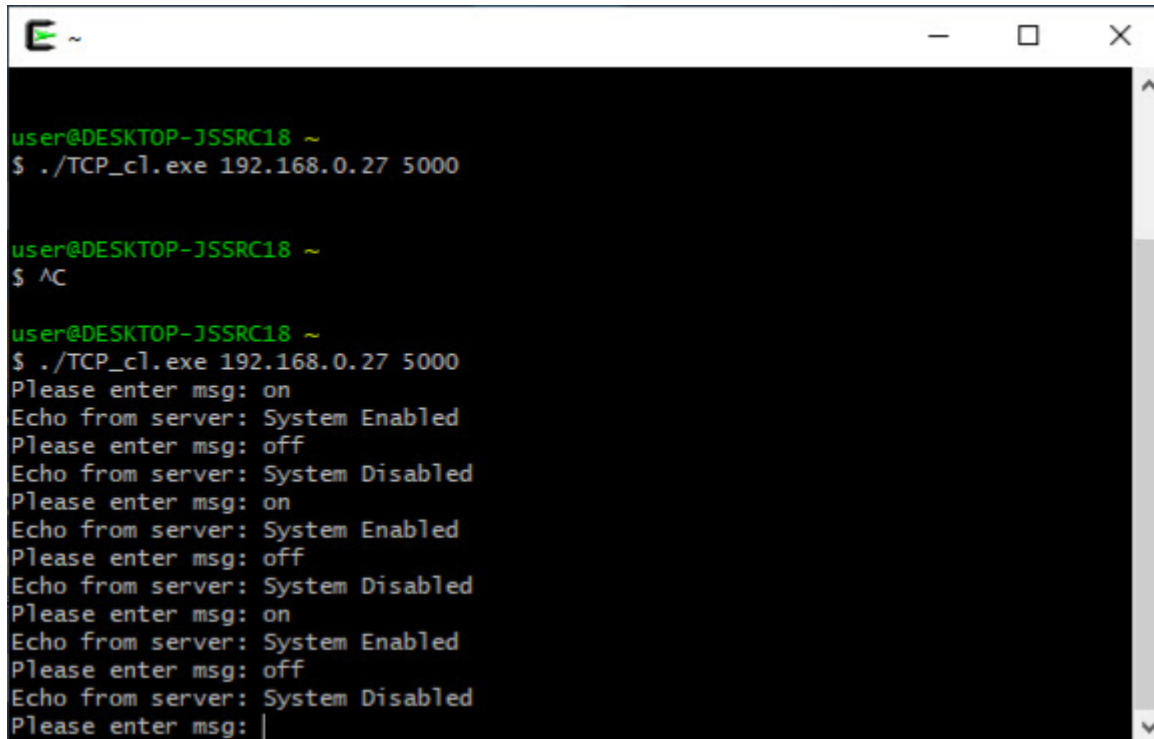
- Connecting unit to 24VDC power supply
- Burning a testing program into the microcontroller
- Testing CAN, Ethernet, IO-Link communication transfers (if applicable for a subsystem)
- Software debugging, stress-tests
- Joining subsystems into networks and monitoring behaviour during joint operation.

Further testing will be based on:

- Generating 3-phase waveforms and observing the Linear Induction Motor behaviour as a critical actuator for the design.
- Integrating and demonstrating operation of the braking pneumatic system
- Configuring internal PoE Wi-Fi module to establish wireless TCP/IP communication.

5.1.5.3 Expected Results

Preliminary communication tests can be found in the figure below. As shown, a simple TCP/IP communication is established, and relevant data and commands can be exchanged between the control station and all the pod subsystems.



```

user@DESKTOP-JSSRC18 ~
$ ./TCP_cl.exe 192.168.0.27 5000

user@DESKTOP-JSSRC18 ~
$ ^C

user@DESKTOP-JSSRC18 ~
$ ./TCP_cl.exe 192.168.0.27 5000
Please enter msg: on
Echo from server: System Enabled
Please enter msg: off
Echo from server: System Disabled
Please enter msg: on
Echo from server: System Enabled
Please enter msg: off
Echo from server: System Disabled
Please enter msg: on
Echo from server: System Enabled
Please enter msg: off
Echo from server: System Disabled
Please enter msg: |

```

Figure 5.1.5.3.1 Successful Ethernet and CAN bus testing

5.1.6 Software

Table 5.1.6.1 Software testing procedure

Test	Method	Expected Result
Ensure motherboard is responding	Once the computer is on, ping the main motherboard via the PC. The Motherboard should send a ping back to the PC. The remote PC should be placed approximately 200m away to ensure that the range of the connection is suitable.	The board should be connected to the PC. This test should return true over a 200m range test. There should be 1% loss within this range when transferring data.
Ensure propulsion board is responding	Once the motherboard is connected the motherboard can then ping the propulsion	should return True (propulsion board is connected)

	board. If the propulsion board is connected it will return true, otherwise it will return false.	
Ensure braking board is responding	Once the motherboard is connected the motherboard can then ping the braking board. If the braking board is connected it will return true, otherwise it will return false.	should return True (braking board is connected)
Ensure sensors are responding	On the remote computer use the interface to navigate to the pod data interface and view what data is being presented.	If data being presented is coherent and no specific data source is missing, then we know that data has been transferred from the given sensors to the remote computer.
Make sure temperature sensors are accurate	Compare the temperature shown on the pod data interface menu on the remote computer to the temperature on the pod using a digital thermostat.	The difference between the temperature on the pod and the the temperature being read should be accurate to +/-20%
making sure failsafes work including loss of connectivity and telemetry	Disengage the brakes and exit the application on the remote computer. We can then observe what happens to the brakes and propulsion when there is a loss of signal.	The brakes should engage and the propulsion should remain disengaged.
make sure interconnectivity tests are accurate	On the remote computer use the interface to navigate to the pod data interface and view the connection of a given board (braking for example). Disconnect the board and view changes on the pod data interface.	The braking board should appear as disconnected on the remote computers interface.
Ensure software functions as expected.	The software will have been tested intensively for weeks to ensure that functionality and safety measures have been met. On site some functionality of the software will be tested using the boards to review inputs and	The inputs and outputs should appear manipulated according to the functions which we execute.

	outputs of specific wires and pins	
Ensure propulsion works as expected	We will disengage brakes and use the minimum possible current through the propulsion. The force will be too small to allow the pod to move but we will be able to extract information allowing us to understand if the propulsion system is working as expected.	The propulsion should engage and disengage when expected. When not instructed to engage it should automatically default to disengaged
Ensure both brakes work as expected	On both brakes the brakes for a short period of time will be commanded to disengage. Once the short time is over they will be commanded to engage again (this is the default anyway)	The brakes should engage and disengage as expected.